LUCAS

DOE/NASA/0069-79/1
NASA CR-159592
AiR 31-3328

CONCEPT DEFINITION STUDY OF SMALL BRAYTON CYCLE ENGINES FOR DISPERSED SOLAR ELECTRIC POWER SYSTEMS

Lyle D. Six, Thomas L. Ashe, Frank X. Dobler, and Ron T. Elkins
AiResearch Manufacturing Company of Arizona
A Division of the Garrett Corporation

January 1980

Prepared for
NATIONAL AERONAUTICS AND SPACE ADMINISTRATION
Lewis Research Center
Under Contract DEN 3-69

for
U.S. DEPARTMENT OF ENERGY
Office of Solar Geothermal Electric and Storage Systems
Division of Central Solar Technology

NOTICE

1. Report No. NASA CR-159592	2. Government Accession No.	3. Recipient's Catalog No.
4. Title and Subtitle CONCEPT DEFINITION STUDY OF SMALL BRAYTON CYCLE ENGINES FOR DISPERSED SOLAR ELECTRIC POWER SYSTEMS		5. Report Date January, 1980
		6. Performing Organization Code
7. Author(s) L. D. Six, T. L. Ashe, F. X. Dobler, R. T. Elkins		8. Performing Organization Report No. 31-3328
		10. Work Unit No.
9. Performing Organization Name and Address AiResearch Manufacturing Company of Arizona 111 South 34th Street Phoenix, Arizona 85010		11. Contract or Grant No. DEN3-69
		13. Type of Report and Period Covered Contractor Report - Sept., 1978-June, 1979
12. Sponsoring Agency Name and Address NASA-Lewis Research Center 21000 Brookpark Rd. Cleveland, Ohio 44135		14. Sponsoring Agency Code

15. Supplementary Notes
Project Manager, J. A. Heller
NASA-Lewis Research Center

16. Abstract

This is the final report for the Concept Definition Study of Small Brayton Cycle Engines for Dispersed Solar Electric Power Systems, NASA Contract DEN3-69. This study addressed three first-generation Brayton cycle engine types for solar application: a near-term open cycle (Configuration A), a near-term closed cycle (Configuration B), and a longer-term open cycle (Configuration C).

The existing AiResearch GTP36-51 turbocompressor and a 400-Hz generator, both suitably modified, were selected for Configuration A. The existing AiResearch PFE turbocompressor and a 400-Hz generator were selected for Configuration B. Configuration C utilizes a turbocompressor also, based on the GTP36-51 aerodynamics, but scaled to an optimum flow and mounted on gas bearings, together with a permanent magnet generator.

For a thermal input of 72.7 kW_t to the engine, Configuration C has an efficiency of 31.4 percent at the engine shaft and will generate 19.1 kW_e (net) at the 60-Hz busbar with an overall efficiency of 26.3 percent on a sea level, 80°F day. Initial high-production rate and maintenance costs also were estimated.

Related reports in the Solar Thermal-Electric Power Conversion Conceptual Design study are:

Free Piston Stirling System	NASA CR-159587
Kinematic Stirling System	NASA CR-159588
Steam Rankine Turbine System	NASA CR-159589
Steam Rankin Reheat Reciprocator System	NASA CR-159590
Steam Rankine Reciprocator System	NASA CR-159591

17. Key Words (Suggested by Author(s))	18. Distribution Statement
Brayton Cycle, Production Costs, Solar Electric Power, Gas Turbines Durability	Unclassified - Unlimited STAR Category 44 DOE Category 62B

19. Security Classif. (of this report)	20. Security Classif. (of this page)	21. No. of Pages	22. Price*
Unclassified	Unclassified	132	

* For sale by the National Technical Information Service, Springfield, Virginia 22161

NASA-C-168 (Rev. 10-75)

DOE/NASA/0069-79/1
NASA CR-159592
AiR 31-3328

CONCEPT DEFINITION STUDY OF SMALL BRAYTON CYCLE ENGINES FOR DISPERSED SOLAR ELECTRIC POWER SYSTEMS

Lyle D. Six, Thomas L. Ashe, Frank X. Dobler, and Ron T. Elkins
AiResearch Manufacturing Company of Arizona
Phoenix, Arizona 85010

January 1980

Prepared for
NATIONAL AERONAUTICS AND SPACE ADMINISTRATION
Lewis Research Center
Cleveland,Ohio 44135
Under Contract DEN 3-69

for
U.S. DEPARTMENT OF ENERGY
Office of Solar Geothermal Electric and Storage Systems
Division of Central Solar Technology
Washington, D.C. 20545
Under Interagency Agreement EX-76-A-29-1060

TABLE OF CONTENTS

TABLE OF CONTENTS (Contd)

1.0 SUMMARY

This is the Final Report for the Concept Definition Study of Small Brayton Cycle Engines for Point-Focusing Dispersed Solar Electric Power Systems, NASA Contract DEN3-69. A point-focusing dispersed solar electric power system comprises a number of solar modules, each consisting of a point-focusing concentrator, plus a receiver and engine/generator mounted at the focus.

This study addressed three first-generation Brayton cycle engine types designated as Configurations A, B, and C. Configuration A is a near-term* open cycle and Configuration B is a near-term closed cycle gas turbine engine/generator. Both of these configurations are recuperated and were to be based on maximum use of existing hardware. Configuration C also is a recuperated open cycle but will allow the use of customized or scaled hardware that may require a longer development program.**

To meet program cost and schedule objectives for a near-term demonstration engine (Configurations A and B), modified turbocompressors from existing AiResearch engines, the Model GTP36-51 and the Pacific Fruit Express (PFE) respectively, were selected. Each turbocompressor drives a 400 Hz generator through a gearbox. The longer development term allowed for engine Configuration C led to the recommendation of a gas bearing turbocompressor based on the Model GTP36-51 aerodynamics, but customized or scaled, if necessary, to optimum size, and a direct-driven permanent magnet generator (PMG). This configuration requires no lubrication since it uses foil bearings. The PMG also can be utilized to start the turbocompressor. All three configurations require a power conditioning system consisting of a rectifier and inverter.

The cost of a production version of Configuration C, including a turbocompressor, PMG, recuperator, rectifier, controls and other miscellaneous equipment, was estimated to be $5270 in 1978 dollars. This cost was based on a production rate of 10,000 units per year. Operation and maintenance costs, based on component failure rates and scheduled maintenance requirements, were estimated to be $98/year for 3300 hours of operation each year. For a thermal input of 72.7 kW_t, this engine will generate 19.1 kW_e of power (net) at the DC busbar (22.9 kW_m at the engine shaft), with an overall efficiency of 26.3 percent (31.5 percent at the engine shaft) on a sea level, 80°F day.

*Scheduled for initial testing in late 1980.
**Scheduled for initial testing in 1981-1982.

2.0 INTRODUCTION

The Solar Thermal Power Office in the United States Department of Energy's Energy Technology/Solar Division is currently conducting technology and engineering development of point-focusing dispersed solar power systems for applications in electrical power generation. This is a part of DOE's total program directed toward evaluating the potential for commercializing dispersed solar energy conversion. Responsibility for implementing these systems has been delegated by interagency agreement to the National Aeronautics and Space Administration (NASA) team consisting of the Jet Propulsion Laboratory (JPL) and the Lewis Research Center (LeRC). The LeRC responsibilities include investigating the technical and economic characteristics of heat engines applicable to point-focusing, distributed solar power systems. One of the system concepts being considered by JPL and LeRC consists of a number of solar power modules, each consisting of a parabolic solar concentrator (a point-focusing dished mirror), a high-temperature solar receiver operating in the range of 650°C to 815°C (1200-1500°F), and a recuperated Brayton cycle engine/generator (BE/G). The engine/generator, and receiver would be mounted as an assembly at the focus of the concentrator. This assembly is depicted in Figure 2-1 for one of the possible Brayton engine/generator and receiver configurations. The assembly is shown mounted on a solar power module in the artist's rendering in Figure 2-2.

Figure 2-2 illustrates how modules might be combined to form a solar power system or plant. Hundreds and even thousands of these modules, scattered over uninhabited or unused terrain, each producing 15-20 kW_e of electricity, could contribute substantially to the nation's electrical energy needs while reducing the consumption of fossil fuels.

Alternatively, fewer modules could be used effectively for smaller applications requiring electrical power. These might be remote military bases, shopping centers, housing subdivisions, apartments, co-ops, irrigation pumping, large industries, etc.

The NASA Lewis Research Center awarded a study program* (NASA Contract DEN3-69) to The Garrett Corporation; AiResearch Manufacturing Company of Arizona, to evaluate the availability of engine hardware for and the suitability of BE/G concepts for producing electric power from such distributed solar energy modules.

*Concurrent with this study, a design study was conducted under JPL contract NAS7-100/955136 by the AiResearch Manufacturing Company of California to conceptually design a point-focusing solar receiver unit for use in conjunction with Brayton engine/generators.

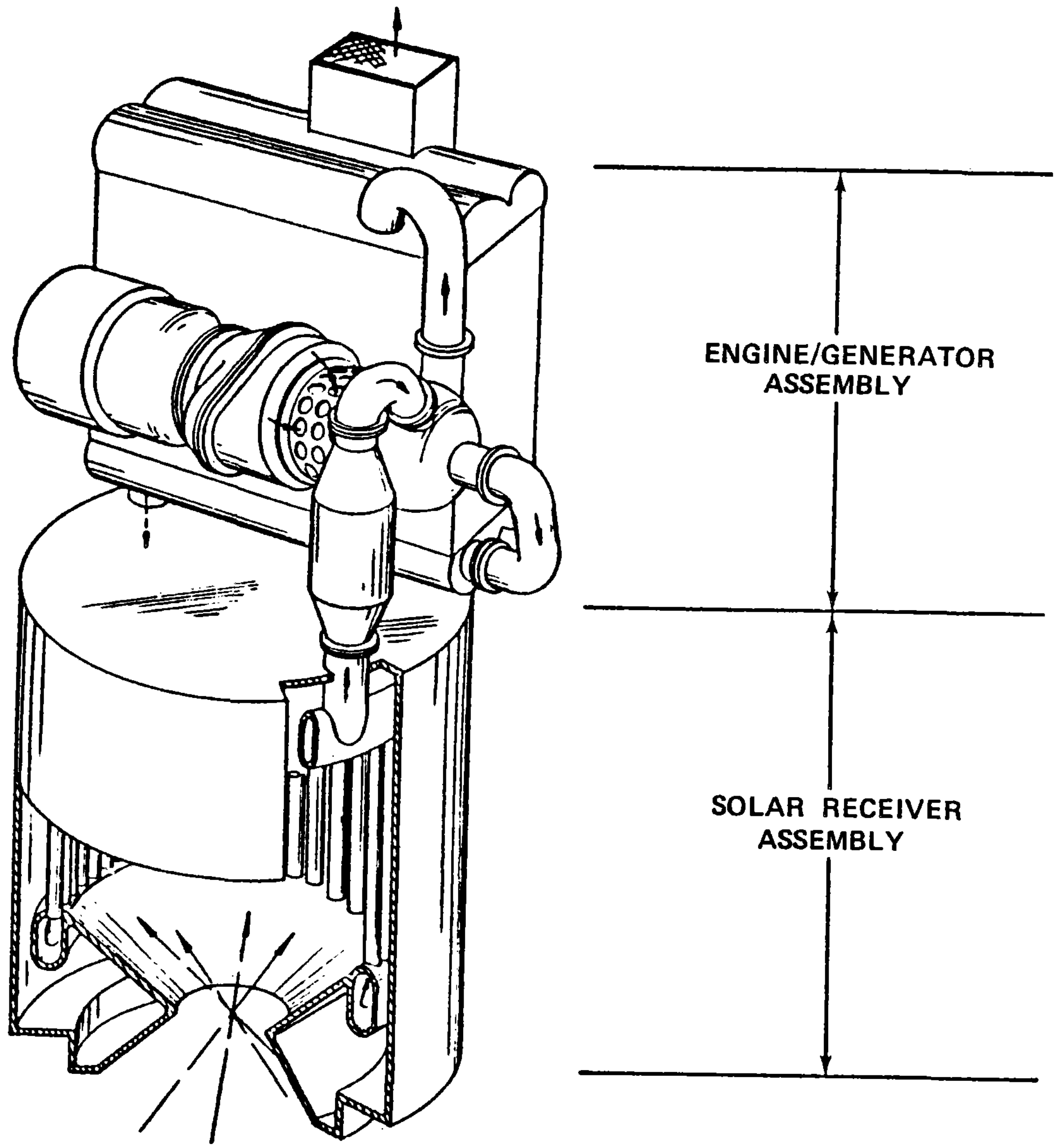

Figure 2-1. Engine/Generator Assembly and Receiver

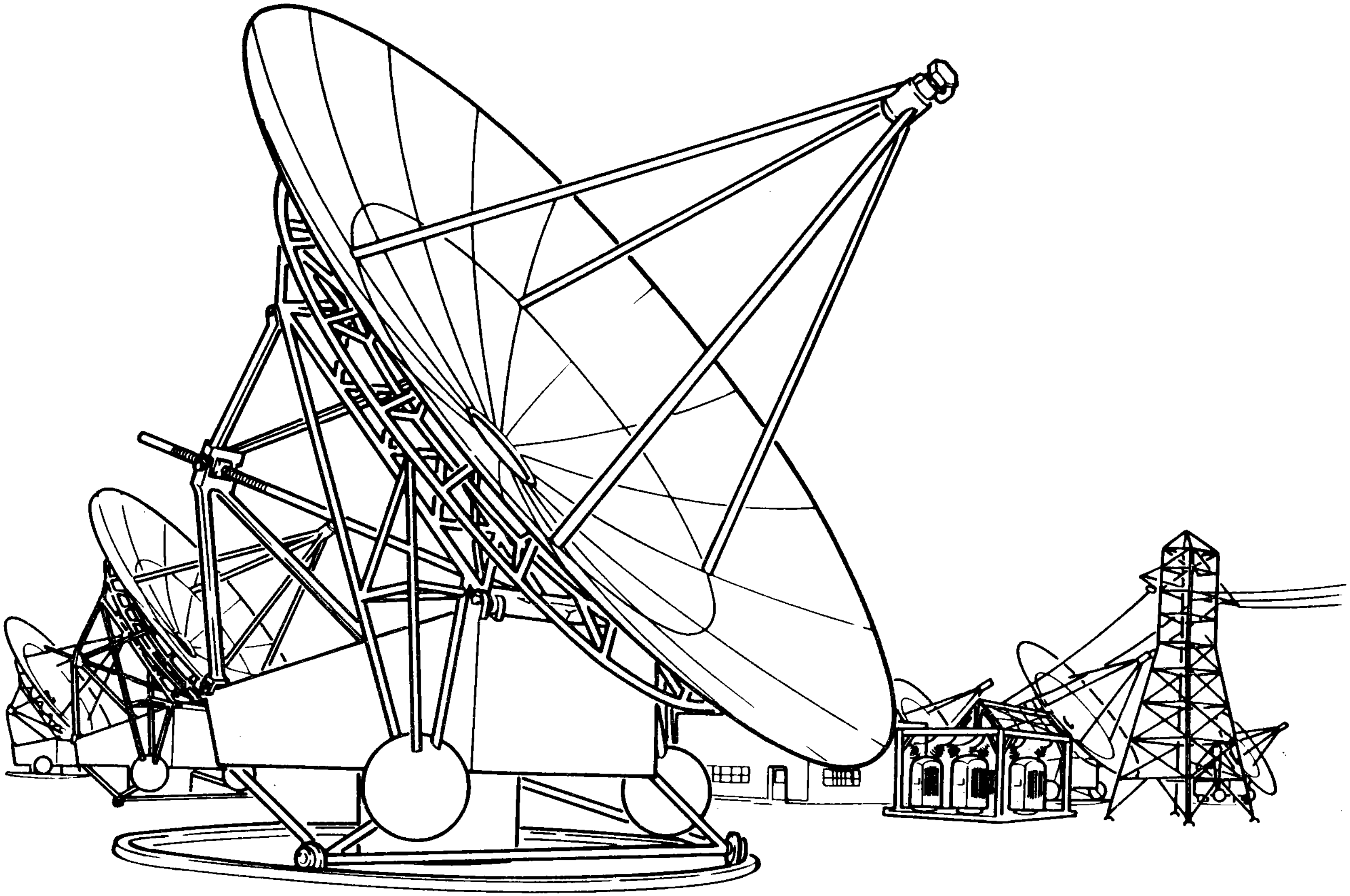

Figure 2-2. Artist's Conception of Dispersed Solar Power Plant.

The study contract objective was to determine the most suitable concept performance and life cycle costs of small gas turbine/generator sets deemed to have economic potential for dispersed power applications.

It was required that the BE/G investigated fall into the two calendar time-dependent categories indicated by the following exerpts from the Statement of Work.

> <u>Configurations A and B</u> - This set shall be a modified engine/generator derived from the contractor's existing product line. Further, the modified Baseline BE/G Module shall be available for testing in a full-scale solar facility in FY 1980. The Baseline BE/G must represent a low risk approach with a high probability and confidence of success for near-term commercialization.
>
> <u>Configuration C</u> - This engine/generator set shall be based on advanced designs incorporating new technology and having an improvement in efficiency over a wide operating range and/or reduction in costs (initial and life cycle) and an increase in design life and reliability. The alternate BE/G module need not necessarily be a direct derivative of the Baseline BE/G; however, if such is the case, the design shall be based on an engine which at this time is a unit well along in the latter phases of development. This alternate E/G module shall be available for testing in a full-scale solar facility in FY 1982. The addition of new technology makes this alternate configuration a higher risk approach than the baseline configurations and will require subsequent development for commercialization some years later.

Configurations A and C are open cycle recuperated Brayton engines, while Configuration B is a closed cycle recuperated Brayton engine. All are configurations that could be built and tested in the 1980 to 1982 period. Production versions of these BE/G were also defined in the study for use as a basis for estimating mass production engine costs.

This study consisted of work under the following four tasks:

<u>Task 1 - Parametric Performance Analyses</u>

The purpose of this task was to conduct a parametric performance analysis to provide necessary data to select a Brayton engine design for each of the three Configurations A, B and C, for further detailed investigation.

<u>Task 2 - Conceptual Designs</u>

The purpose of this task was to establish the conceptual design for each of the three engine types selected in Task 1.

Task 3 - Interface Requirements

The purpose of this task was to briefly evaluate the interface requirements for the BE/G and solar receiver.

Task 4 - Assessment of Production Implementation

The purpose of this task was to assess the technology status, production costs, durability, and growth potential for the selected engine types.

Results of the studies conducted under these tasks are discussed in following sections of this report.

3.0 ANALYSIS AND SELECTION OF THE BRAYTON ENGINE/GENERATOR CONFIGURATIONS

The objective of the analysis was to provide a basis for selecting engine/generator designs suitable for operation with solar input.

3.1 Brayton Engine/Generator Types Defined

The system diagram and general characteristics of the engine types investigated are shown in Figure 3-1. (Nomenclature is defined in Appendix A.) These were the open atmospheric Brayton cycle (ABC), the open subatmospheric Brayton cycle (SABC) and the closed Brayton cycle (CBC).

The ABC engine draws in atmospheric air at the compressor inlet and operates as a conventional recuperated gas turbine. Engine control to accommodate various insolation levels can be achieved by one of two methods -- either varying rotor speed at constant turbine inlet temperature or varying turbine inlet temperature at constant rotor speed.

The CBC engine is a completely closed system utilizing a heat exchanger upstream of the compressor inlet to reject cycle gas waste heat to the atmosphere. The pressure level of the cycle gas inventory is regulated by the engine control system. Control to accommodate various insolation levels is achieved by varying cycle gas inventory. The rotor speed and turbine inlet temperature remain constant. The CBC may, therefore, operate at essentially constant efficiency, temperature, and corrected flow over a wide range of insolation. Typical cycle gases are helium, air, argon, nitrogen, krypton, xenon, or mixtures of these. For dispersed solar power, air is considered the most suitable and was used in this evaluation.

In the subatmospheric engine (SABC), the pressure at the compressor inlet is 1/2 to 1/3 of atmospheric. This cycle type is formed from a conventional cycle by (1) connecting the turbine exhaust through a cooler to the compressor inlet, and (2) venting the high pressure side of the cycle to atmosphere at Point "A" or "B" in Figure 3-1 to establish the cycle high pressure equal to atmosphere. The SABC engine vented at Location "A" and the ABC and CBC engines would utilize a closed receiver conceptually similar to the receiver depicted in Figure 2-1. The SABC engine vented at Location "B" would utilize the open receiver shown conceptually in Figure 3-2. In this receiver concept, ceramic elements are heated by solar insolation. Cycle gas flows around or through the elements and is heated to turbine inlet temperature. The rationale for venting at Point "B" and utilizing the open receiver is the potential for lower production cost of the receiver and the potential for operation at somewhat higher turbine inlet temperatures.

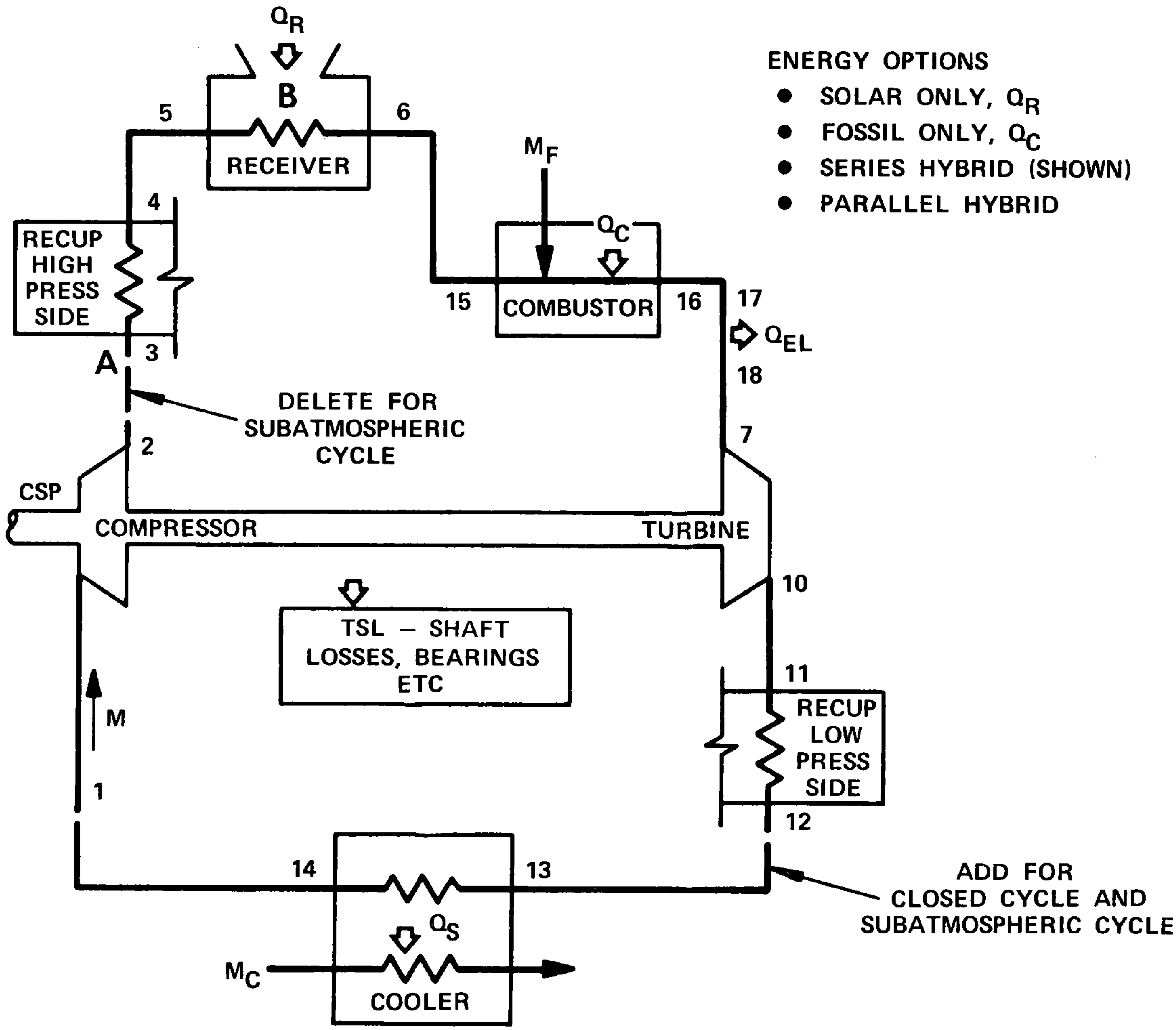

Figure 3-1. Engine System Diagram.

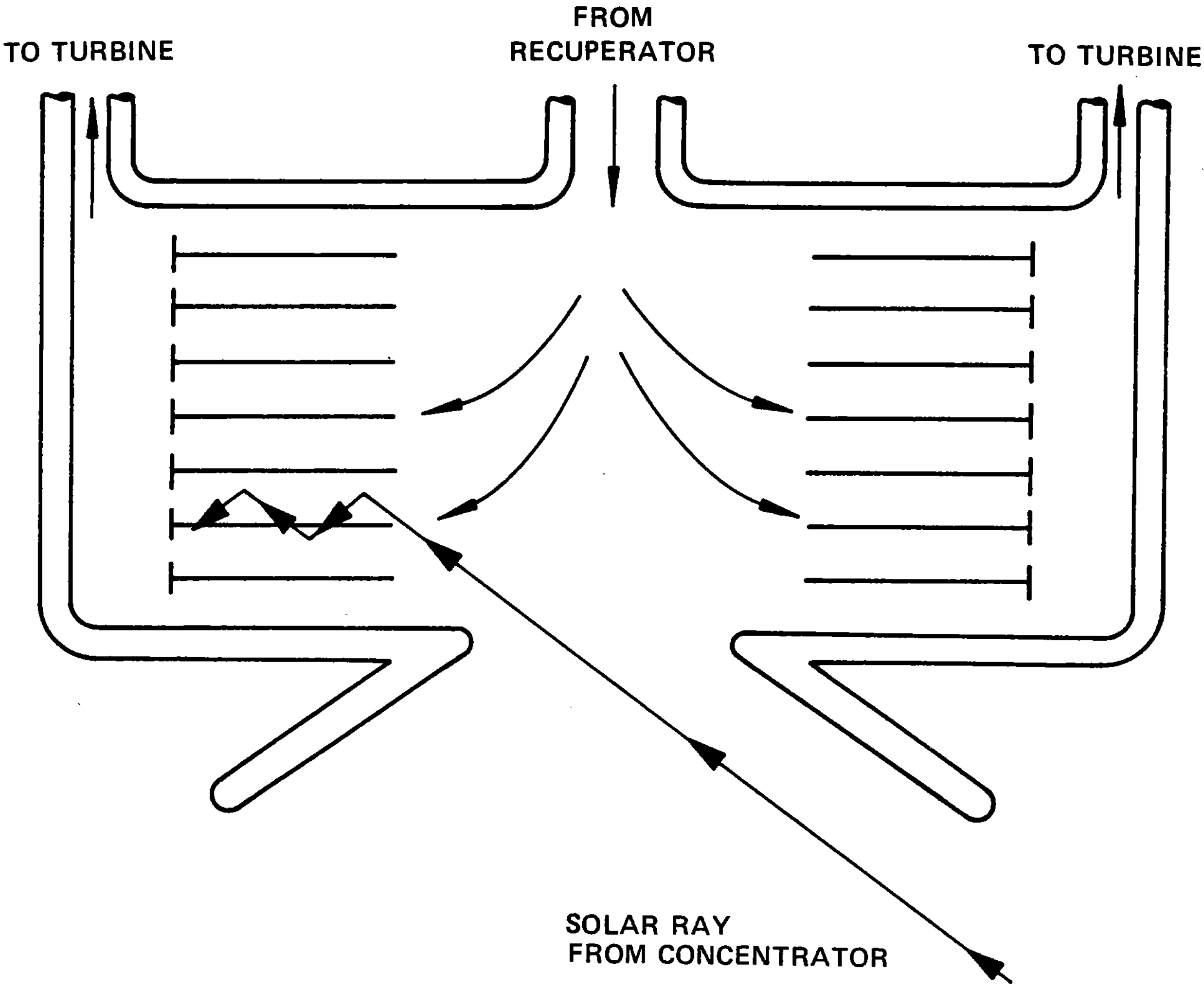

Figure 3-2. Optional Solar Receiver Concept for Subatmospheric Cycle

Although systems heated by insolation only were considered in this analysis, each cycle type is also suitable for adaptation to hybrid configurations, using a combination of insolation and fossil fuel. Fossil heat addition, by means of a heat exchanger in series or in parallel with the solar receiver is applicable to all three engine types. Internal fossil fuel combustion can be used with the ABC type but is applicable to the SABC type only if fresh air is introduced to support combustion and combustion products are vented at Location "A" in Figure 3-1.

Applicability of various electrical generators and corresponding power conditioning systems were considered. For simplicity, the E/G parametric analysis assumed use of a direct drive permanent magnet generator having an efficiency of 0.933. Section 3.5 describes other generators and appropriate electromechanical systems.

3.2 Methodology for Engine Parametric Analysis

Parametric analyses were made of various BE/Gs to provide data for use in selecting designs for cost effective solar electric power modules. Major emphasis was placed on identifying designs that would result in minimum specific cost (dollars per kilowatt) for the complete module rather than attempting to minimize the specific costs of a concentrator, receiver, or BE/G individually. Minimizing specific cost of the BE/G alone will generally not result in a module having minimum specific cost. Low weight and compact packaging were also considered important design goals because of their impact on the support structure and mirror shadowing.

A computer was used to calculate engine power output and engine cost for a range of design variables listed in Table 3-I. Weight, cost and aerodynamic performance models of current production compressors and turbines were placed in the computer data bank, as well as adjustment factors for rotor size and clearance, specific speed, pressure ratio and other variables on which aerodynamic performance depends. With this data bank, the parametric analysis can be used to show the effect on engine performance, cost, and weight of scaling or customizing aerodynamic parameters such as airflow, rotor diameter and rotor speed to optimum values for any given engine power rating. The program also can be used to show the engine speed for best performance of an existing engine for which the rotor diameter is already fixed. Also placed in the computer data bank were models for a system power balance and for the cost, weight and performance of bearings, gearbox and production heat exchangers. A block diagram of the parametric analysis methodology is shown in Figure 3-3.

Literally hundreds of possible engine designs were then calculated for interesting permutations of the design variables. The output of the computer calculations are the engine estimated production costs (ordinate) plotted against the electrical power outputs

TABLE 3-I. MATRIX OF ENGINE DESIGN PARAMETERS.

MATRIX A			
Engine Types			ABC, SABC, CBC
Concentrator Diameters		m	7, 9, 11
MATRIX B			
Engine Speed	N_T	krpm	55, 60, 65, 70, 75, 80, 85
Compressor Pressure Ratio	R_C		1.8, 2.0, 2.2, 2.5, 2.8, 3.1
Recuperator Effectiveness	E_R		0.8, 0.875, 0.90, 0.925, 0.95
Compressor Specific Speed (CBC Only)	$N_{SC}{}^{\ddagger}$		0.075, 0.090, 0.105, 0.120
MATRIX C			
Cycle Pressure Loss Ratio	$\Delta P/P$		0.3, 0.5, 0.7, 0.9
Compressor Inlet to Ambient Delta	T_1-T_∞	°F	10, 20‡ 40 (SABC AND CBC ONLY)
Ambient Temperature	T_∞	°F	0, 40, 80‡ 120
Turbine Inlet Temperature	T_7	°F	1200, 1400, 1500‡
Generator Speed	N_G	rpm	1800, 3600, $N_T{}^{\ddagger}$

‡Denotes values selected for parametric analysis.

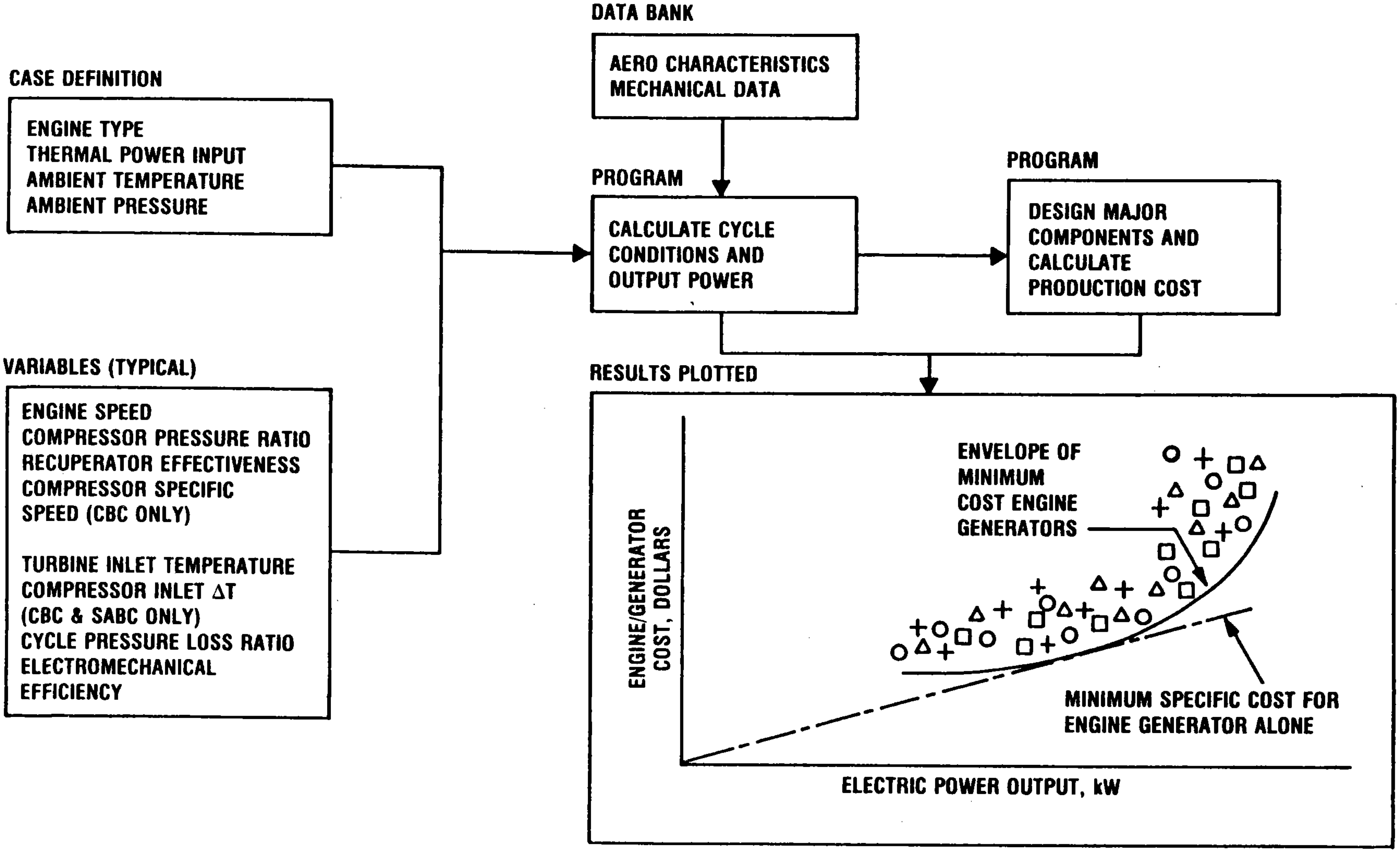

Figure 3-3. Methodology of Parametric Analysis

(abscissa) for each permutation of the engine design variables. The slope of a line drawn from the origin to the coordinates of a particular engine design would be the specific cost of that design in dollars per kilowatt.

All engine designs of a particular type (ABC, CBC or SABC) and for a particular concentrator diameter (7, 9, and 11 meter) were plotted on a single chart like the one shown in Figure 3-3. On this chart, therefore, the values on the abscissa are also proportional to engine efficiency. This is because all values of electrical output power are for engines sized to work with a single concentrator diameter, which produces a single value of thermal input power to the engine. The wide range of electrical output power along the abscissa is primarily a result of the range of recuperator size (or effectiveness) selected for analysis. Likewise, the variation in estimated engine production cost along the ordinate is primarily the result of the recuperator size.

Cost effective engine designs are those falling on or near the envelope of the plotted designs. The minimum engine specific cost is the slope of a line through the origin tangent to this envelope. The engine design determined in this manner would include a recuperator size and values for the other engine design variables, that would result in minimum specific cost for the engine alone.

For a complete solar power module, the choice of engine design must be selected on the basis of module minimum specific cost, not just engine minimum specific cost. The origin of the cost versus electric power plot must therefore be extended to include the cost of the other module components. Since the engine plot is for a single concentrator diameter, providing a single value for the thermal input to the engine, the concentrator and receiver costs were considered approximately constant for all values of power output along the abscissa. The costs of these components were therefore treated as constant values, each added to the variable engine cost, resulting in a plot of module cost like that shown in Figure 3-4. Using this modified plot, an engine design and recuperator size was selected that should result in a minimum specific cost for the entire module.

3.3 Customized Engines for 1981-1982 Time Frame (Including Configuration C)

It was defined that, to be available for full scale solar testing by 1981-1982, the aerodynamic components for Configuration C would utilize current AiResearch production aerodynamic designs (as represented by the Model GTP36-51) but with the rotor speed and diameter customized or scaled, if required, to a size that would result in optimum module cost for the specified thermal input power. Numerous previous gas turbine development programs have demonstrated that such a customizing or scaling can be effectively accomplished with good

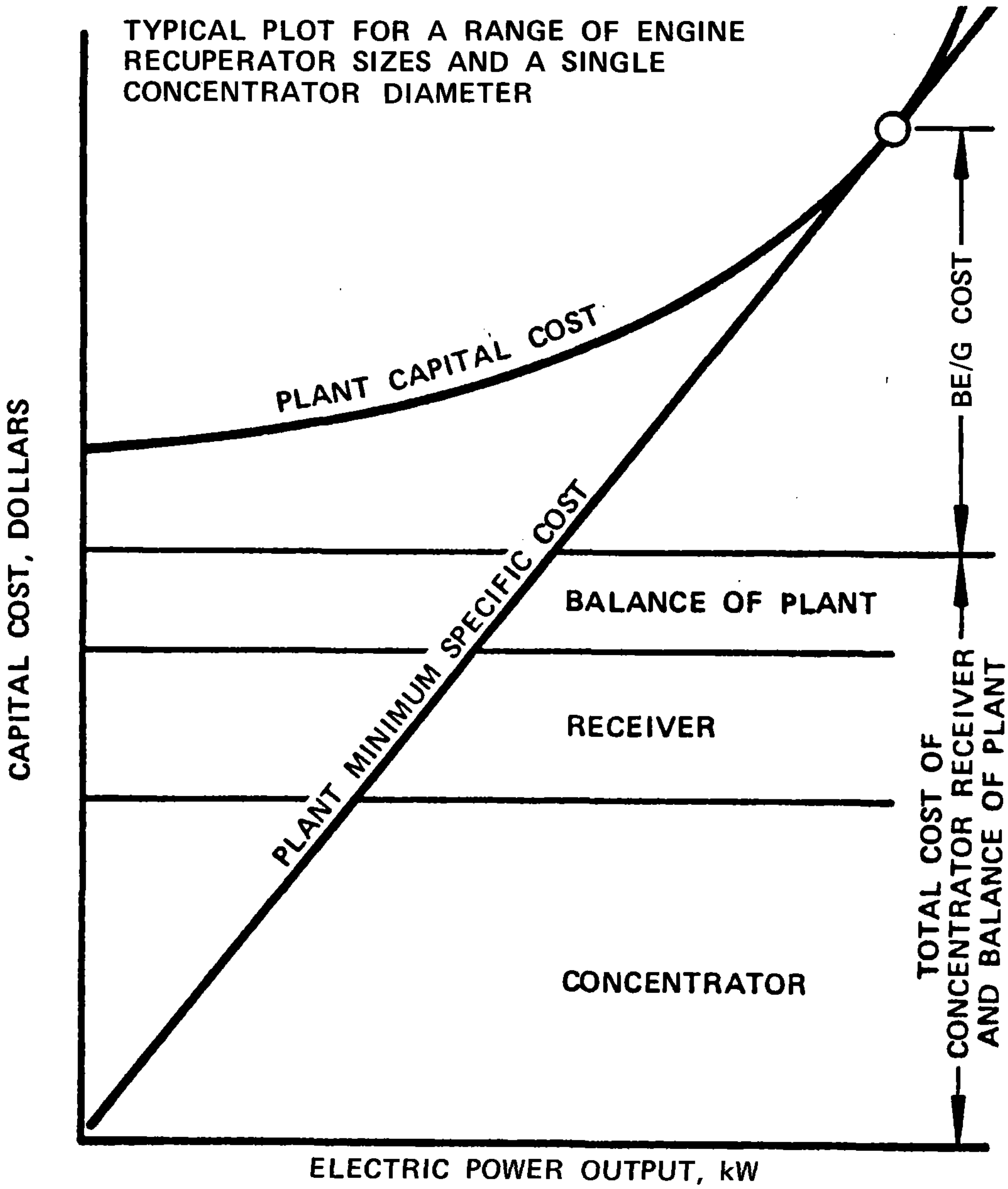

Figure 3.4 Module Cost vs Output Power

confidence in the mechanical and aerodynamic results, and with development periods easily compatible with the requirement for full scale solar testing by 1981-1982.

It was also defined that the turbine inlet temperature would be held at 1500°F, a value selected to accommodate the first-generation metallic solar receiver and the first-generation metallic recuperator, ducting and bellows.

Performance gains that might be expected from higher temperature and improved performance, along with other concepts for further increasing the cost effectiveness of the Brayton engine in mass production are discussed briefly in Section 8.4.

Allowing the compressor and turbine rotor diameter and speed to be customized or scaled to optimum values, the methodology described in Section 3.2 above was used to define design points for nine engine/generator cases. These nine cases consisted of three engine types, (ABC, CBC*, and SABC), customized for each of three parabolic concentrators (diameters 7, 9, and 11 meters).

The design point thermal input power to the engines from each concentrator size was calculated using the initial assumption listed in Table 3-II. These values are based on a NASA-provided schedule of insolation for an average year, and the premise that the engine design point should be optimized at the mean insolation intensity. For the insolation schedule provided, the mean insolation was calculated to be 0.722 kW/m^2. With this insolation, the thermal input to the engine from an 11-meter concentrator and receiver, for example, was calculated to be 45.2 kW$_t$. The calculated trend of engine cost versus output power for the ABC type engine, for example, was as shown in Figure 3-5. Each point in this figure represents a complete engine design based on one combination of the parameters displayed in Table 3-I. A curve referred to as the envelope of minimum cost, can then be drawn also as shown in Figure 3-5, which identifies the locus of minimum possible E/G costs for a given electric power output. Similar analyses were performed and plotted for the other engine types and concentrator sizes. The envelopes of minimum cost for the three engine types using an 11-meter concentrator for example, are displayed in Figure 3-6.

The minimum specific cost for the E/G alone could then be determined by constructing the tangent to the envelope of minimum cost that intersects the origin. These are the minimums indicated by the triangle symbols in Figure 3-6.

*This section also evaluates closed cycle cases to be used as a reference for comparing closed cycle engines based on existing aerodynamics.

TABLE 3-II. THERMAL INPUT POWER ASSUMPTIONS.

Parameter	Original			Revised
Collector Size, (m)	7	9	11	11
Collector Efficiency, (η_C)	0.72	0.72	0.72	0.9
Receiver Efficiency, (η_R)	0.92	0.92	0.92	0.85
Design Point Insolation, (kW/m^2)	0.722	0.722	0.722	1.00
Design Solar Input to E/G, (kW)	18.4	30.4	45.2	72.7
Rated Insolation, (kW/m^2)	0.900	0.900	0.900	1.00
Rated Solar Input to E/G, (kW)	23.1	37.8	56.4	72.7

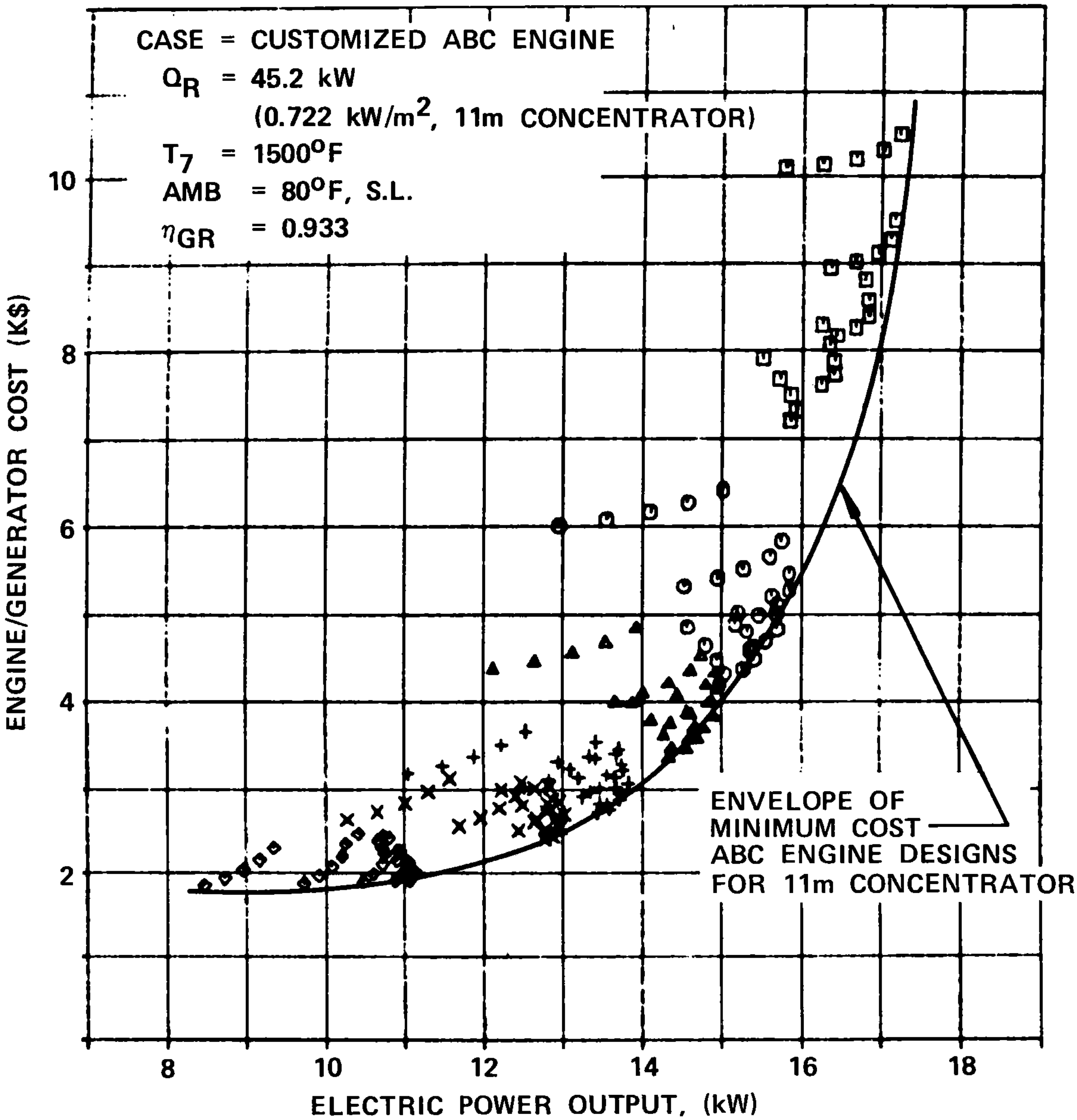

Figure 3-5. Example of Plotted Design Point Calculations for Customized Engine.

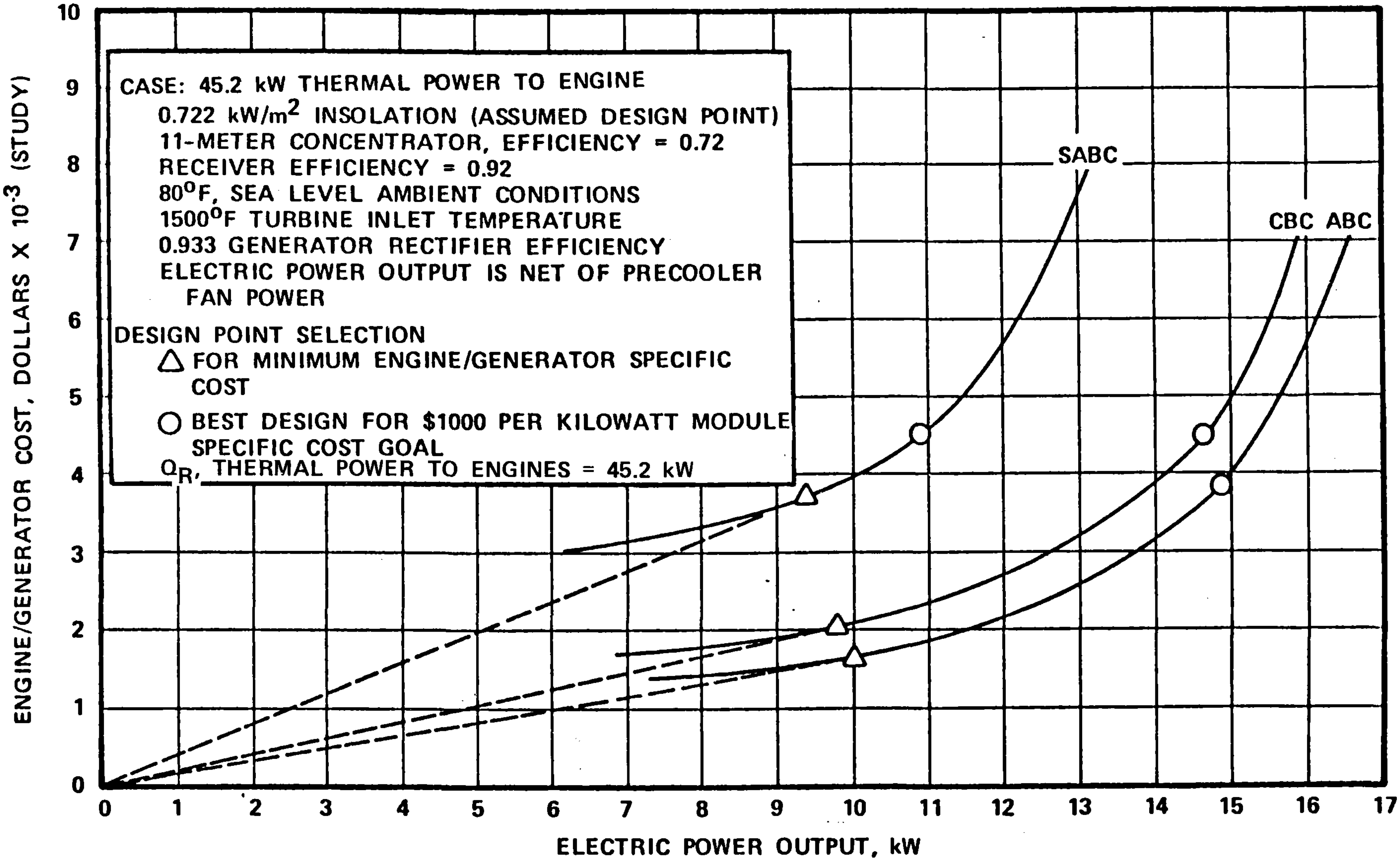

Figure 3-6. Selected Design Points for 3 Cycle Types.

For the purpose of this study however, the E/G design point that results in a minimum specific cost for the total module was to have been the basis for selecting the optimum design point, as discussed in Section 3.2 and 3.4 and depicted in Figure 3-4. Since values for the cost of the concentrator, receiver, and balance of the plant needed to establish the origin for the curve of total module cost on Figure 3-4 were not well established at the time of this analysis, a value was assumed for the total plant specific cost. This assumption, 1000 dollars/kW, fixed the slope of the straight line labeled "plant minimum specific cost" in Figure 3-4. The E/G that will result in minimum specific cost of the module is thus determined by finding the points on the curves in Figure 3-6 where the tangent to the curves has a slope of 1000 dollars/kW. These points are indicated by the circle symbols in Figure 3-6. These circles thus define the selected E/G design points for the three engine types customized for an 11-meter concentrator with 0.722 kW/m^2 insolation.

This type of analysis was repeated for each of 3 concentrator diameters to establish design points for customized engines over a range of power ratings. Table B-1 in Appendix B presents a tabulation of customized engine design points selected for the three cycle types and for each of the power levels corresponding to each of the 7-, 9-, and 11-meter diameter concentrators.

Evaluation of the above results especially those depicted in Figure 3-6, led to the conclusion that, for the first generation open cycle engine requirement the atmospheric type (ABC) engine is superior to the subatmospheric type (SABC). This conclusion would require review if some unique or unusual requirement were to impact the engine design, such as an input that a major cost benefit might accrue from the use of an engine type whose loop high pressure was exactly atmospheric, thus permitting use of a lower cost reciever. For the purposes of this study, however, no further consideration of subatmospheric engines was considered fruitful.

While the study was in progress, technical direction was received from NASA changing the design point thermal input energy, Q_E, from the original values shown in Table 3-II to 72.7 kW_t for the 11-meter concentrator. Performance characteristics for this engine are described in detail in Section 4.3.

3.4 Existing Turbocompressors for Configurations A and B

To meet the requirement for full scale solar testing by 1980, first-generation near-term Configuration A (open cycle) and B (closed cycle) were to make maximum use of existing hardware, modified as required since this 1980 test schedule would allow considerably less development work than for Configuration C.

The existing AiResearch engines (or turbocompressors) considered as candidates for the near-term Configurations A and B, with appropriate characteristics are shown in Table 3-III. Each of these engines was classified according to its suitability for operation with various modes of solar heat input including hybrid operation and the results listed in Table 3-IV. As shown, only the AGA and PFE turbocompressors were recommended for further evaluation for use with the original design point thermal input power fuels (up to 45.2 kW_t) and the GTP36-51 for the revised design point power level (72.7 kW_t). Figures 3-7, 3-8, and 3-9 are cross-sectional drawings of these candidate engines.

Applicability of these existing engines or turbocompressors was parametrically evaluated for a range of the open cycle (A) and closed cycle (B) E/G systems design variables on the basis of performance and cost. For example, Figure 3-10 shows the cost plot for the PFE turbocompressor evaluated over a range of closed cycle (CBC) engine design variables. This analysis was similar to the analysis described in Section 3.3 except that the compressor and turbine hardware were fixed and only the recuperation, cooling, pressure drop, N_T, etc. were allowed to vary. This type of evaluation resulted in selecting design points for each power level for the AGA and PFE turbocompressors as shown in Section 4.2 and Tables B-II and B-III in Appendix B, and for the GTP36-51 in Section 4.1.

Results of this analysis for the open cycle Brayton engine plotted in Figure 3-11, shows that at the lower power inputs to the engine and depending on the input power, the AGA, PFE or GTP36-51 would all be suitable, the AGA engine best fitting the range. For the higher input power (72.7 kW_t), only the GTP36-51 turbocompressor is suitable. This engine is a modern state-of-the-art engine developed for the U.S. Army as a 30 kW_e generator set. Although this engine has not yet been produced in quantity, it is designed for high-volume, low-cost production through the use of simple elements and rugged cast components wherever possible.

Figure 3-12 shows a comparison of the closed cycle engine candidates. The PFE turbocompressor produces higher performance.

On the basis of these comparisons, the GTP36-51 was selected for the first-generation near-term open cycle engine Configuration A. The PFE was selected for the closed cycle engine Configuration B. Detailed performance characteristics of these engine/generators are described in Chapter 4.

3.5 Part Power Characteristics

Part power characteristics for the various engine types were evaluated. The ABC and SABC types can vary either rotor speed or turbine inlet temperature to accommodate power changes, while the CBC type normally relies on changing inventory to vary system pressure level for power level control.

TABLE 3-III. EXISTING ENGINE HARDWARE.

Identifying Application	AGA	BRU	CCPS40	PFE	JFS100	T048	GTP36-51
Hours Operation	60 Dev	32,000 Endurance	300 Dev	40 Dev	Production	Production	336 Dev
Rating, kW	9.5	6.0	30	10.8	95		30
Cycle Flow, Actual, lb/sec Flow, Corrected, lb/sec Working Fluid Turbine Inlet Temp, T_2, °F Control Variable[3] Cycle Type	 0.267 0.732 Air 1500 T_7 SABC	 0.798 0.840 XeHe 1600 P_1 CBC	 1.510 0.584 Argon 1500 P_1 CBC	 0.655 0.409 Air 1500 P_1 CBC	 1.7 -- Air 1760 T_7, N_{PT} ABC	 -- -- Air[1] 1350 T_7, N_{GG} Turbo-charger	 1.03 0.950 Air[1] 1675 T_7 ABC
Combustor Type/Fuel	Internal Combustor Nat. Gas	External Electric Heater	External Electric Heater w/diesel	External Radiant Burner	Internal Annular JP-4 etc.	IC or Diesel Engine	Internal Can JP-4 etc.
Rotor Number Speed, rpm Compressor dia., inches Cold End Bearing Hot End Bearing Arrangement[2] Power Output Method	 88,800 3.85 Foil (3) SBBCT Magnetic Coupling to Freon Pump	 36,000 4.25 Pad Pad CBABT Integral Electrical	 52,000 4.25 Foil Foil SBCBT Carbon Seal & Quill & Gearbox to 8000 rpm	 60,000 4.25 Oil/ Journal Foil SBCBT Buffered Labyrinth Quill & Gearbox to 1200 rpm	 72,500 4.47 Ball Ball Two Rotors Integral Free Turbine Driven Gearbox to rpm	 116,000 2.76 Oil/Journal Oil/Journal CSBBST No Provision	 80,000 4.86 Ball (3) BBSCT Integral Gearbox to 3000/3600 rpm
Electro-Mechanical Equipment		Integral Wound Field Alternator 1200 Hz					

(1) Plus combustion products

(2) S-Seal, B-Bearing, C-Compressor, T-Turbine, A-Alternator

(3) Cantilever Configuration with two cold bearings

TABLE 3-IV. SCREENING OF EXISTING TURBOCOMPRESSOR HARDWARE

	AGA	BRU	CCPS40	PFE	T04B	GTCP36-51
Ready Adaptability to Various Cycle Types						
Pure Solar Applications						
Open Cycle w/Closed Receiver	ABC SABC			ABC SABC	ABC	ABC
Open Cycle w/Vented Receiver	SABC			SABC		
Closed Cycle	CBC	CBC	CBC	CBC		
Externally Fired Hybrid Applications (Parallel Receiver Only)						
Open Cycle W/Closed Receiver	ABC SABC			ABC SABC	ABC	ABC
Open Cycle w/Vented Receiver	SABC			SABC		
Closed Cycle	CBC	CBC	CBC	CBC		
Internally Fired Hybrid Applications (Either Parallel or Series Receiver)						
Open Cycle w/Closed Receiver	ABC SABC			ABC SABC	ABC	ABC
Minimal Bearing and Rotor Dynamics Modifications	X		X	X		
Minimum Mechanical Output Mods	X	X	X	X		
Some Production Study Background Available	X			X	X	X
Adaptability to 1980 Objectives	X	X	X	X	X	X
Recommended for Continued Study as Applied to Original Power Level	X			X		
Recommended for Revised Power Level						X

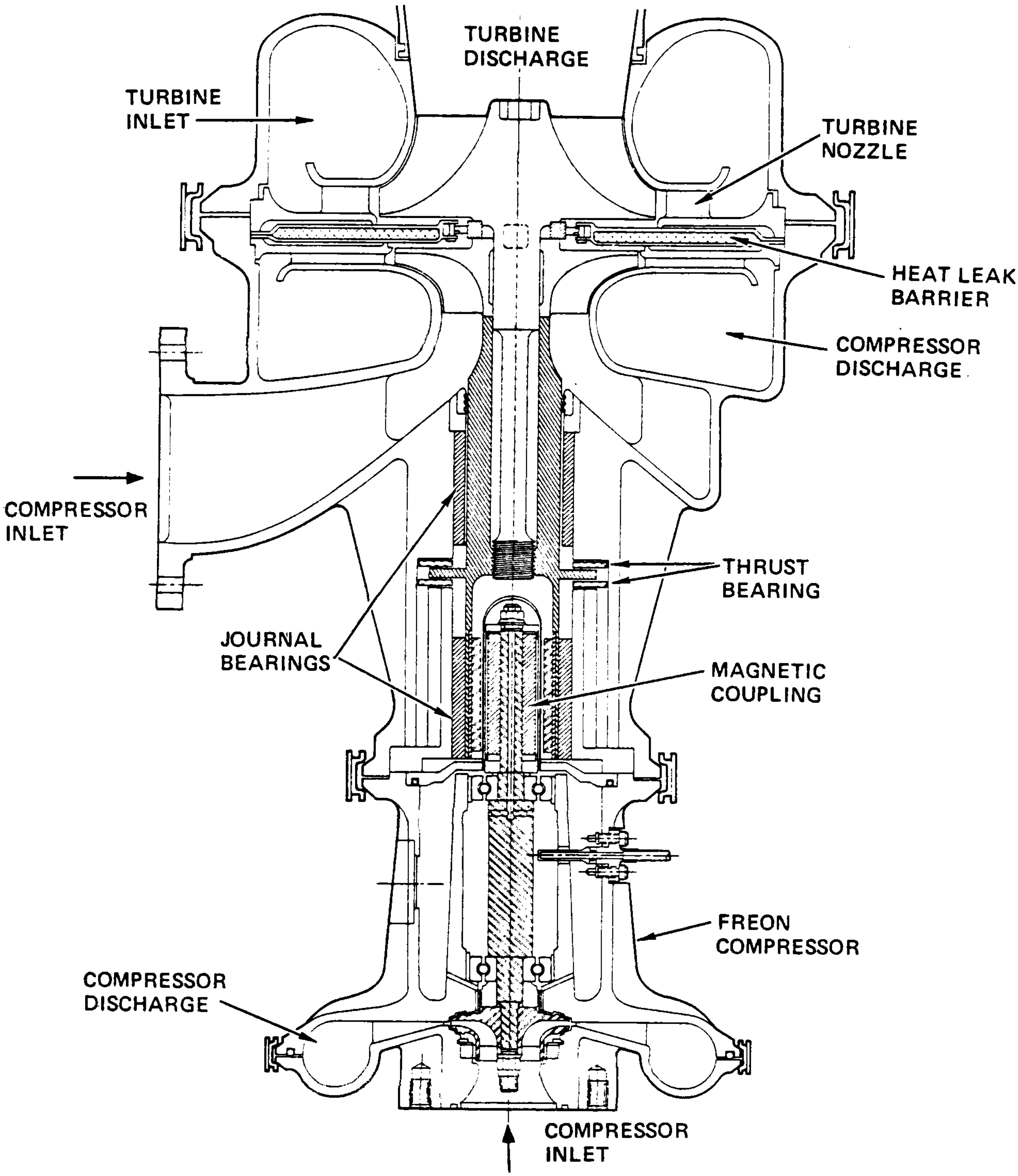

Figure 3-7. AGA 10-Ton Rotating Group Cross-Section.

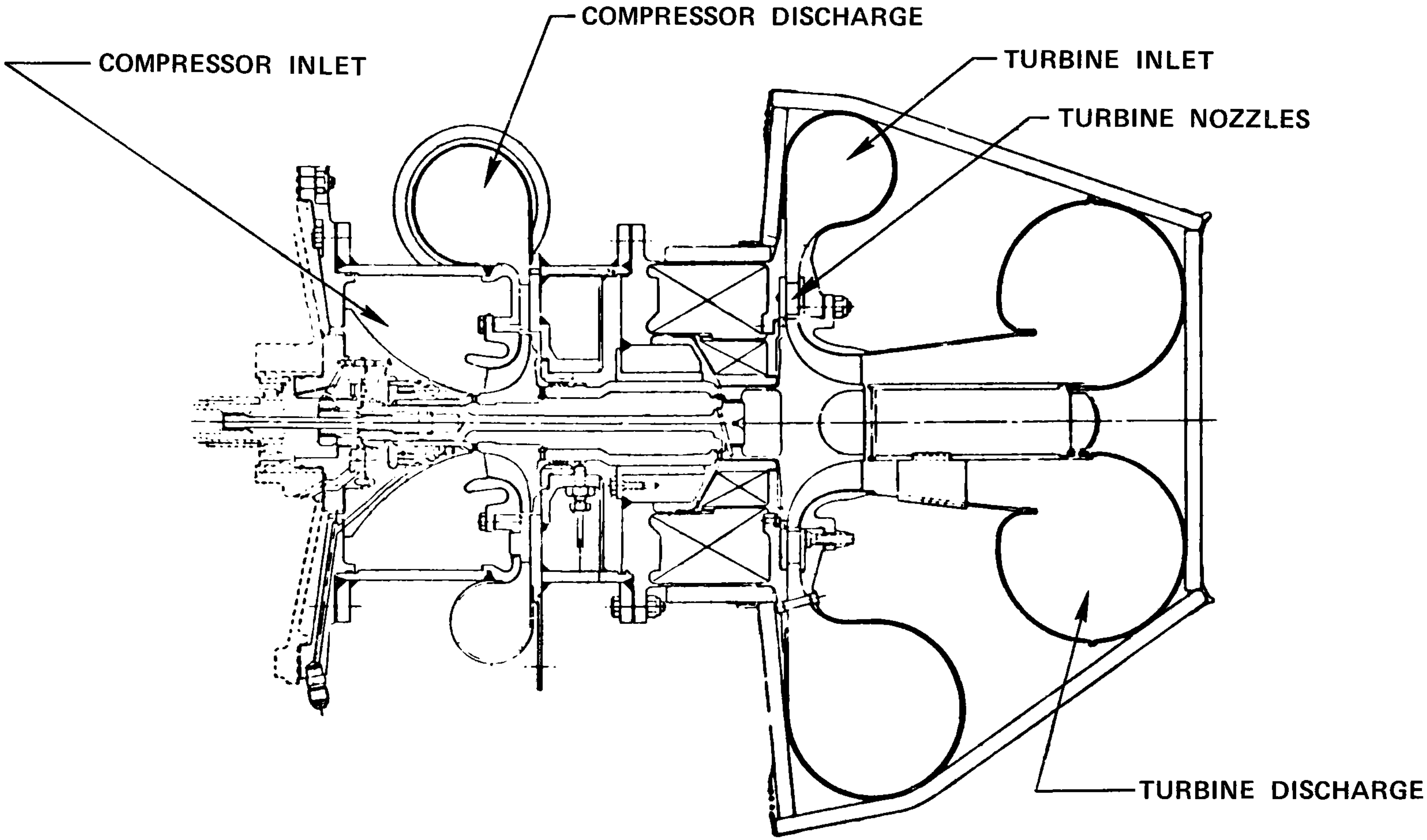

Figure 3-8. PFE Engine Cross-Section.

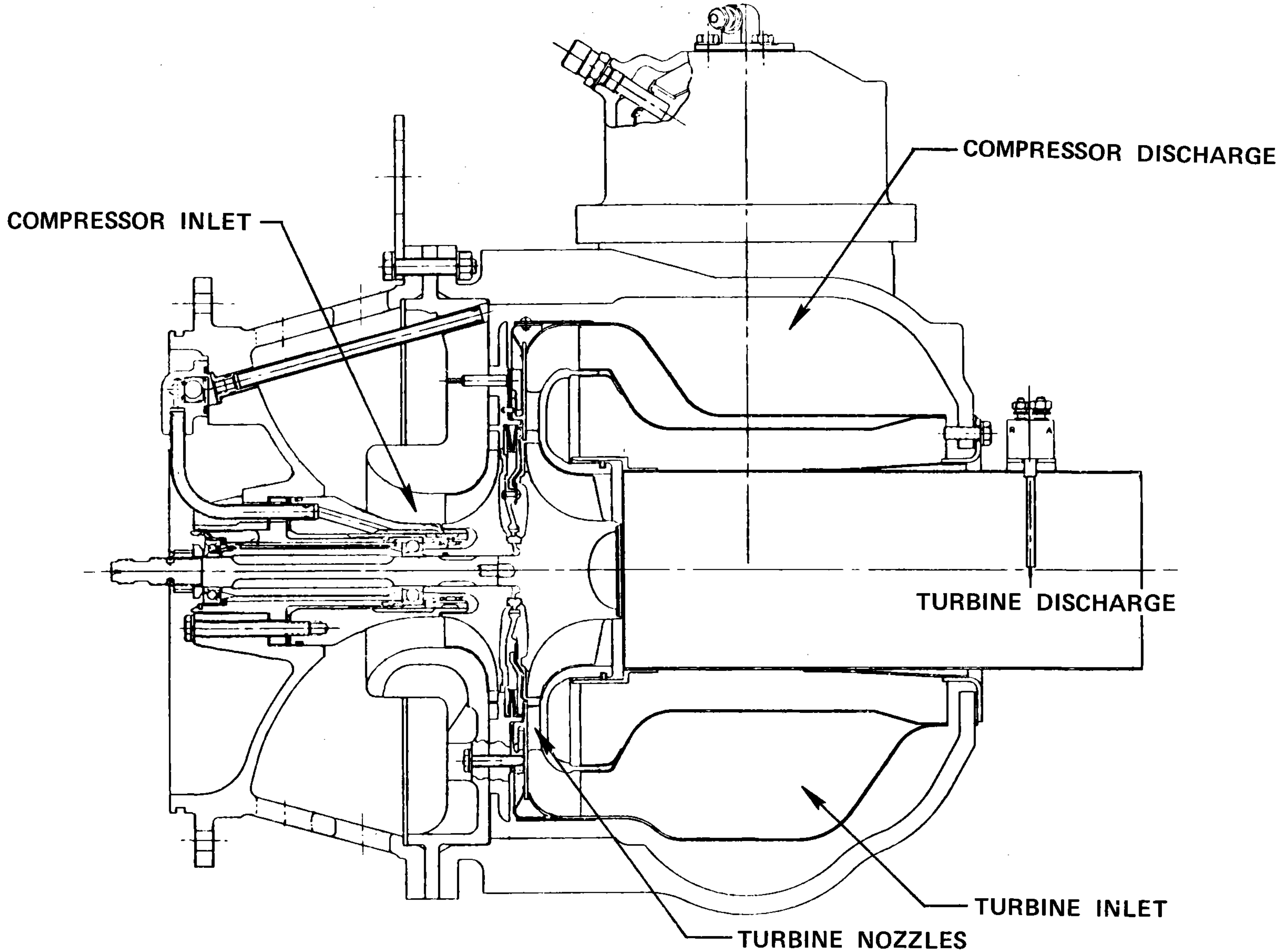

Figure 3-9. GTP36-51 Cross-Section.

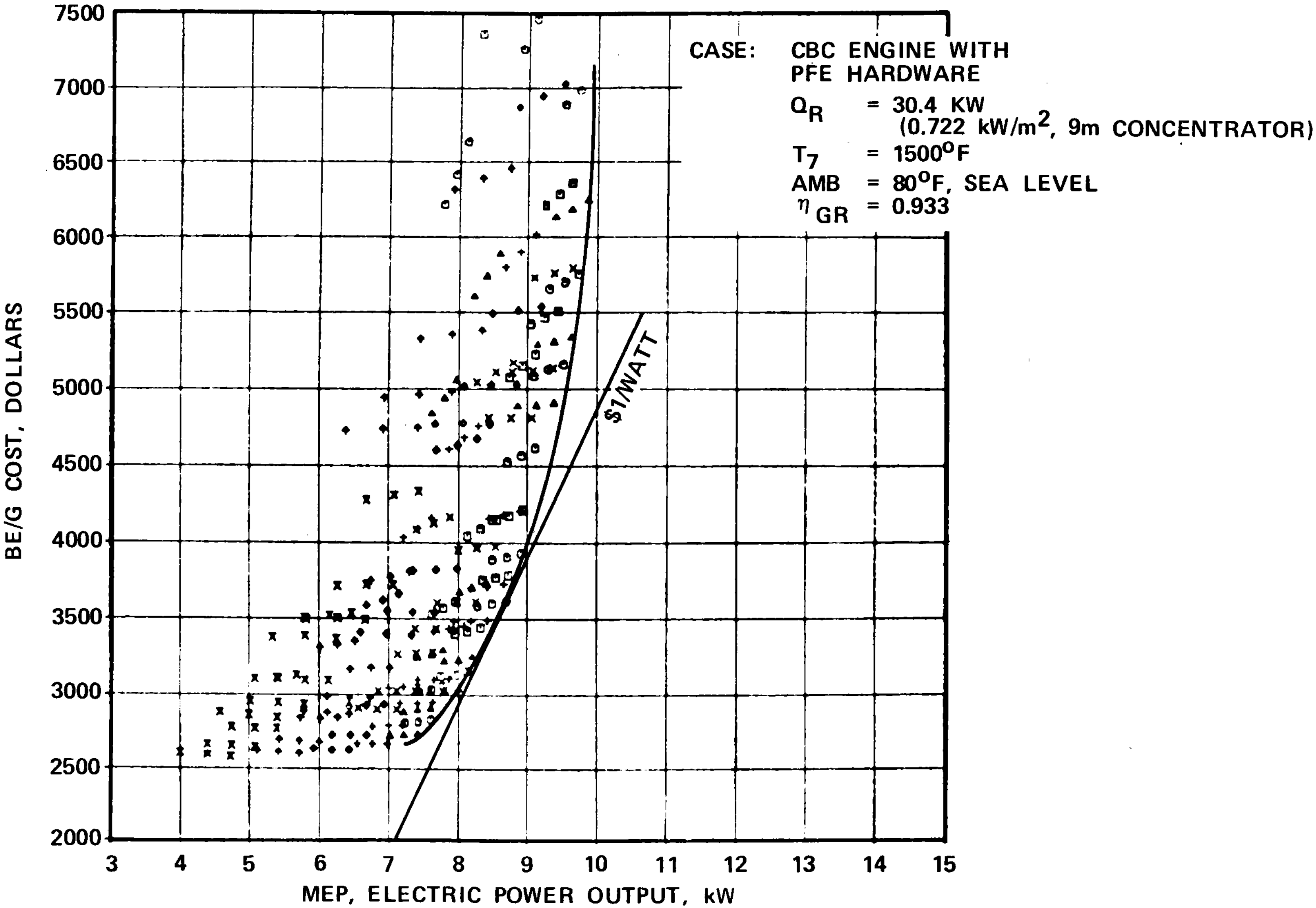

Figure 3-10. Example of Plotted Design Point Calculations for an Engine Based on Existing Turbocompressor Hardware.

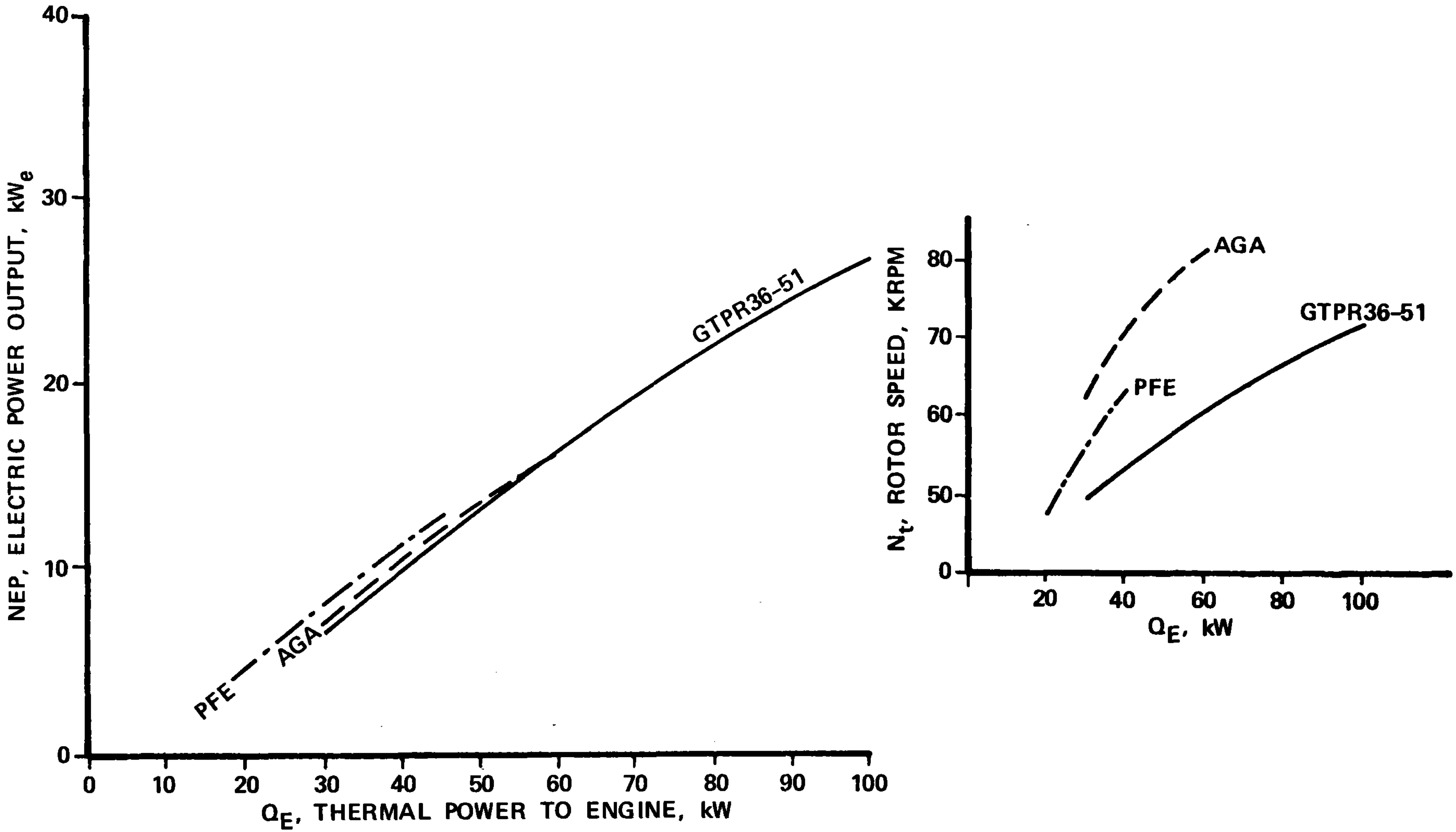

Figure 3-11. Suitability of Existing Hardware for ABC Engine.

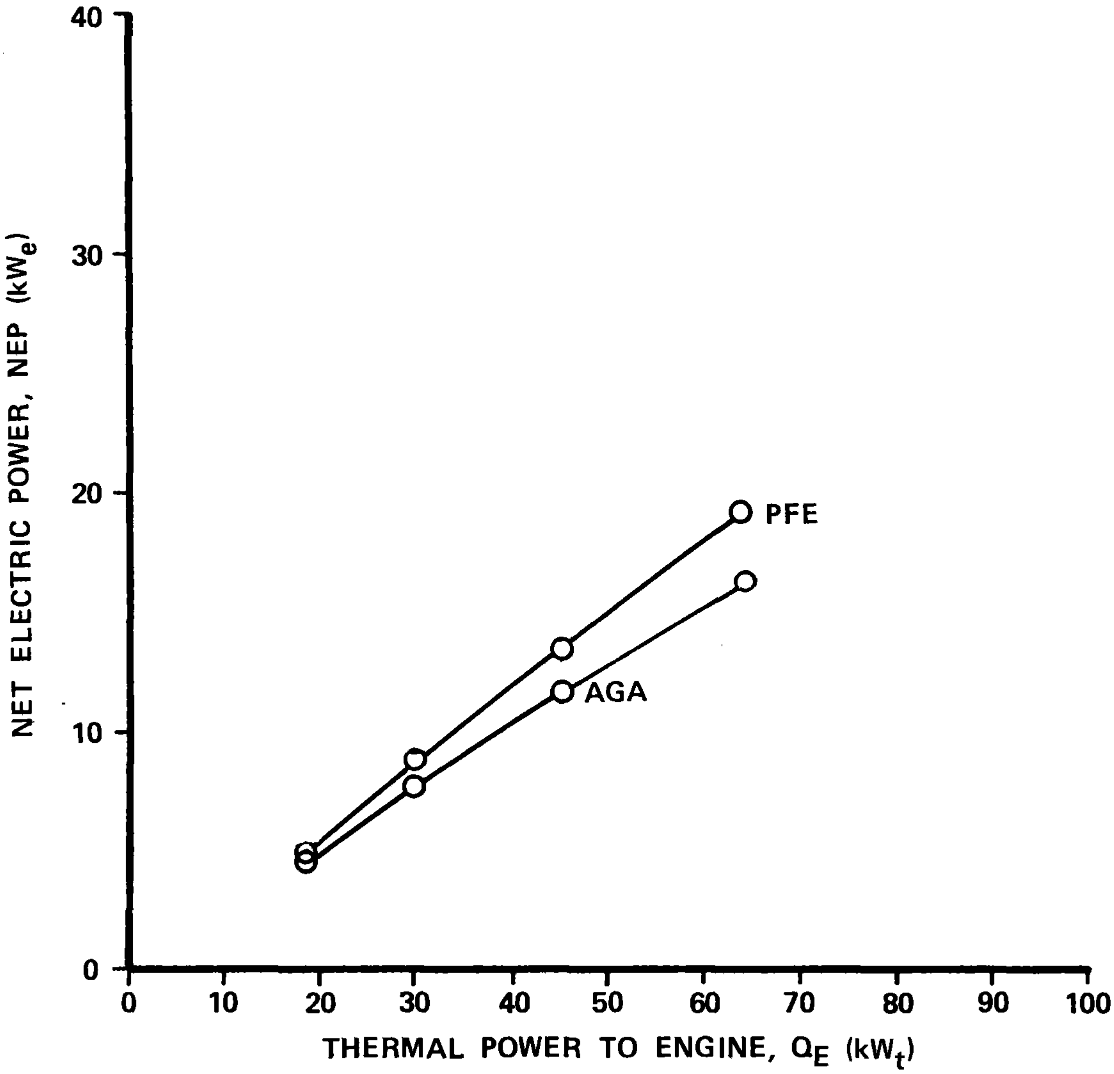

Figure 3-12. Suitability of Existing Hardware for CBC Engines.

Figure 3-13 shows the part power performance of the open cycle ABC with both constant speed and constant turbine inlet temperature (T_7) control modes. It can be seen that higher part power efficiency for this engine type will be attained with a variable speed-constant T_7 system than with a variable T_7 constant N_t control mode. (Even though it is an open cycle, the subatmospheric Brayton cycle SABC was found to suffer a significant decrease in efficiency at part power levels with either control mode.) The constant turbine inlet temperature, variable rotor speed control mode for part load was selected for the open cycle engines as being in keeping with the objective for maximizing engine performance over a wide range of operating conditions.

3.6 Generator Selection, Power Conditioning and Management

3.6.1 Generator Selection

A tradeoff study of generators in the 20 kW size was undertaken to determine the optimum generator for the application described in this report. The main concerns were weight, cost, and reliability. Table 3-V shows a comparison of generator types versus weight, efficiency and size. The table also summarizes the main advantages and disadvantages of each. Both generator efficiency and efficiency defined as busbar electric power (NEP) divided by engine shaft power (CSP) are listed in Table 3-V. The latter efficiency includes the gearbox efficiency, if a gearbox is required, and the power conditioning equipment, if required. The 60 Hz synchronous, 60 Hz induction, 400 Hz and DC generators require speed reduction gearboxes. The assumed gearbox efficiency is 98 percent. The permanent magnet, Rice-wound field and 400 Hz generators also require power conditioning systems consisting of a rectifier and an inverter. The assumed rectifier and inverter efficiencies are 96 and 94 percent respectively. The DC generator requires an inverter with assumed efficiency of 94 percent.

Further consideration of synchronous, induction and DC generators was dropped because of weight and electrical system constraints. The field-modulated alternator (FMA) is in the initial stages of development(1) and, therefore, it was not considered appropriate for the first-generation engine/generators. In addition, the output of the FMA is single phase, so that three FMAs must be driven by one engine and phased 120° apart or several FMAs must be summed together into a set and the sets fixed at different phases. For these reasons, the FMA was eliminated from further consideration. The PMG and Rice generators are smaller, lighter, and more efficient than the 400 Hz generator, but use of the 400 Hz generator was judged most appropriate for the near-term 1980 time period.

Thus, for near-term demonstrator Engines A or B, the 400 Hz generator was selected. The permanent magnet generator (PMG) is more efficient, lighter and requires no gearbox. It is therefore a

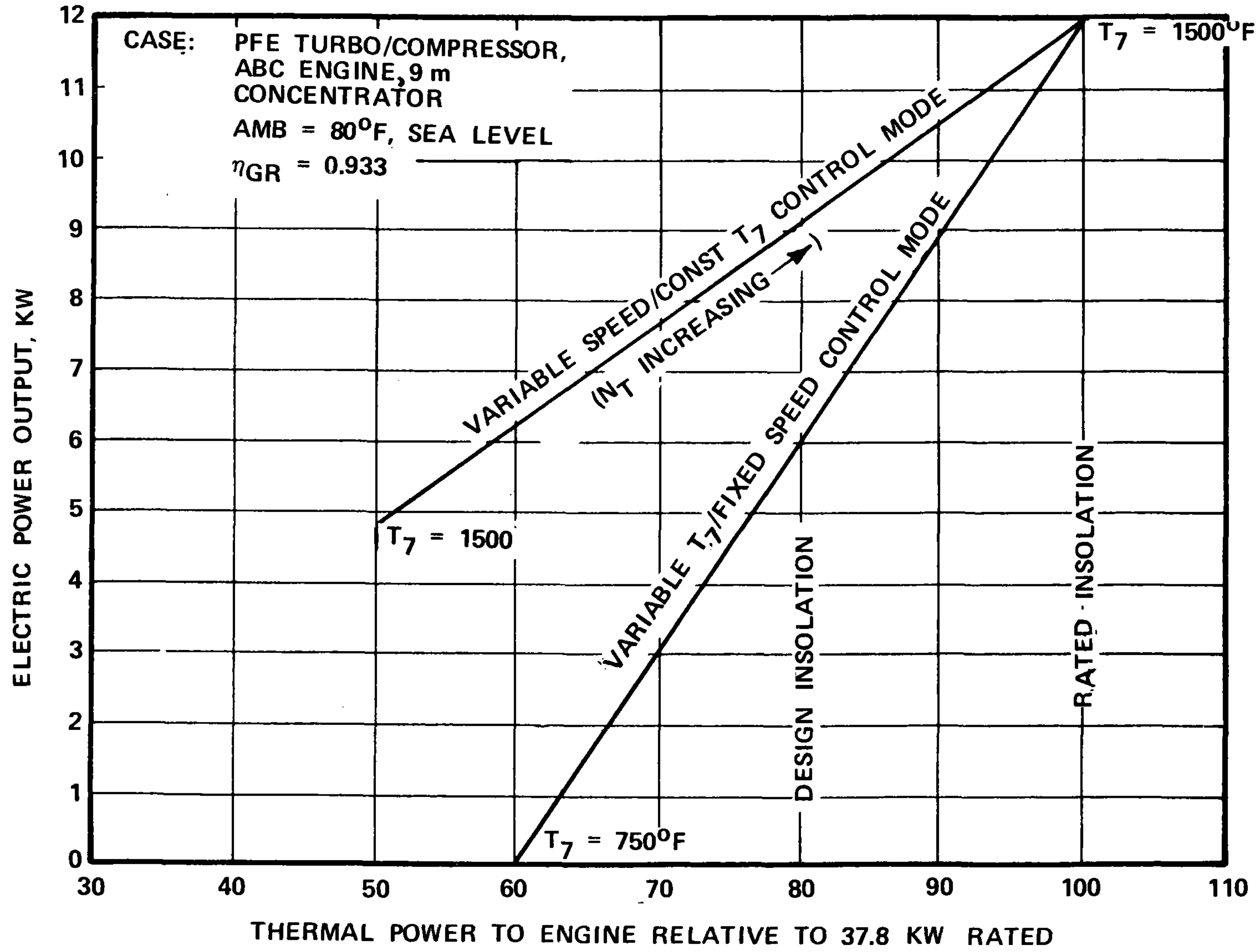

Figure 3-13. Part Power Performance Comparison of a PFE/ABC Engine

TABLE 3-V. COMPARISON OF GENERATORS.

Generator Types	Weight LB	Efficiency	Size Generator	Advantages	Disadvantages
60 Hz synchronous + gearbox (3600 rpm)	370/65	0.90/0.88	16 in. diameter 22 in. long	Reliable, moderate cost, experience, can use as starter motor	Heavy, difficult to synchronize, can absorb power (motor)
Permanent magnet generator	10	0.94/0.85	4.8 in. diameter 5.61 in. long	Direct drive, lightweight, can use as starter motor	Limited experience
DC generator and gearbox	370/65	0.78/0.81	16 in. diameter 24 in. long	Reliability, can use as starter motor	Heavy, voltage required beyond present experience
Field modulated	70	0.93/0.93	9.75 in. diameter 7.75 in. long	Direct drive, lightweight, easy to synchronize and control	No experience, single phase output, high cost can't use as starter
60 Hz induction and gearbox	390/65	0.92/0.90	16 in. diameter 29 in. long	Reliable, commercially available, moderate cost, experience, can use as starter motor	Heavy, not applicable to stand-alone operation
400 Hz generator and gearbox (380-420 Hz) 7600-8400 rpm)	50/65	0.91/0.81	6.5 in. diameter 13.75 in. long	Moderate weight, reliable, experience	Difficult to synchronize
Rice wound field	40	0.92/0.83	7 in. diameter 15 in. long	Direct drive, lightweight easy to synchronize and control, can use as starter motor	Limited experience,
	Generator/ gearbox	Generator/ NEP/CSP			

strongly favored candidate for the first-generation Configuration C engine and even the A and B engines if sufficient development time could be programmed into the schedule. (A cross-section of the PMG is shown in Figures 5-11 and 12 in Chapter 5.)

The performance and characteristics of the PMG and 400 Hz generators were investigated so the power conditioning requirements could be determined, and are shown in Figures 3-14 and 3-15 respectively. The 400 Hz generator output voltage is maintained constant by a voltage regulator as the speed varies (Figure 3-14). The efficiency of this generator increases slowly with increasing speed.

As shown in Figure 3-15, the PMG output voltage is linearly proportional to input speed, therefore voltage regulation must be included in the power conditioning electronics. It can also be seen that the PMG efficiency increases slowly with speed and then levels off.

3.6.2 Power Conditioning and Parallel Operation

Possible power conditioning schemes for the 400 Hz, permanent magnet, and 60 Hz induction generators are shown in Figure 3-16. For the 400 Hz and PMG systems, the rectifier converts the AC output of the generator to DC, which is tied to a DC link bus. This DC voltage is converted to three phase, 60 Hz AC by the inverter.

The inverter would utilize transistors fired by the timing of an integral 60 Hz crystal oscillator to set the 60 Hz frequency. During grid operation, the inverter is line-commutated. During stand-alone operation, the 60 Hz frequency is set by the oscillator.

The PMG would require a more complicated rectifier and inverter system than the 400 Hz generator since the output voltage of the PMG is proportional to speed. Constant AC line voltage must be maintained by the rectifier and inverter for this generator.

For parallel operation of the 400 Hz and PMG, it is envisioned that a number of 20 kW engine/generator modules will be summed into a DC bus of 200 volts or more and converted to 60 Hz by one large inverter also as shown in Figure 3-16. Other constraints have been placed on the generator and rectifier since they are used as integral parts of the engine control system described in Section 6.1. The control philosophy requires that the generator and electrical system absorb all power delivered by the engine as it in turn absorbs all heat energy produced by the solar receiver. If the power delivered cannot be beneficially used, or if it persists for a time longer than the buffer storage is capable of accommodating, the excess energy would be dissipated in an energy load bank. If the user requirement is for more power than the maximum rating of the modules, the buffer storage batteries can supply energy to the system for short periods of time. In addition, the buffer storage batteries eliminate voltage transients due to engine/generator control fluctuations.

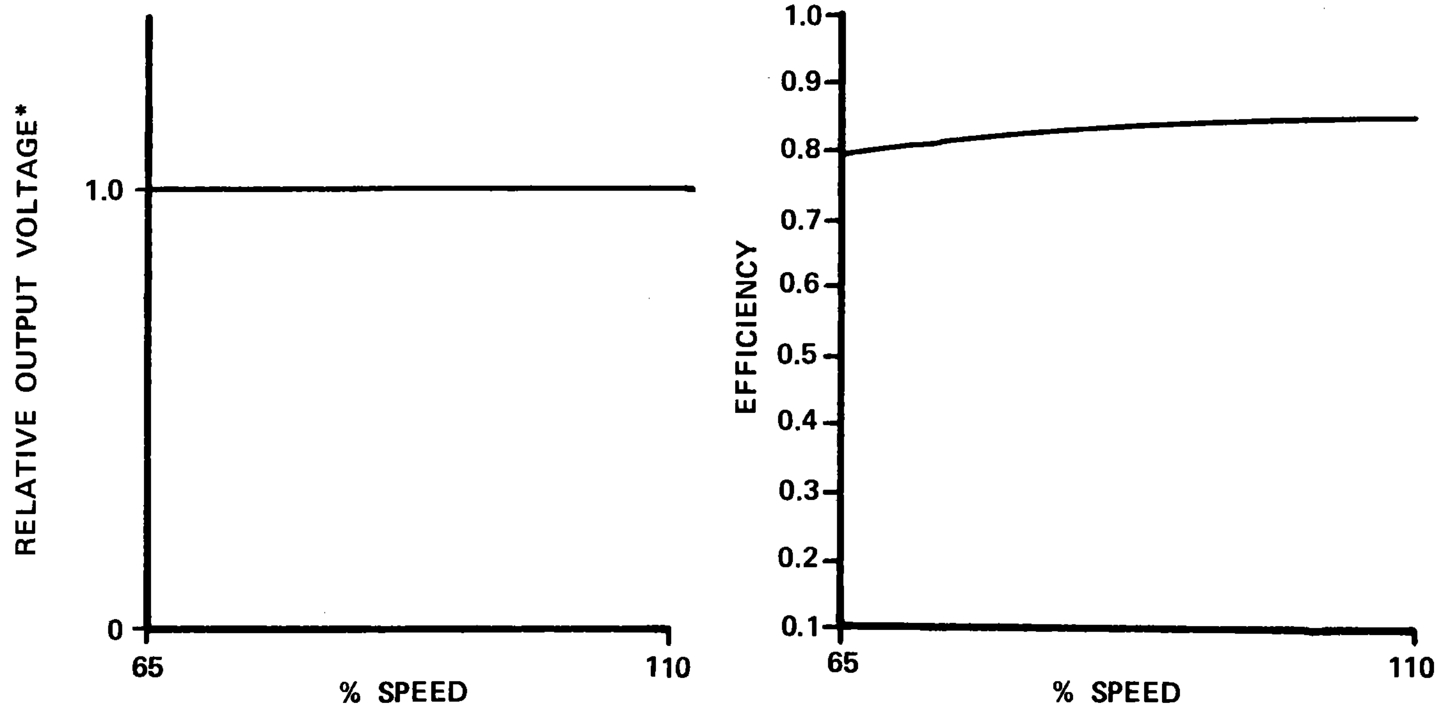

*VOLTAGE REGULATOR WILL MAINTAIN CONSTANT OUTPUT VOLTAGE OVER THE DESIGN RANGE.

Figure 3-14. Performance of 400 Hz Generator.

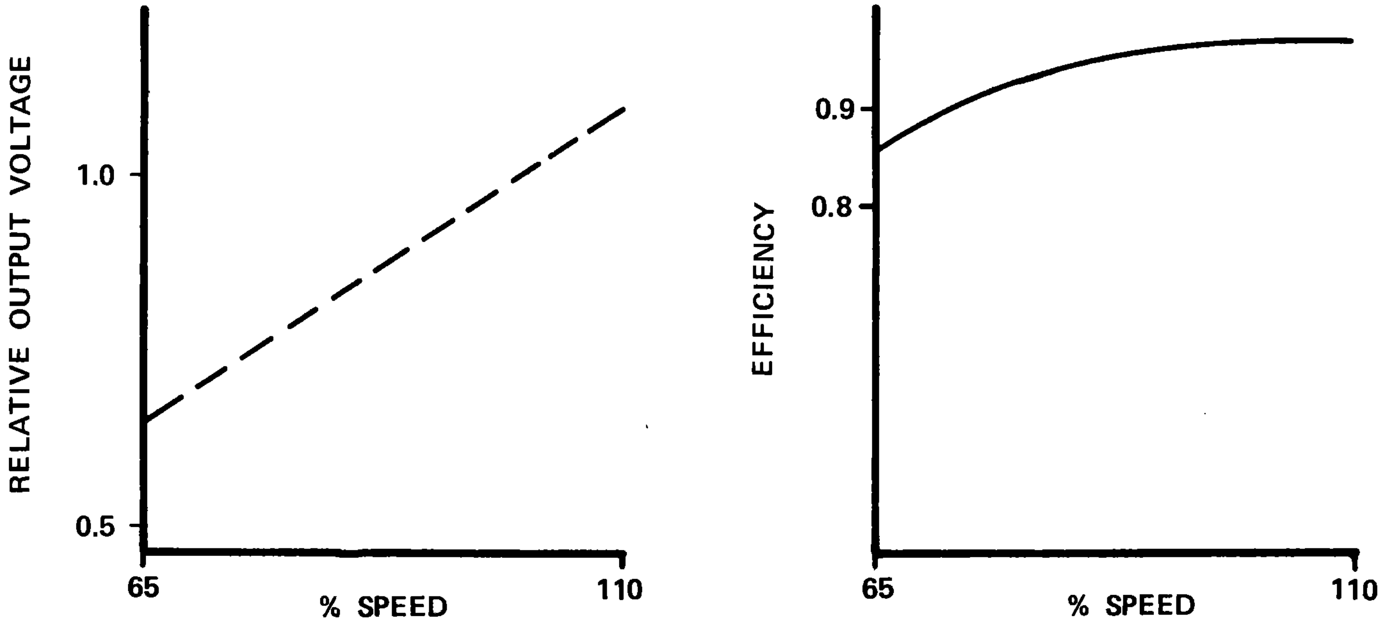

Figure 3-15. Performance of Permanent Magnet Generator.

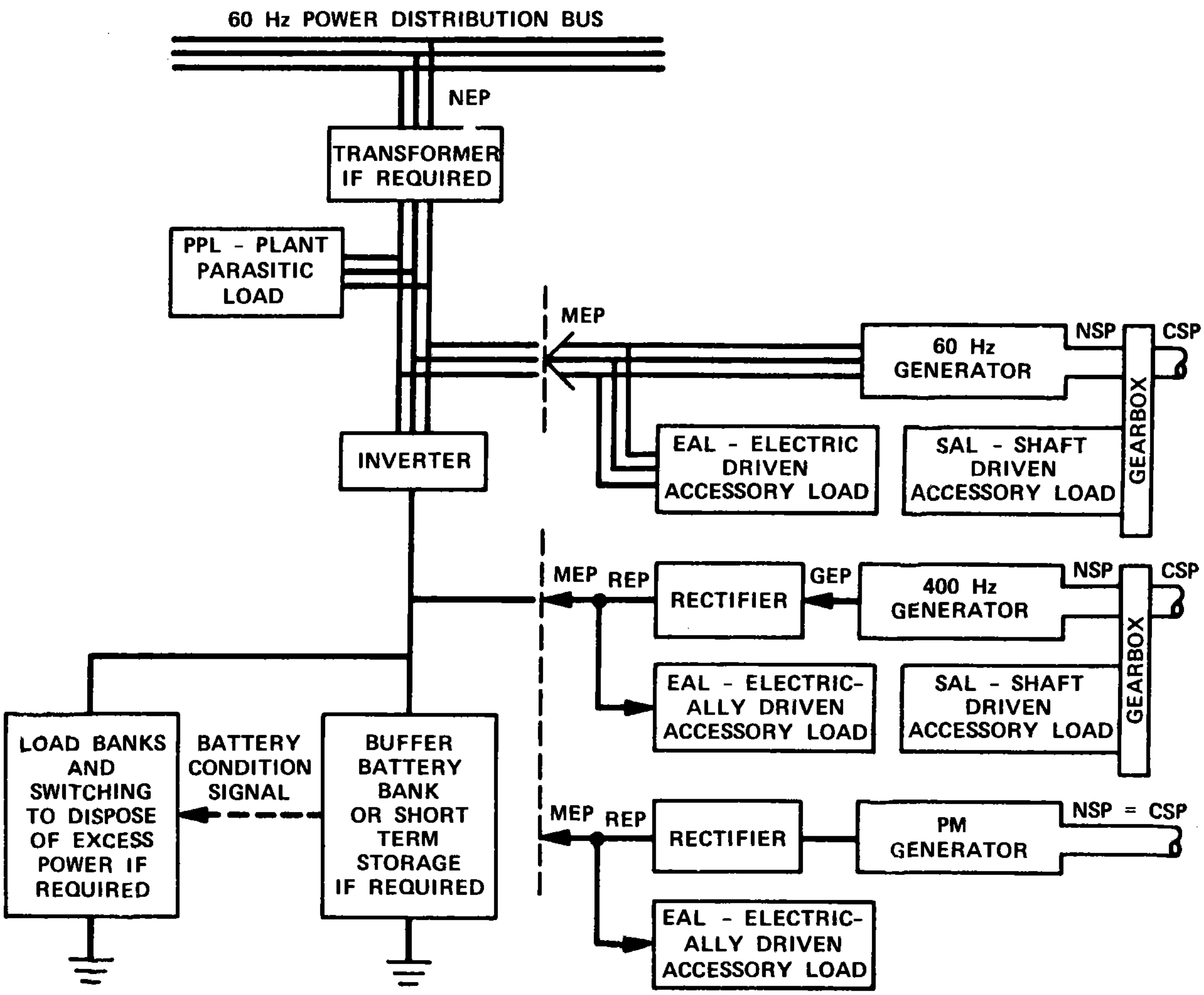

Figure 3-16. Generator and Power Conditioning System Diagram.

No rectifier or inverter would be required for the 60 Hz induction generator shown in Figure 3-16. A stiff 60 Hz bus powered by other sources would be relied on for controlling the speed of these induction generator modules.

4.0 PERFORMANCE OF ENGINE/GENERATORS FOR 72.7 kW_t

4.1 Configuration A

The Configuration A engine selected for the 72.7 kW_t thermal power design requirement consists of a GTP36-51 type turbocompressor and a 269 lb recuperator with a nominal effectiveness (E_r) equal to 0.92. The off-design and part load performance characteristics are plotted in Figures 4-1 and 4-2, and tabulated in Tables 4-I and 4-II. The data in these tables is given in terms of the cycle shaft power (CSP), cycle efficiency, η_{CSP}, recuperator effectiveness (E_r), compressor pressure ratio, (r_c), turbine pressure ratio (r_t), engine mass flow (M_1), and speed (N_t). Cycle efficiency η_{CSP} is the ratio of CSP to the thermal input power to the engine (Q_E). Also given is the mass flow (M) and inlet and outlet temperatures (T), and pressures (P) of the receiver and recuperator. Cycle station locations are shown in Figure 3-1. A complete list of symbols is provided in Appendix A.

Figure 4-1 shows sea level shaft output power plotted as a function of heat input to the cycle, Q_E, and compressor inlet temperature (T_1). Figure 4-2 shows similar data for 5000 feet above sea level.

Table 4-I shows estimated engine performance at design solar insolation of 1 kW/m^2 and corresponding thermal input (Q_E), of 72.7 kW_t. The data is portrayed for sea level and 5000 ft elevation with ambient air temperature from 10°F to 140°F. These data show that the system would produce 22.9 kW_m of mechanical shaft power (CSP) on an 80°F day with a cycle efficiency η_{CSP} of 31.5 percent.

Table 4-2 shows similar data for the case of a typical low solar insolation of 0.4 kW/m^2 and corresponding thermal input, Q_E, of 30 kW_t. Here the system would produce 8.1 kW_m at 80°F ambient temperature with a cycle efficiency of 27.1 percent.

The electric power appearing at the 60 Hz AC busbar will be less than the mechanical shaft power due to inefficiencies and losses in the generator and power conditioning system. A 400 Hz generator was selected for Engine A. This generator requires an AC-DC-AC power conditioning system as shown in Figure 3-16. This system consists of a rectifier and inverter. The following is an estimate of the net electric power (NEP) appearing at the AC busbar for sea level, 80°F ambient temperature operation with thermal input power Q_E of 72.7 kW_t.

Cycle Shaft Power, CSP*		22.9 kW_m
Gearbox Efficiency, 0.98	0.456 ΔkW	
Shaft Accessory Load, SAL	0.073 ΔkW	
Generator Efficiency, 0.91	2.01 ΔkW	
Rectifier Efficiency, 0.96	0.813 ΔkW	
Electric Accessory Load, EAL	0.428 ΔkW	

*Refer to Figure 3-16 for location.

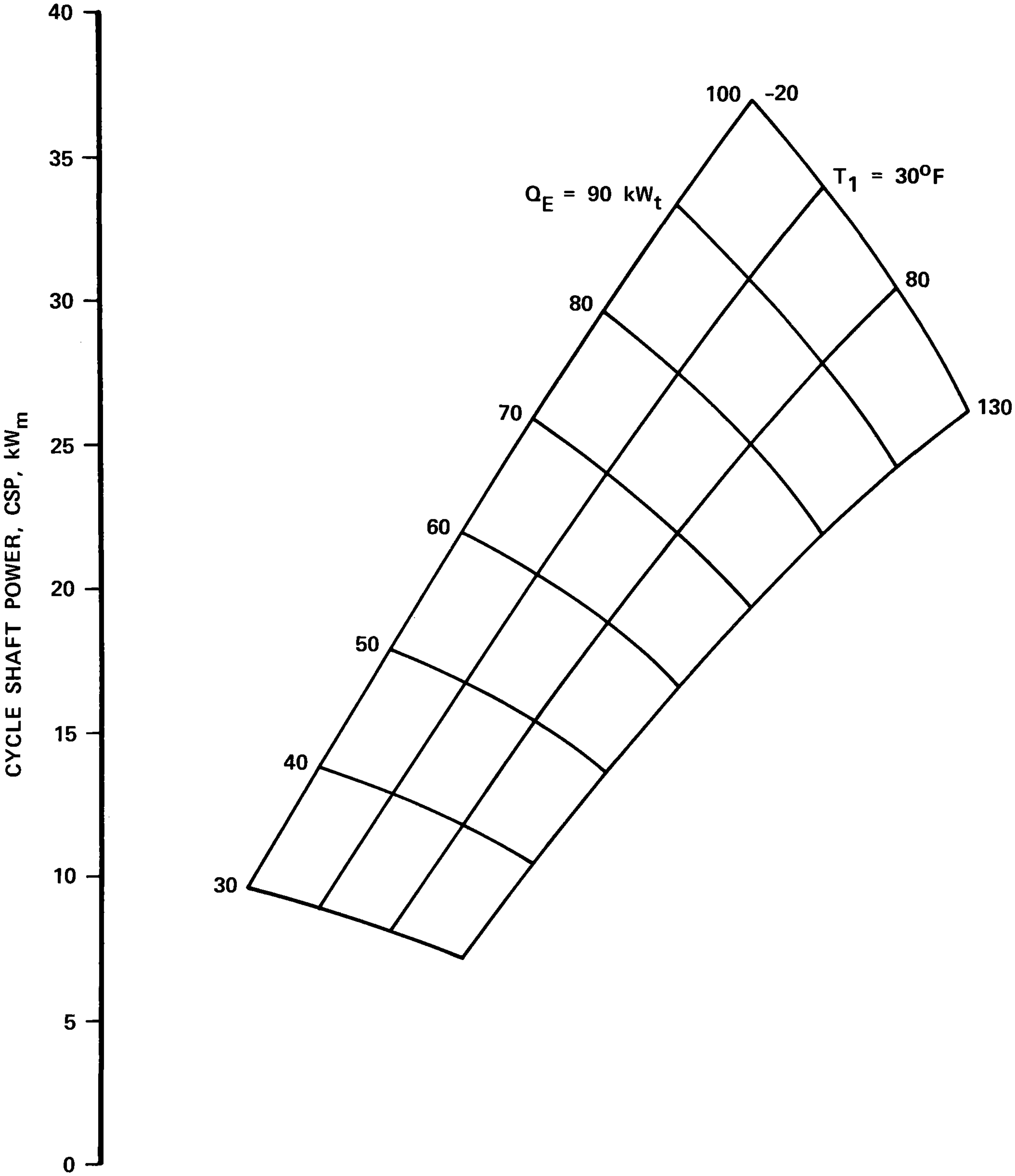

Figure 4-1. Engine A Performance at Sea Level Altitude.

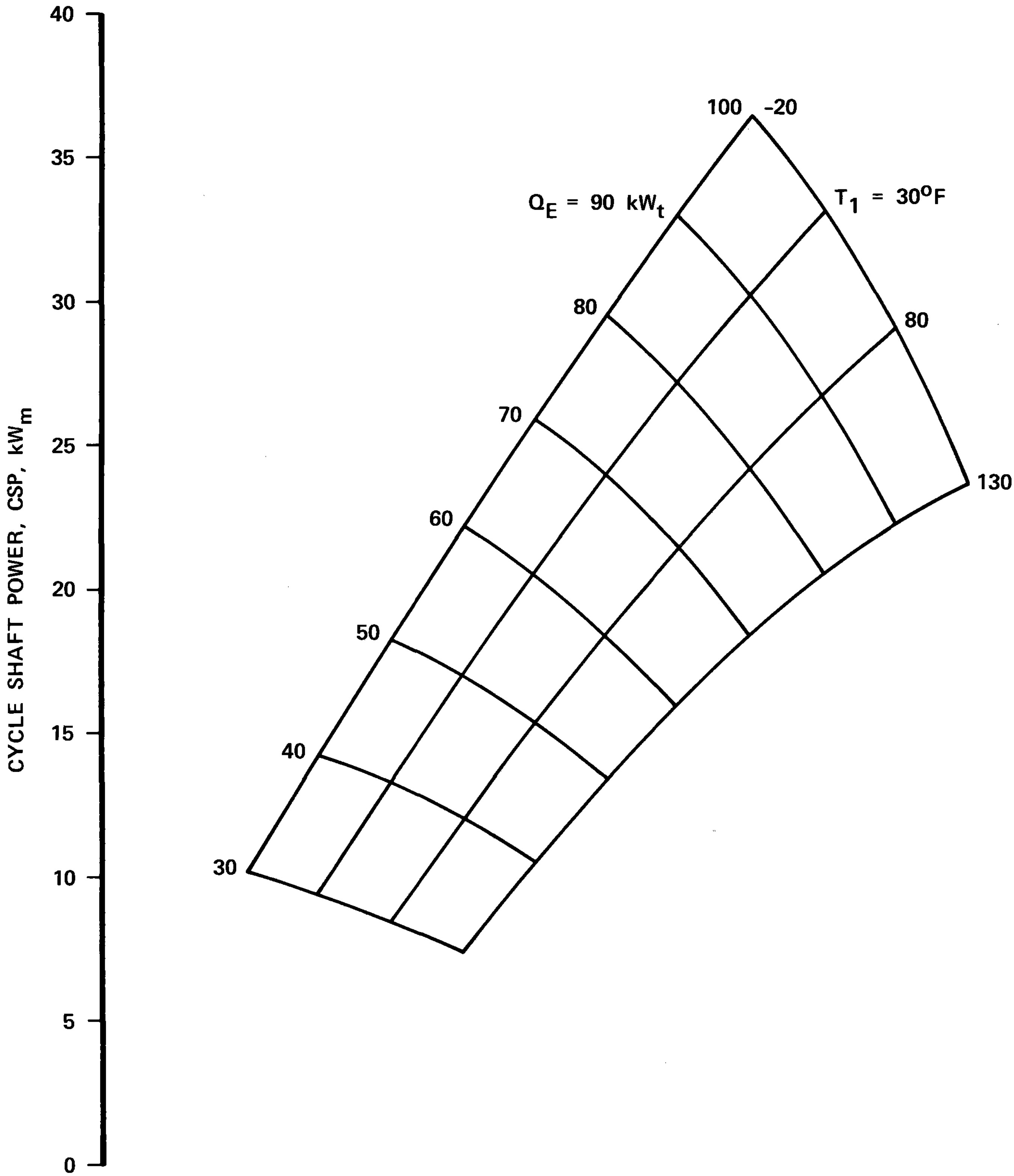

Figure 4-2. Engine A Performance at 5000 Ft Altitude.

TABLE 4-I. ENGINE A PERFORMANCE AT DESIGN INSOLATION.

		S.L. 10°F	S.L. 80°F	S.L. 140°F	5000 Ft -20°F	5000 Ft 109°F
GENERAL	Q_E (kW_t)	72.7	72.7	72.7	72.7	72.7
	CSP (kW_m)	25.899	22,879	19.4543	27.114	20.474
	ηCSP (CSP/Q_E)	0.3562	0.3147	0.2676	0.3730	0.2816
	E_r	0.9155	0.9163	0.9168	0.9176	0.9190
	r_c	2.6699	2.6844	2.7076	2.9874	3.0184
	r_t	2.4084	2.4139	2.4275	2.6572	2.6640
	M_1 (lb/sec)	0.6161	0.6161	0.6179	0.5797	0.5799
	N_t (rpm)	58,023	62,773	66,941	59,839	69,175
RECUPERATOR HP SIDE	M_3 (lb/sec)	0.6131	0.6131	0.6148	0.5768	0.5770
	P_{in} (psia)	38.778	38.979	39.308	36.114	36.471
	P_{out} (psia)	38.516	38.700	39.014	35.860	36.185
	T_{in} (°F)	209	307	396	191	384
	T_{out} (°F)	1092	1092	1093	1066	1066
RECEIVER	M_5 (lb/sec)	0.6131	0.6131	0.6148	0.5768	0.5770
	P_{in} (psia)	38.516	38.700	39.014	35.860	36.185
	P_{out} (psia)	36.917	37.109	37.425	34.357	34.693
	T_{in} (°F)	1092	1092	1094	1066	1066
	T_{out} (°F)	1500	1500	1500	1500	1500
RECUPERATOR LP SIDE	M_{11} (lb/sec)	0.6161	0.6161	0.6179	0.5797	0.5799
	P_{in} (psia)	15.220	15.266	15.311	12.819	12.914
	P_{out} (psia)	14.690	14.711	14.729	12.249	12.289
	T_{in} (°F)	1174	1164	1157	1145	1125
	T_{out} (°F)	302	389	469	282	453

NOTE: Numeric subscripts refer to station locations shown on Figure 3-1.

TABLE 4-II. ENGINE A PERFORMANCE AT A TYPICAL LOW INSOLATION.

		S.L. 10°F	S.L. 80°F	S.L. 140°F	5000 Ft -20°F	5000 Ft 109°F
GENERAL	Q_E (kW_t)	30.0	30.0	30.0	30.0	30.0
	CSP (kW_m)	9.1904	8.1268	7.0095	10.099	7.8926
	CSP (CSP/Q_E)	0.3064	0.2709	0.2336	0.3366	0.2631
	E_r	0.9353	0.9360	0.9365	0.9371	0.9384
	r_c	1.7643	1.7794	1.7951	1.9196	1.9454
	r_t	1.6299	1.6425	1.6556	1.7564	1.7761
	M_1 (lb/sec)	0.3786	0.3771	0.3767	0.3518	0.3487
	N_t (rpm)	43,170	46,997	50,248	44,611	52,067
RECUPERATOR HP SIDE	M_3 (lb/sec)	0.3768	0.3753	0.3748	0.3500	0.3469
	P_{in} (psia)	25.637	25.851	26.075	23.215	23.519
	P_{out} (psia)	25.412	25.616	25.830	22.995	23.278
	T_{in} (°F)	122	212	290	100	271
	T_{out} (°F)	1235	1234	1234	1214	1212
RECEIVER	M_5 (lb/sec)	0.3768	0.3753	0.3748	0.3500	0.3469
	P_{in} (psia)	25.412	25.616	25.830	22.995	23.278
	P_{out} (psia)	24.364	24.584	24.809	21.999	22.312
	T_{in} (°F)	1235	1234	1234	1214	1212
	T_{out} (°F)	1500	1500	1500	1500	1500
RECUPERATOR LP SIDE	M_{11} (lb/sec)	0.3787	0.3772	0.3768	0.3518	0.3487
	P_{in} (psia)	14.902	14.922	14.941	12.479	12.517
	P_{out} (psia)	14.603	14.610	14.617	12.161	12.175
	T_{in} (°F)	1312	1304	1298	1298	1274
	T_{out} (°F)	214	295	366	190	344

NOTE: Numeric subscripts refer to station locations shown on Figure 3-1.

Module Electric Power, MEP*		19.1 kW_e
Inverter Efficiency, 0.94	1.143 ΔkW	
Plant Parasitic Load, PPL	Neglected	
Transformer Efficiency	Not Required	
Net Electric Power, NEP*		18.0 kW_e

The electric accessory load (EAL) includes power to run the controls (28 watts) and the generator and gearbox compartment cooling fan (400 watts). The shaft accessory load (SAL), in this case, is power required to drive the oil pump (73 watts).

The net electric power produced is 18.0 kW_e. The estimated overall thermal input to AC busbar efficiency (NEP/Q_E) is therefore 24.8 percent.

4.2 Configuration B

The B engine selected for the 72.7 kW_t thermal power design requirement consists of the PFE turbocompressor and a 269 pound recuperator design and part load performance characteristics are shown in Figure 4-3 and Tables 4-III and 4-IV. Since this is a closed cycle engine, it is insensitive to elevation except for cooling airflow.

Figure 4-3 shows shaft output power (CSP) versus heat input (Q_E) and compressor inlet temperature. Table 4-III shows the engine cycle performance at design insolation of 1 kW/m^2 and corresponding thermal input (Q_E) of 72.7 kW_t. These data show that the system would produce 21.6 kW_m of shaft power (CSP) at design insolation with a cycle efficiency η_{CSP} of 29.7 percent. Table 4-IV shows system performance at a typical low insolation of 0.4 kW/m^2 and corresponding thermal input Q_E of 30 kW_t.

The 400 Hz generator was also selected for Engine B. The following is an estimate of the net electric power (NEP) appearing at the AC busbar for sea level, 80°F ambient temperature operation with Q_E equal to 72.7 kW_t:

Cycle Shaft Power, CSP		21.6 kW_m
Gearbox Efficiency, 0.98	0.432 ΔkW	
Shaft Accessory Load, SAL	0.076 ΔkW	
Generator Efficiency, 0.91	1.90 ΔkW	
Rectifier Efficiency, 0.96	0.767 ΔkW	
Electric Accessory Load, EAL	0.861 ΔkW	
Module Electric Power, MEP		17.6 kW_e
Inverter Efficiency, 0.94	1.053 ΔkW	
Plant Parasitic Load, PPL	Neglected	
Transformer Efficiency	Not required	
Net Electric Power, NEP		16.5 kW_e

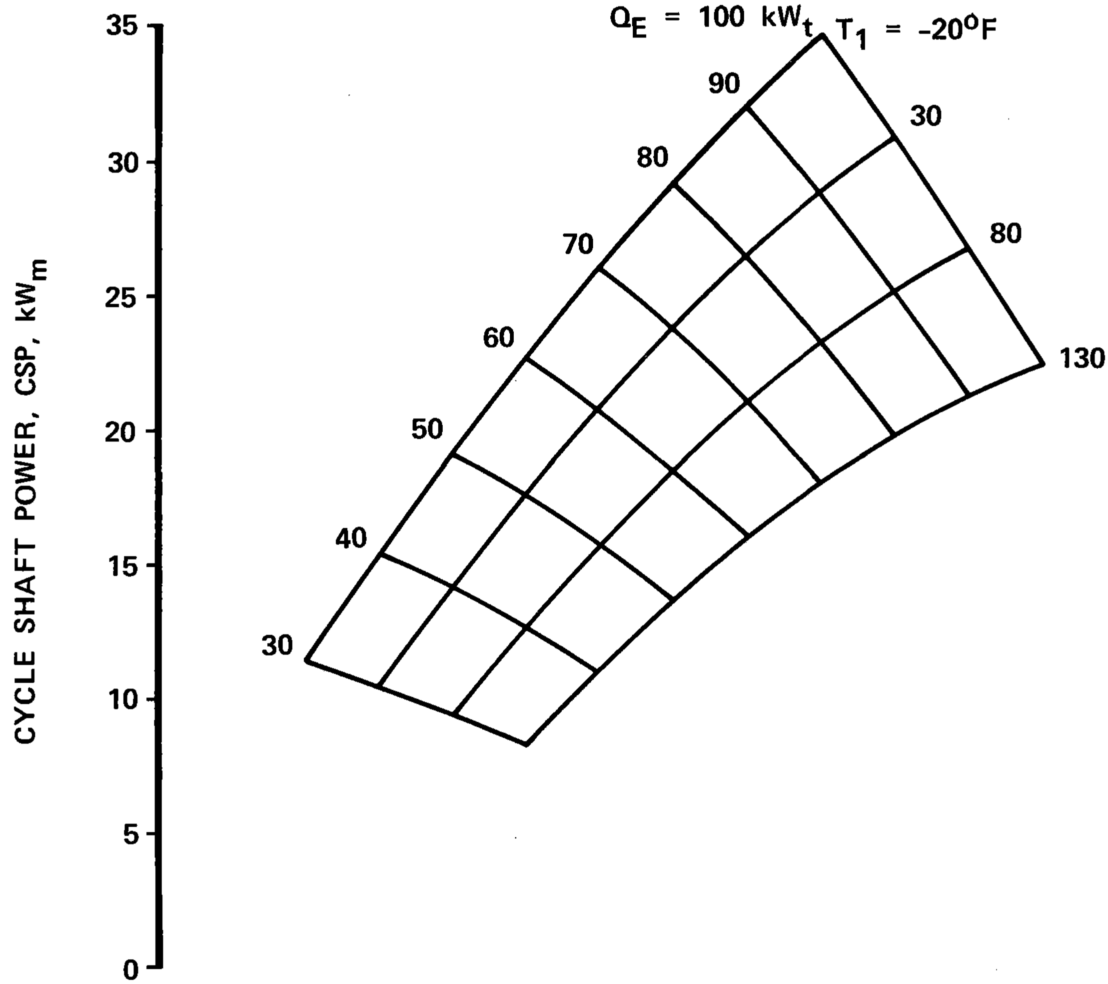

Figure 4-3. Engine B Performance.

TABLE 4-III. ENGINE B PERFORMANCE AT DESIGN INSOLATION.

		S.L. 10°F	S.L. 80°F	S.L. 140°F
GENERAL	Q_E (kW_t)	72.7	72.7	72.7
	CSP (kW_m)	25.489	21.591	17.923
	η_{CSP} (CSP/Q_E)	0.3505	0.2969	0.2466
	E_r	0.9164	0.9134	0.9105
	r_c	2.4083	2.1715	2.0116
	r_t	2.1717	1.9805	1.8521
	M_1 (lb/sec)	0.6480	0.7064	0.7615
	N_t (rpm)	65,433	65,433	65,433
RECUPERATOR HP SIDE	M_3 (lb/sec)	0.6318	0.6887	0.7425
	P_{in} (psia)	45.877	51.350	57.182
	P_{out} (psia)	45.645	51.102	56.923
	T_{in} (°F)	212	285	347
	T_{out} (°F)	1102	1135	1162
RECEIVER	M_5 (lb/sec)	0.6318	0.6887	0.7425
	P_{in} (psia)	45.645	51.102	56.923
	P_{out} (psia)	43.790	49.090	54.788
	T_{in} (°F)	1100	1134	1161
	T_{out} (°F)	1502	1502	1502
RECUPERATOR HP SIDE	M_{11} (lb/sec)	0.6381	0.6957	0.7503
	P_{in} (psia)	19.777	24.394	29.184
	P_{out} (psia)	19.351	23.985	28.790
	T_{in} (°F)	1183	1216	1242
	T_{out} (°F)	311	382	443
COOLER WORKING FLUID SIDE	M_{13} (lb/sec)	0.6478	0.7062	0.7617
	P_{in} (psia)	19.351	23.985	28.790
	P_{out} (psia)	19.191	23.815	28.611
	T_{in} (°F)	309	380	442
	T_{out} (°F)	34	108	172
COOLER COOLANT	M_c (lb/sec)	2.0	2.0	2.0
	T_{in} (°F)	10	80	140

NOTE: Numeric subscripts refer to station locations shown on Figure 3-1.

TABLE 4-IV. ENGINE B PERFORMANCE AT A TYPICAL LOW INSOLATION.

		S.L. 10°F	S.L. 80°F	S.L. 140°F
GENERAL	Q_E (kW_t)	30.0	30.0	30.0
	CSP (kW_m)	10.780	9.2990	7.8365
	η_{CSP} (CSP/Q_E)	0.3592	0.3098	0.2612
	E_r	0.9452	0.9440	0.9425
	r_c	2.4830	2.2555	2.0845
	r_t	2.1728	2.0027	1.8756
	M_1 (lb/sec)	0.2806	0.3053	0.3302
	N_t (rpm)	65,433	65,433	65,433
RECUPERATOR HP SIDE	M_3 (lb/sec)	0.2735	0.2976	0.3219
	P_{in} (psia)	19.965	22.204	24.727
	P_{out} (psia)	19.773	22.000	24.515
	T_{in} (°F)	193	262	321
	T_{out} (°F)	1126	1157	1183
RECEIVER	M_5 (lb/sec)	0.2735	0.2976	0.3219
	P_{in} (psia)	19.773	22.000	24.515
	P_{out} (psia)	18.958	21.116	23.572
	T_{in} (°F)	1123	1153	1180
	T_{out} (°F)	1505	1505	1504
RECUPERATOR HP SIDE	M_{11} (lb/sec)	0.2763	0.3006	0.3252
	P_{in} (psia)	8.558	10.372	12.393
	P_{out} (psia)	8.217	10.043	12.075
	T_{in} (°F)	1180	1210	1235
	T_{out} (°F)	262	330	388
COOLER WORKING FLUID SIDE	M_{13} (lb/sec)	0.2806	0.3052	0.3302
	P_{in} (psia)	8.217	10.043	12.075
	P_{out} (psia)	8.099	9.915	11.942
	T_{in} (°F)	260	328	386
	T_{out} (°F)	11	81	142
COOLER COOLANT	M_c (lb/sec)	2.0	2.0	2.0
	T_{in} (°F)	10	80	140

NOTE: Numeric subscripts refer to station locations shown on Figure 3-1.

With reference to Figure 3-16, the electric accessory load (EAL) includes power to run the controls (28 watts), the cooler fan (433 watts), and the generator and gearbox compartment cooling fan (400 watts). The shaft accessory load (SAL) in this case, is power required to drive the oil pump (76 watts).

The net electric power produced is 16.7 kW_e. The estimated overall thermal output to AC busbar efficiency (NEP/Q_E) is therefore 23.0 percent.

4.3 Configuration C

Engine C, selected for the 72.7 kW_t thermal power design requirement, is based on current production aerodynamics (of which the GTP36-51 compressor and turbine are typical), customized or scaled to a diameter and speed that will result in the most cost effective 1500°F solar power modules. Engine C also includes a 269-pound recuperator. Engine C performance is depicted in Figures 4-4 and 4-5 and Tables 4-V and 4-VI. The salient design point performance parameters for the customed ABC engine configuration at this increased power level are summarized below:

Thermal Input, kW_t	72.7
Cycle Efficiency, η_{CSP}	0.3137
Shaft Output Power, kW_m	22.807
Compressor Inlet Temperature, °F	80
Turbine Inlet Temperature, °F	1500
Rotating Speed, RPM	75,085
Compressor Pressure Ratio	2.799
Recuperator Effectiveness	0.92
Bleed Flow Fraction	0.01
Pressure Loss Parameter, β	0.8971
Compressor Diameter, in.	3.921
Turbine Diameter, in.	5.057

Figure 4-4 shows sea level shaft output power (CSP) plotted as a function of heat input to the system (Q_E) and compressor inlet temperatures (T_1). Figure 4-5 shows similar data for 5000 ft elevation above sea level.

Table 4-V shows estimated engine performance with an 11-meter dish at design solar insolation of 1 kW/m^2 and corresponding thermal input (Q_E) of 72.7 kW_t. The data is portrayed for sea level and 5000 ft elevation with ambient air temperatures from 10°F to 140°F.

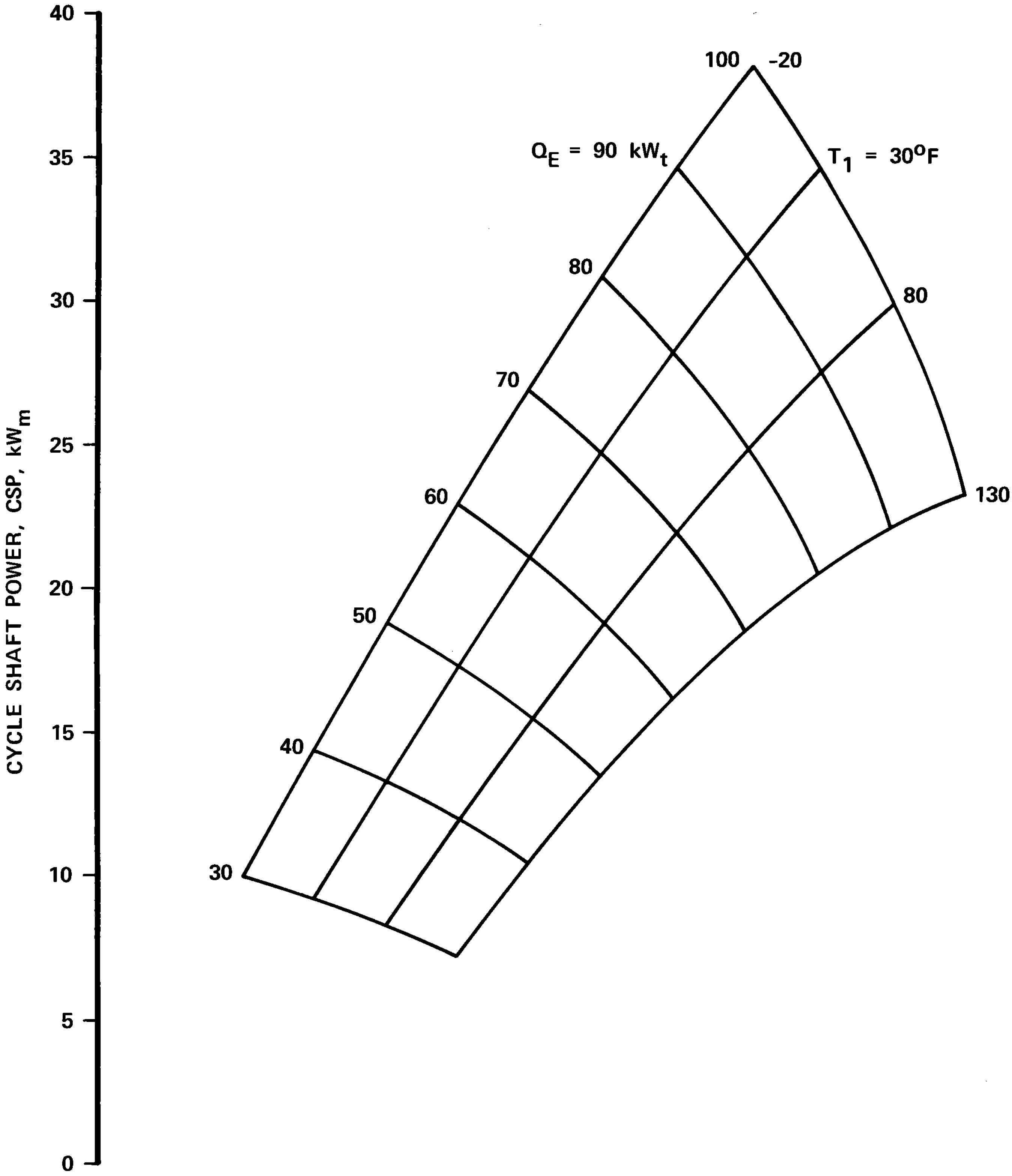

Figure 4-4. Engine C Performance at Sea Level Altitude.

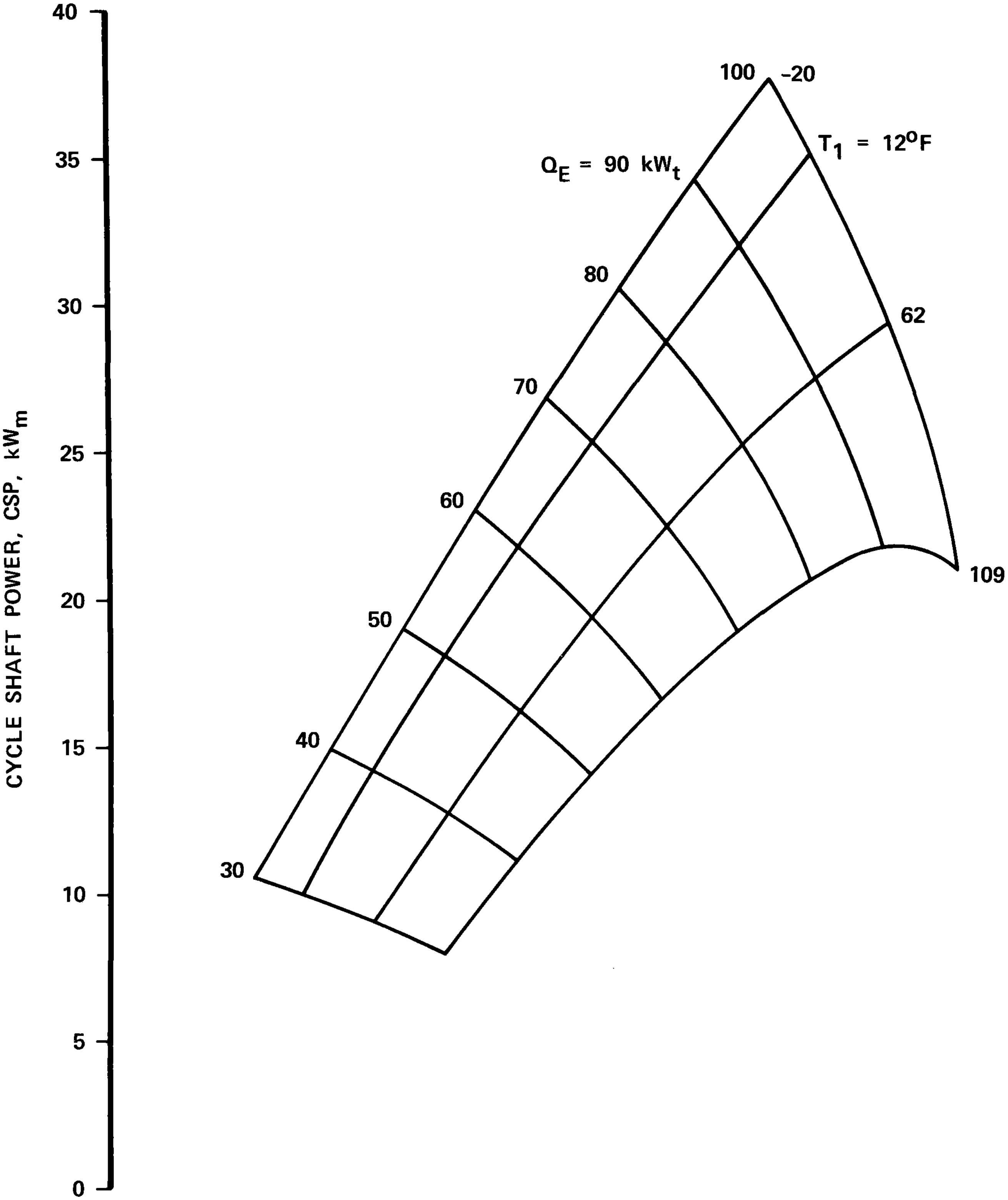

Figure 4-5. Engine C Performance at 5000 Ft Altitude.

TABLE 4-V. ENGINE C PERFORMANCE AT DESIGN INSOLATION.

		S.L. 10°F	S.L. 80°F	S.L. 140°F	5000 Ft -20°F	5000 Ft 109°F
GENERAL	Q_E (kW_t)	72.7	72.7	72.7	72.7	72.7
	CSP (kW_m)	26.752	22.807	18.313	28.005	19.613
	η_{CSP} (CSP/Q_E)	0.3680	0.3137	0.2519	0.3852	0.2698
	E_r	0.9193	0.9200	0.9202	0.9215	0.9225
	r_c	2.7734	2.7990	2.8394	3.1036	3.1647
	r_t	2.4982	2.5110	2.5373	2.7605	2.7880
	M_1 (lb/sec)	0.5913	0.5945	0.6005	0.5558	0.5627
	N_t (rpm)	69,119	75,085	80,528	71,101	83,056
RECUPERATOR HP SIDE	M_3 (lb/sec)	0.5854	0.5885	0.5945	0.5503	0.5571
	P_{in} (psia)	40.289	40.651	41.228	37.524	38.245
	P_{out} (psia)	40.053	40.398	40.959	37.297	37.984
	T_{in} (°F)	215	320	414	199	401
	T_{out} (°F)	1073	1075	1079	1045	1050
RECEIVER	M_5 (lb/sec)	0.5854	0.5885	0.5945	0.5503	0.5571
	P_{in} (psia)	39.905	40.250	40.810	37.160	37.846
	P_{out} (psia)	38.293	38.632	39.177	35.658	36.328
	T_{in} (°F)	1073	1075	1079	1045	1050
	T_{out} (°F)	1500	1500	1500	1500	1500
RECUPERATOR LP SIDE	M_{11} (lb/sec)	0.5913	0.5945	0.6005	0.5558	0.5627
	P_{in} (psia)	15.191	15.249	15.303	12.790	12.904
	P_{out} (psia)	14.695	14.722	14.744	12.258	12.304
	T_{in} (°F)	1148	1141	1137	1117	1105
	T_{out} (°F)	306	399	483	287	466

NOTE: Numeric subscripts refer to station locations shown on Figure 3-1.

These data show the system would produce 22.8 kW_m of shaft power on an 80°F day with a cycle efficiency η_{CSP} of 31.4 percent.

Table 4-VI shows similar data for the case of a typical low solar insolation of 0.4 kW/m^2 and corresponding Q_E of 30 kW_t. Here, the system would produce 8.3 kW_m of shaft power at 80°F with a cycle efficiency of 27.5 percent.

A permanent magnet generator (PMG) was selected for Engine C. This generator also requires a power conditioning system as shown in Figure 3-16. The following is an estimate of the net electric power (NEP) appearing at the AC busbar for design point operation (sea level, 80°F, Q_E = 72.7 kW_t):

Cycle Shaft Power, CSP		22.8 kW_m
Gearbox Efficiency	Not required	
Shaft Accessory Load, SAL	None	
Generator Efficiency, 0.94	1.369 ΔkW	
Rectifier Efficiency, 0.96	0.857 ΔkW	
Electric Accessory Load, EAL	0.299 ΔkW	
Module Electric Power, MEP		20.3 kW_e
Inverter Efficiency, 0.94	1.217 ΔkW	
Plant Parasitic Load, PPL	Neglected	
Transformer Efficiency	Not required	
Net Electric Power, NEP		19.1 kW_e

With reference to Figure 3-16 the electric accessory load, EAL, includes power to run the controls (28 watts) and the generator fan (271 watts). Engine C utilizes foil bearings, which do not require an oil lubrication system and there is therefore no shaft accessory load.

The net electric power produced is 19.1 kW_e. The estimated overall engine thermal input to busbar efficiency (NEP/Q_E) is 26.3 percent.

TABLE 4-VI. ENGINE C PERFORMANCE AT A TYPICAL LOW INSOLATION.

		S.L. 10°F	S.L. 80°F	S.L. 140°F	5000 Ft -20°F	5000 Ft 109°F
GENERAL	Q_E (kW_t)	30	30	30	30	30
	CSP (kW_m)	9.463	8.255	6.925	10.471	7.942
	η_{CSP} (CSP/Q_E)	0.3154	0.2752	0.2308	0.3490	0.2647
	E_r	0.9388	0.9394	0.9398	0.9406	0.9418
	r_c	1.8035	1.8223	1.8434	1.9638	1.9975
	r_t	1.6620	1.6780	1.6957	1.7950	1.8213
	M_1 (lb/sec)	0.3616	0.3612	0.3622	0.3349	0.3341
	N_t (rpm)	51,466	56,171	60,301	53,043	62,272
RECUPERATOR HP SIDE	M_3 (lb/sec)	0.3576	0.3576	0.3585	0.3316	0.3308
	P_{in} (psia)	26.209	26.477	26.780	23.752	24.152
	P_{out} (psia)	26.004	26.262	26.554	23.551	23.931
	T_{in} (°F)	127	218	298	104	278
	T_{out} (°F)	1221	1221	1221	1198	1198
RECEIVER	M_5 (lb/sec)	0.3576	0.3576	0.3585	0.3316	0.3308
	P_{in} (psia)	25.911	26.170	26.463	23.465	23.846
	P_{out} (psia)	24.894	25.165	25.463	22.513	22.915
	T_{in} (°F)	1221	1221	1221	1198	1198
	T_{out} (°F)	1500	1500	1500	1500	1500
RECUPERATOR LP SIDE	M_{11} (lb/sec)	0.3616	0.3612	0.3622	0.3349	0.3341
	P_{in} (psia)	14.885	14.905	14.925	12.457	12.499
	P_{out} (psia)	14.604	14.611	12.618	12.161	12.177
	T_{in} (°F)	1292	1285	1280	1267	1254
	T_{out} (°F)	218	301	374	194	351

NOTE: Numeric subscripts refer to station locations shown on Figure 3-1.

5.0 CONCEPTUAL DESIGNS FOR ENGINE/GENERATORS

Conceptual designs were defined for each of the three Configurations A, B and C, and included evaluating and selecting or defining each turbocompressor, and the other components comprising a Brayton Engine/Generator (BE/G) or Power Conversion Unit (PCU).

Typical PCU components are listed in Table 5-I. Applicability of these components to Configurations A, B and C is shown in Table 5-II, along with a comparison of the estimated component and total weights for each arrangement. A summary of conceptual design work and results is presented in following paragraphs and Section 6.0.

5.1 Turbocompressor and Generator Arrangements

Candidate turbocompressor and generator arrangements were defined for both the open and closed cycle engines.

Open cycle engine candidates are illustrated by the schematic representations on Figure 5-1. With two exceptions, the arrangements for near-term Configuration A engines (Mod "O") were based on modifying the existing GTP36-51 power section, and using it to drive various gearbox and generator combinations. The exceptions, (Arrangements A-7 and -8) are based on the modified AGA turbocompressor. The latter two are applicable only if the design point thermal input power level becomes established at values lower than 72.7 kW_t.

Figure 5-1 also illustrates arrangements for the customized Configuration C engines (MOD "I"). All use gas bearings, PMGs and current production aerodynamics. The aerodynamic components would be scaled or customized to an optimum diameter and speed to be established by the solar power module system analysis.

A similar definition and analysis of closed cycle turbocompressor and generator arrangements was also accomplished.

Evaluation of these candidate arrangements consisted of assessing development cost, schedule, and risks associated with each, to determine which arrangement would best meet the objectives for the three Configurations A, B and C. Figure 5-2 shows the relationship among some of the more attractive open cycle arrangements. As illustrated by the figure, varying amounts of investment in terms of schedule time and program costs will be required to move from near-term first-generation demonstrator arrangements like A-1, which make maximum use of existing engine hardware, to more prototypical arrangements like A-5, C-2 or C-5. With this consideration in mind, arrangements selected were as follows:

TABLE 5-I. COMPONENTS COMPRISING A BRAYTON ENGINE GENERATOR POWER CONVERSION UNIT.

Turbocompressor
Turbine
Compressor
Housing
Bearings
Shaft
Seals
Recuperator
Controls
Control Logic Module*
Control Sensors
Control Panel*
Control and Power Harnesses
Other
Ducts
Bellows
Insulation
Enclosure
Miscellaneous Brackets, Fasteners
Instrumentation
Pressure Transducer, Oil
Thermocouples, Turbine Exit, Oil Sump
Speed Sensor (Use Alternator Frequency)
Auxiliaries - Starter Motor and Subsystem*
Generator and Voltage Regulator
Gearbox
Housing
Bearings and Seals
Gears and Shafts
Auxiliaries - Lube Pump and Subsystem
Accessories
Compartment Fan
Control Rectifier*

*Indicates PCU components that probably will not be mounted on the concentrator at its focus.

TABLE 5-II. 20 kW ENGINE/GENERATOR ASSEMBLIES - WEIGHT ESTIMATES (LBS).

	Arrangements				
Concentrator-Mounted Components	A-1	A-2	A-3	B-3	C-5
Turbocompressor	148	118	118	125	97
Generator	50	50	10	50	6
Recuperator	269	269	269	269	269
Gearbox	50	50	-	50	-
Cooler	-	-	-	80	-
Combustor	-	-	-	-	-
Other Parts -					
Ducts, Bellows, Filter	35	35	35	45	25
Insulation	15	15	15	15	15
Structure and Enclosure	40	40	40	40	30
Auxiliaries -					
Lube Pump and System	15	15	15	15	-
Starter Motor	15	15	15	15	-
Adapter Gearbox	-	-	10	-	-
Controls and Accessories -					
Sensors, Harness, Etc.	10	10	10	10	10
Fan for Cooler	-	-	-	20	-
Gas Management System	-	-	-	30	-
Fan for Generator	-	-	10	-	10
TOTAL*	647	617	547	764	462

*Excludes components that probably would not be concentrator-mounted.

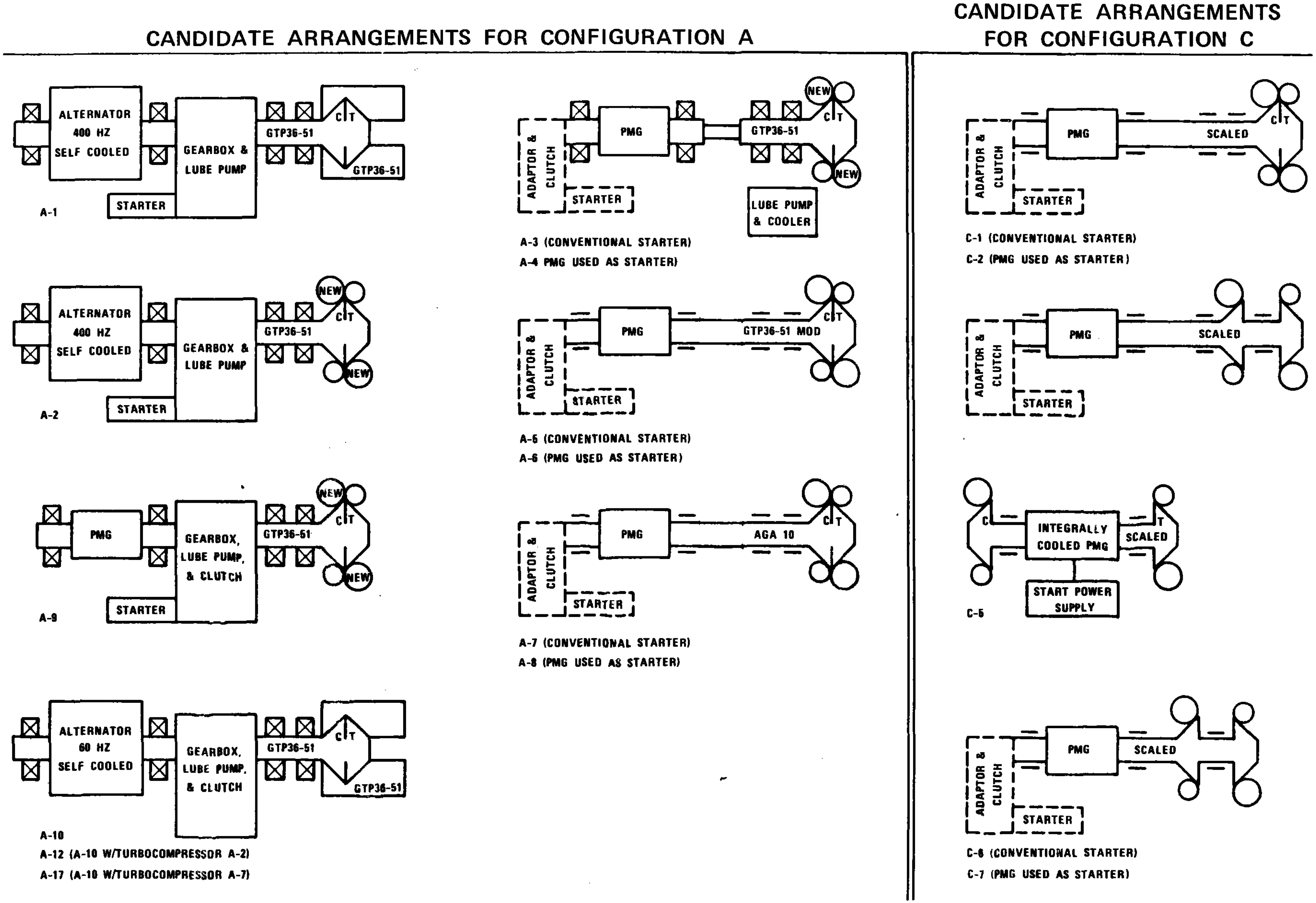

Figure 5-1. Open Cycle Turbocompressor and Generator Arrangements.

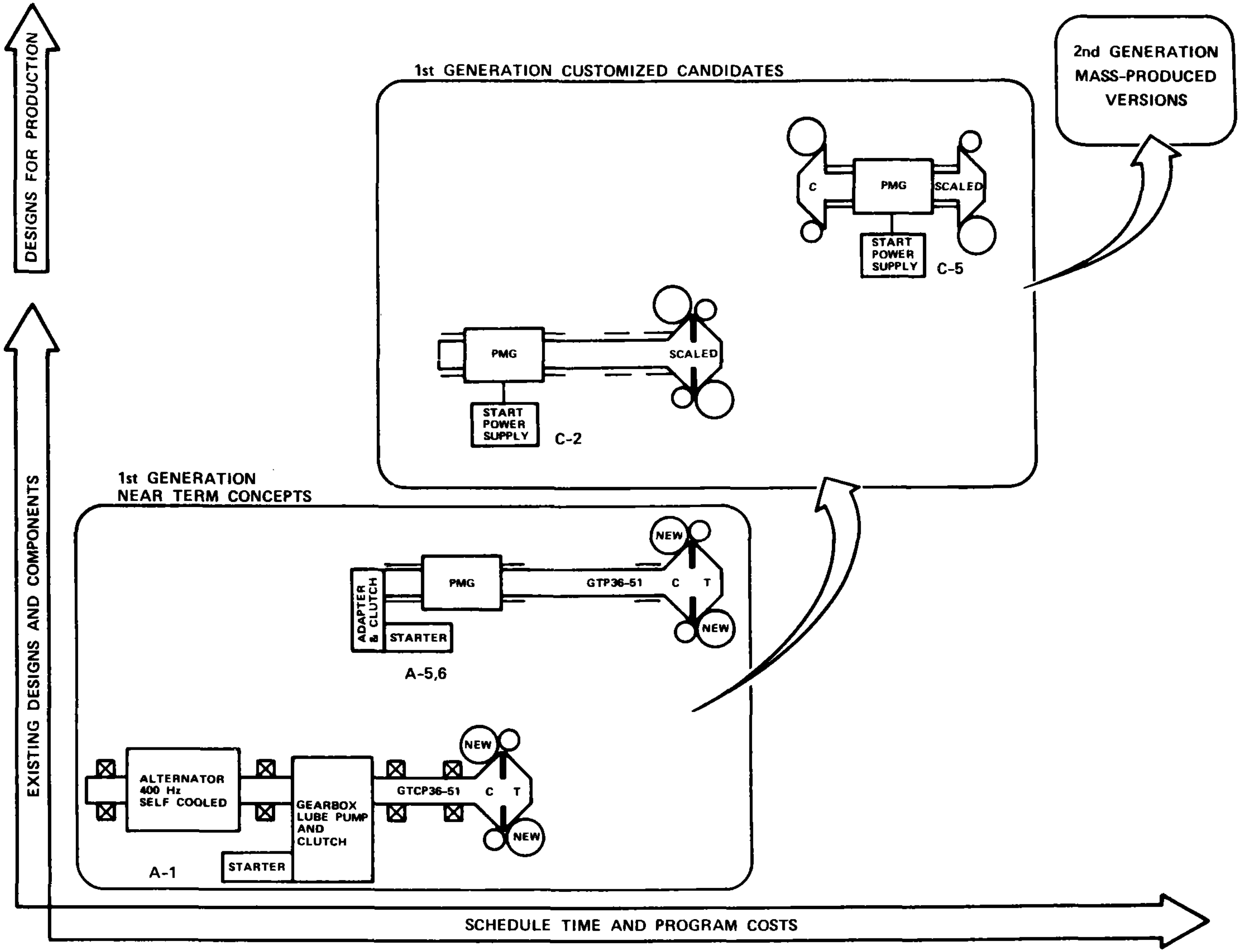

Figure 5-2. Engine Generator Arrangements - Open Cycle.

- Configuration A - Arrangement A-1 using the GTP36-51 with oil bearings, a gearbox and a 400 Hz alternator
- Configuration B - Arrangement B-3 using the PFE with one gas and one oil bearing, a gearbox, and a 400 Hz alternator
- Configuration C - Arrangement C-5 using a customized turbocompressor based on production (GTP36-51) aerodynamics, gas bearings, and a direct drive permanent magnet generator

5.2 Configuration A

5.2.1 PCU

A conceptual layout and center of gravity for the Configuration A PCU is illustrated in Figure 5-3, with the PCU profile as assembled on top of the solar receiver, and relative locations indicated for the connecting ducts. The compressor discharge and turbine discharge ducts extend slightly beyond the shadow outline of the receiver, as illustrated in the plan view.

The PCU is shown with a possible mounting structure. A mounting ring consisting of an aluminum channel bent into a circle is located near the combined center of gravity of the PCU and receiver. The ring has 3 pintles projecting radially outward on which to connect the support struts from the concentrator structure. The PCU and receiver are supported from this mounting ring by tubular struts or other suitable brackets. The PCU concept is shown enclosed within a sheet metal shroud for protection from the elements. Air is drawn into the unit through a filtered inlet and exhausted to the atmosphere through a diesel engine type exhaust pivot cap or other suitable device.

Ducts connecting the components would be 4.0 inch diameter CRES 347. The turbine inlet duct would be fabricated from Hastelloy-X or a non-cobalt containing alloy suitable for the temperature level. Hot ducts would be insulated as required with MIN-K or other suitable high temperature insulation. The materials initially considered for the various components are listed in Table 5-III. Miscellaneous design and specification data for the PCU is listed in Table 5-IV.

5.2.2 Turbocompressor

The turbocompressor and generator Arrangement A-1 derived from the GTP36-51 power section is shown in Figure 5-4. This unit has been modified for external heat addition by removing the outer cast turbine housing containing the tangential combustor and replacing it with a housing containing duct connections for directing the compressor gas flow outside the machine and the turbine gas flow into the turbine nozzle inlet torus. The turbine torus would be modified, and insulation provided to minimize heat transfer to the compressor discharge

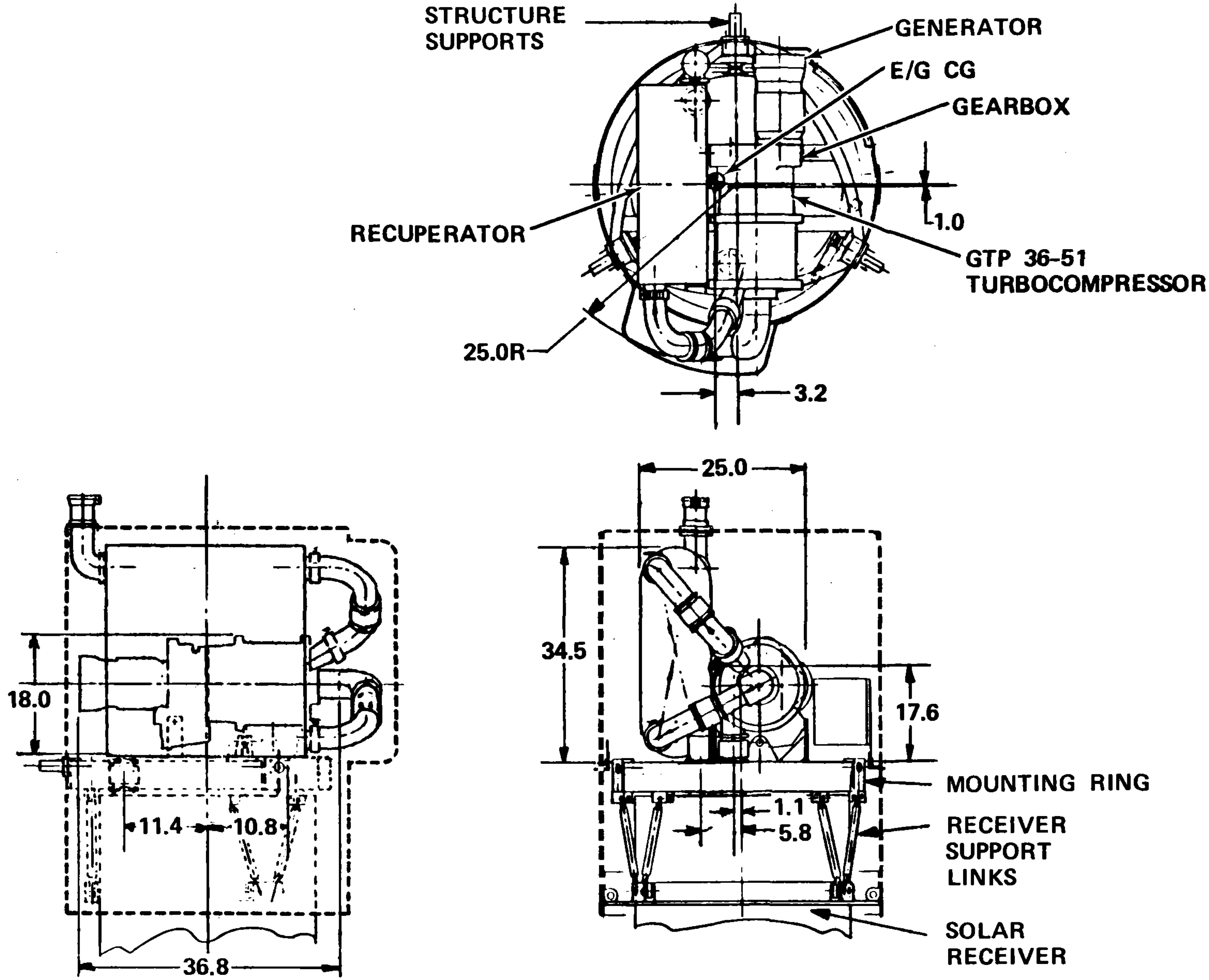

Figure 5-3. PCU Configuration A.

TABLE 5-III. ENGINE A - MATERIALS.

	Component	Material
Turbocompressor	Turbine Wheel	Cast IN713LC
	Turbine Shroud/Nozzle	Hastelloy-X
	Compressor Impeller	CRES 15-5 PA
	Compressor Housing	Sand Cast Ductile Iron
	Shaft	SAE 4340 Alloy Steel
	Bearing Carriers	SAE 8620 Alloy Steel
	Exhaust Duct	Hastelloy-X
	Gearcase	Aluminum Alloy
	Gears (Typical)	SAE 6260 Alloy Steel
Recuperator	Fins	CRES 347
	Plates	CRES 347
	Manifolds	CRES 347
	Shell	CRES 347
Ducting	Turbine Inlet Duct	Hastelloy-X
	Turbine Discharge Duct	CRES 300

TABLE 5-IV. PCU DESIGN AND SPECIFICATION SUMMARY.

Configuration A

Mode of Operation	Solar (adaptable to fossil and hybrid)
Rated Thermal Power Input	72.7 kW
Rated Ambient Condition	80°F, sea level
Ambient Temperature Extremes	10°F to +140°F at sea level -20°F to +109°F at 5000 ft
Voltage	200 volts, DC, nominal
Turbine Inlet Temperature	1500°F, nominal
Test Unit Life	4000 hr, minimum objective
Attitude Capability	0 to +90° roll
Polar Moments of Inertia	
Turbocompressor	0.0212 lb-in/sec^2 at 63,200 rpm
400 Hz Generator	0.104 lb-in/sec^2 at 8000 rpm

Rectifier: 20 kVA, 94 amps, 213 volts, located on ground, 20 by 15 by 21 inches in size (generator and rectifier can be modified to produce voltage required by system over a wide frequency range)

Accessory Loads

Electrical: Generator/gearbox compartment cooling fan - 400 watts, controls - 28 watts

Mechanical: Oil pump, 73 watts

Regular Maintenance Items: Oil, oil filter, air filter

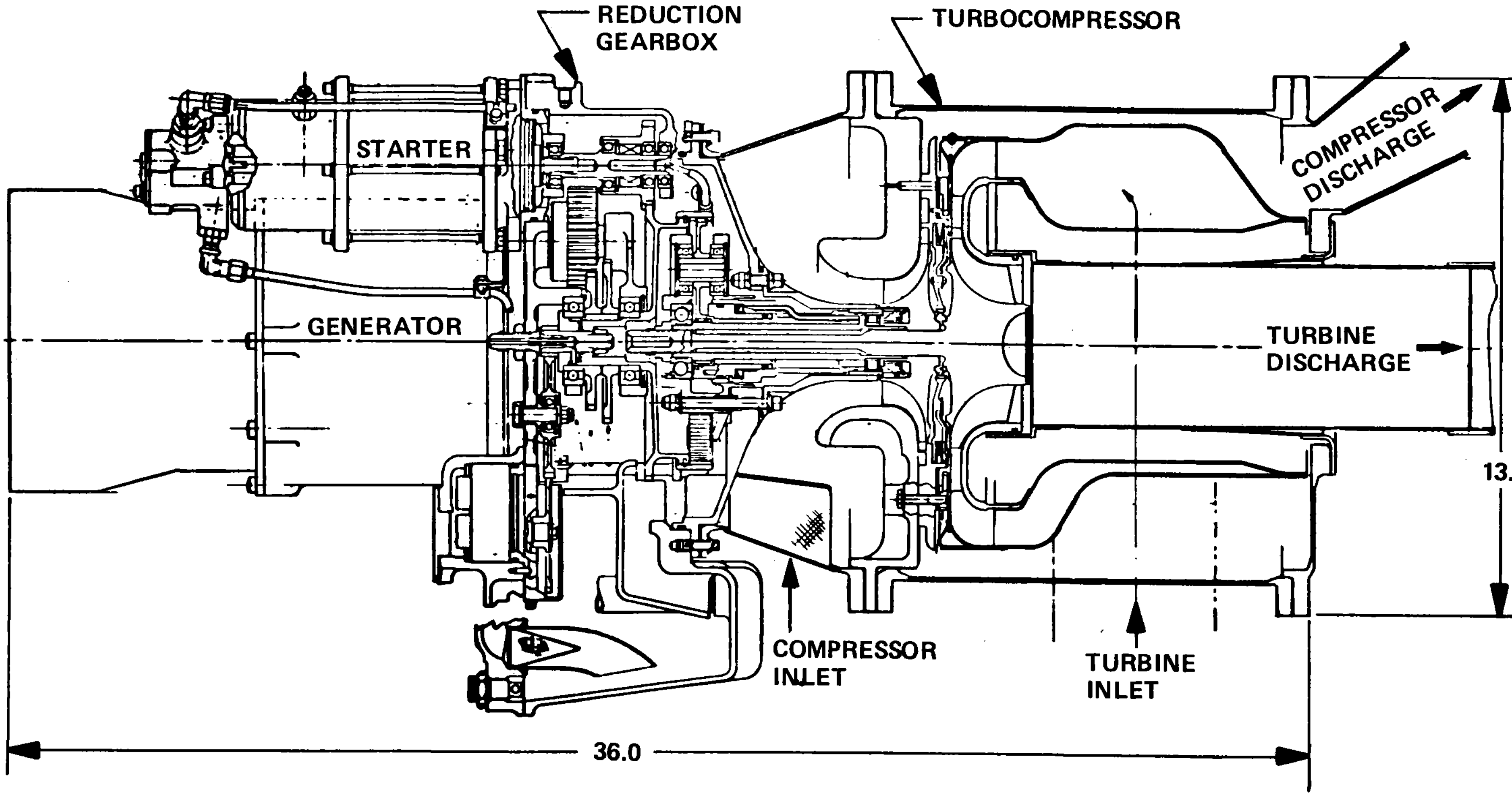

Figure 5-4. Turbocompressor and Generator - Arrangement A-1.

flow from the turbine inlet flow. The unit, including the gearbox and 400 Hz generator, would have an overall length of 36 inches and a diameter of 13.7 inches.

Arrangement A-1 meets the requirement for a demonstration type unit based on minimum modifications to an existing unit, and consequently is the recommended design.

A more easily packaged alternate arrangement was investigated. This unit (A-2) is shown in Figure 5-5 and involves additional departure from the basic GTP36-51 design. The heavy outer housing has been replaced by involute scrolls to provide more efficient direction and control of the gas stream. This arrangement shortens the overall length to 29.8 in. and reduces total weight by 30 lbs as compared to Arrangement A-1, (Table 5-I).

5.2.3 Generator

A 400 Hz generator was selected as the most reliable small power source using present state-of-the-art technology. The proposed machine contains a permanent magnet generator to provide the excitation required for the rotating field. No brushes are used, thereby reducing maintenance and increasing the time between overhaul. The range of speed expected during operation will result in a variation of almost 100 Hz from the basic rated frequency of the machine.

The normal efficiency at rated speed and load conditions will be 91-percent. Operation at the extreme ends of the speed range will result in reduced efficiency due to increased internal machine losses and reduced input/output power. However, this would be compensated to some extent by the lower cooling fan losses at the low end of the speed range. A solid state voltage regulator would be used to maintain the correct voltage required by the rectifier connected between the generator and load bank. The generator weight is about 49 lbs. The voltage regulator weighs 1.0 pound.

The electrical power rating is 400 Hz, 3 phase, 20 kVA, 56 amps, 120 volts line to neutral, and 208 volts line to line.

5.2.4 Lubrication System

The PCU lubrication system consists of an oil pump assembly, filter assembly, miscellaneous control components and the engine gearbox sump, as shown in Figure 5-6. The system provides lubrication and cooling flow to the engine bearings, bearing mounts, and geartrain.

The oil pump is a positive displacement gear-mesh pump with the gear shafts mounted in bronze sleeve bearings. The gears are fabricated by powdered metal techniques providing low cost, high accuracy, and long life. This technique has been used successfully in thousands of small gas turbines. The oil pump is mounted in the gearbox under the filter housing, and is readily accessible.

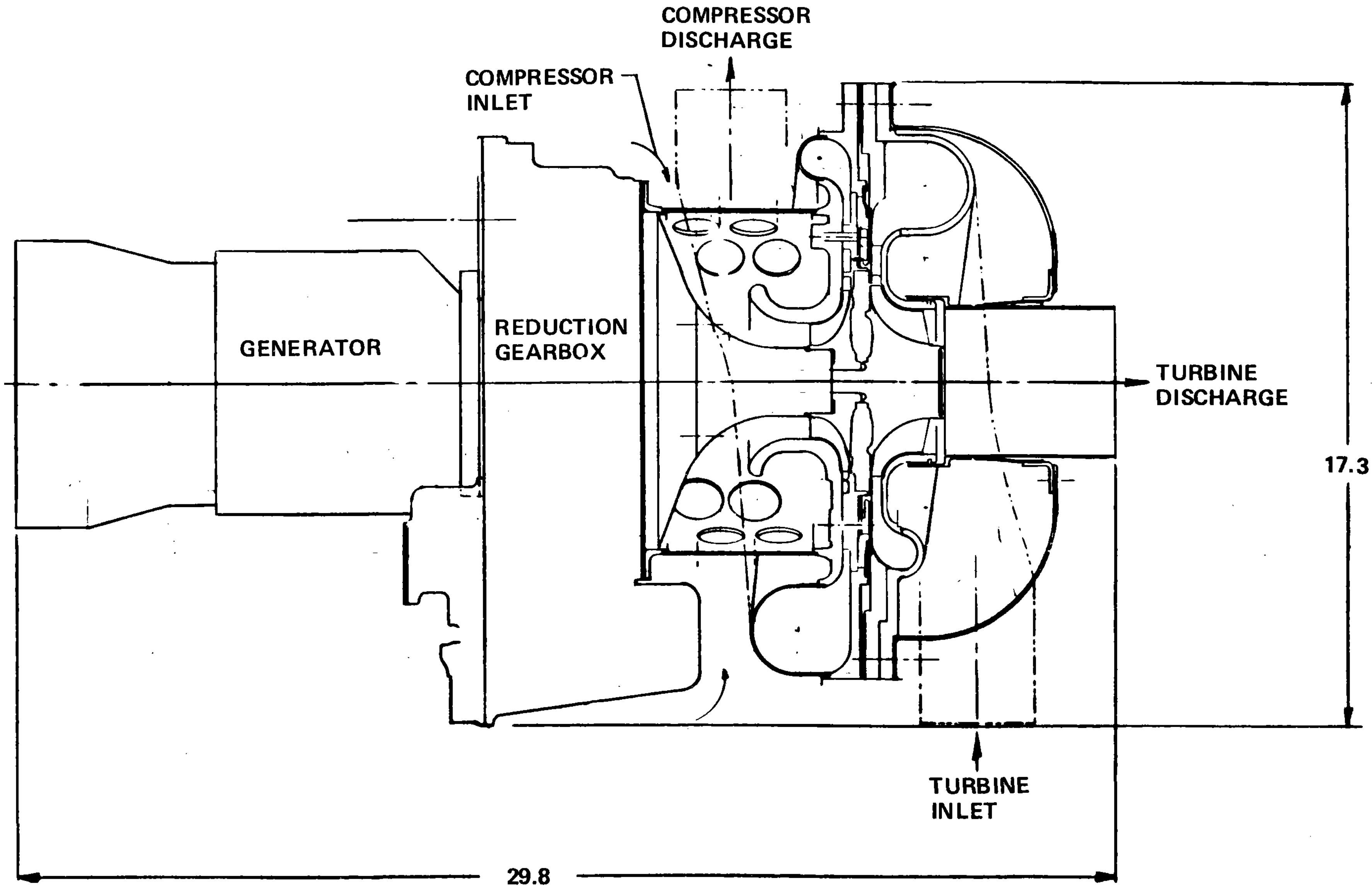

Figure 5-5. Turbocompressor and Generator - Arrangement A-2.

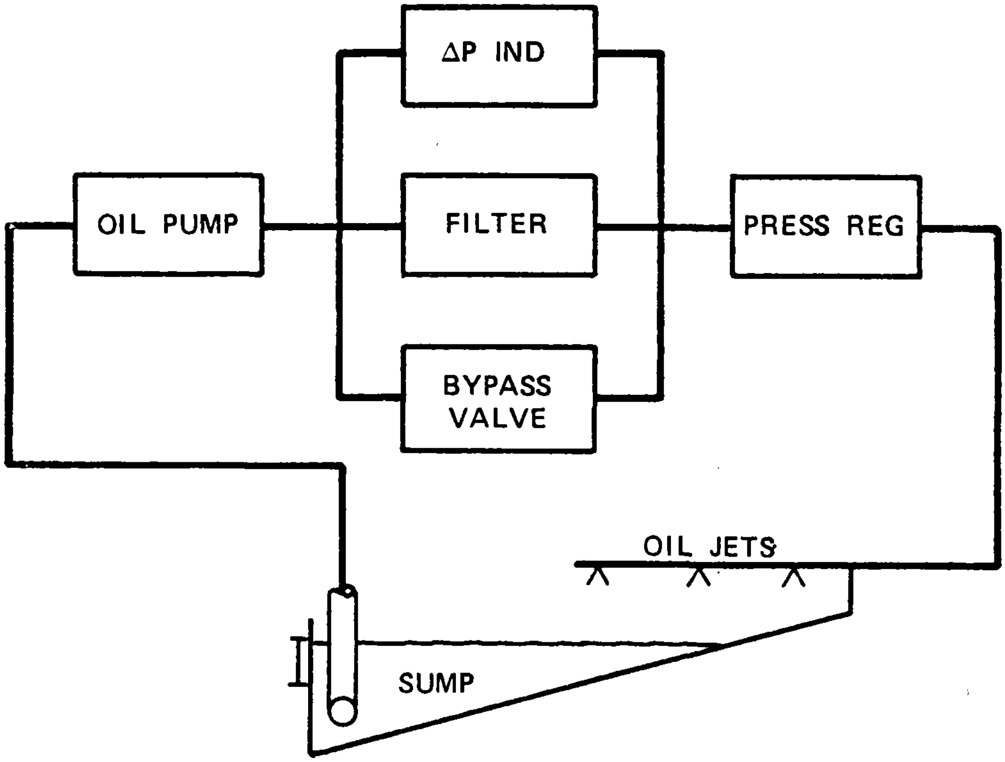

Figure 5-6. PCU Lubrication System Schematic.

The filter assembly consists of a 10 micron filter, filter cover, filter pressure drop warning indicator, filter bypass valve, and the system pressure regulating valve.

The engine gearbox sump is designed to collect return oil from the bearings, mounts, and gear jets, into a sump configured to provide lube pump pickup at any attitude from 0° to 90° in Plane "A", as shown in Figure 5-7. This technique ensures a continuous supply of oil to the pump. The design also provides gravity scavenge, sufficient dwell time, and prevents the foaming normally associated with mechanically scavenged lube systems. The sump incorporates fill and drain ports and an oil level sight glass that is located for servicing during "park" (non-operating) position.

The sump is constructed with fins to provide convection cooling of the lube system without supplemental cooling. This technique is adaptable to forced convection if unusual packaging or operating conditions dictate.

5.2.5 Starter and Subsystem

The starting energy for the gas turbine will be supplied by two 12 volt lead acid batteries connected in series and rated for 62 amp-hrs.

An automotive type 24 vdc starter will be used for starting the turbine. The starter is constructed with a solenoid-operated sliding gear to provide positive engagement during turbine start and acceleration. The starter engagement mechanism incorporates an overrunning clutch to prevent overspeeding the unit. Starter cutout is provided at approximately 65 percent speed by electronic speed sensing circuits in the engine control unit.

The starter weight is 25 pounds. A larger starter can be fitted to the same mounting pad for operation at temperatures below 25°F.

Starting energy is estimated to be 0.025 to 0.050 kW-hr per start.

5.2.6 Performance Verification Instrumentation

The instrumentation to be provided on the PCU is as follows:

(a) Thermocouples

- (1) Compressor inlet
- (2) Compressor exit
- (3) Turbine inlet
- (4) Turbine exit
- (5) Recuperator exit (exhaust)

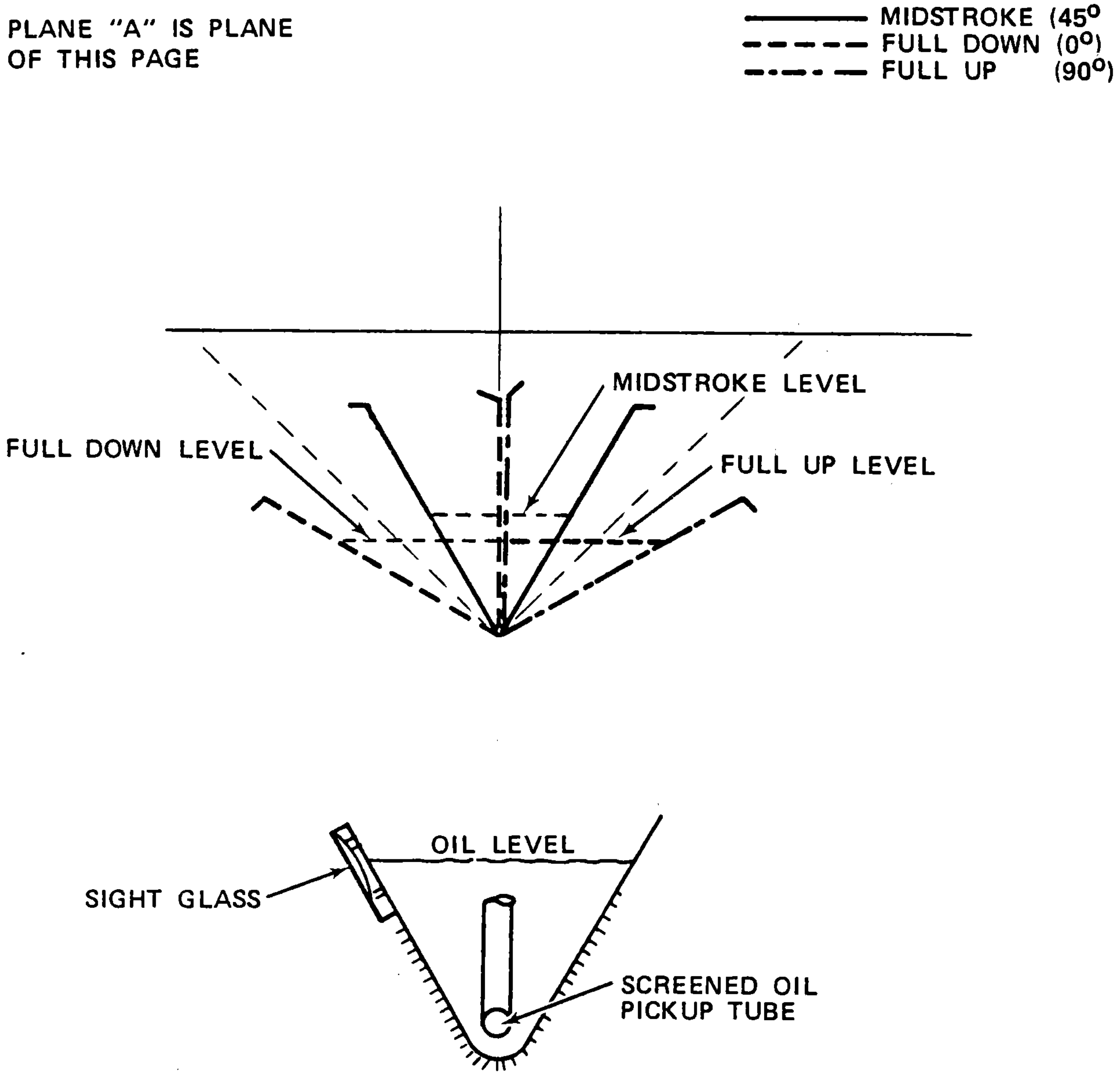

SUMP SHOWN AT 45° ~ MID TRAVEL

Figure 5-7. Engine Gearbox Sump.

(6) Recuperator-to-receiver
(7) Turbine bearing
(8) Oil sump
(9) Generator winding hot spots (external)

(b) Shaft speed sensor, independent of alternator frequency and speed

(c) Pressure sensors:

(1,2) Compressor discharge and inlet

(3,4) Recuperator pressure drops (ΔP on both high and low pressure sides)

(5,6) Turbine inlet and discharge

(7,8) Oil and fuel supply

(9) Filter pressure drop (ΔP)

(d) Vibration meters, 3 planes, (1), (2), (3)

(e) Flowmeters

(1) Fuel
(2) Oil

5.3 Configuration B

5.3.1 PCU

Configuration B is a closed gas turbine engine/generator PCU comprised of components from an existing design. The turbocompressor recommended is a development model originally designed for operation as a railcar refrigeration unit driving a 400 Hz generator. The unit was designated "PFE" as it was designed and tested under a contract with the Pacific Fruit Express.

A conceptual layout for the Configuration B engine/generator is shown on Figure 5-8. This layout illustrates the system profile as assembled on top of the solar receiver, and the relative location of the connecting ducts. The 400 Hz generator is driven by a reduction gearbox on the turbocompressor.

The unit packages completely within the shadow envelope of the reference receiver. This unit extends 51 inches beyond the top of the receiver because of the heat rejection heat exchanger (cooler). Engine B, at a total weight of 764 lbs, is the heaviest of the three configurations (A, B and C), as shown in Table 5-II. This is due

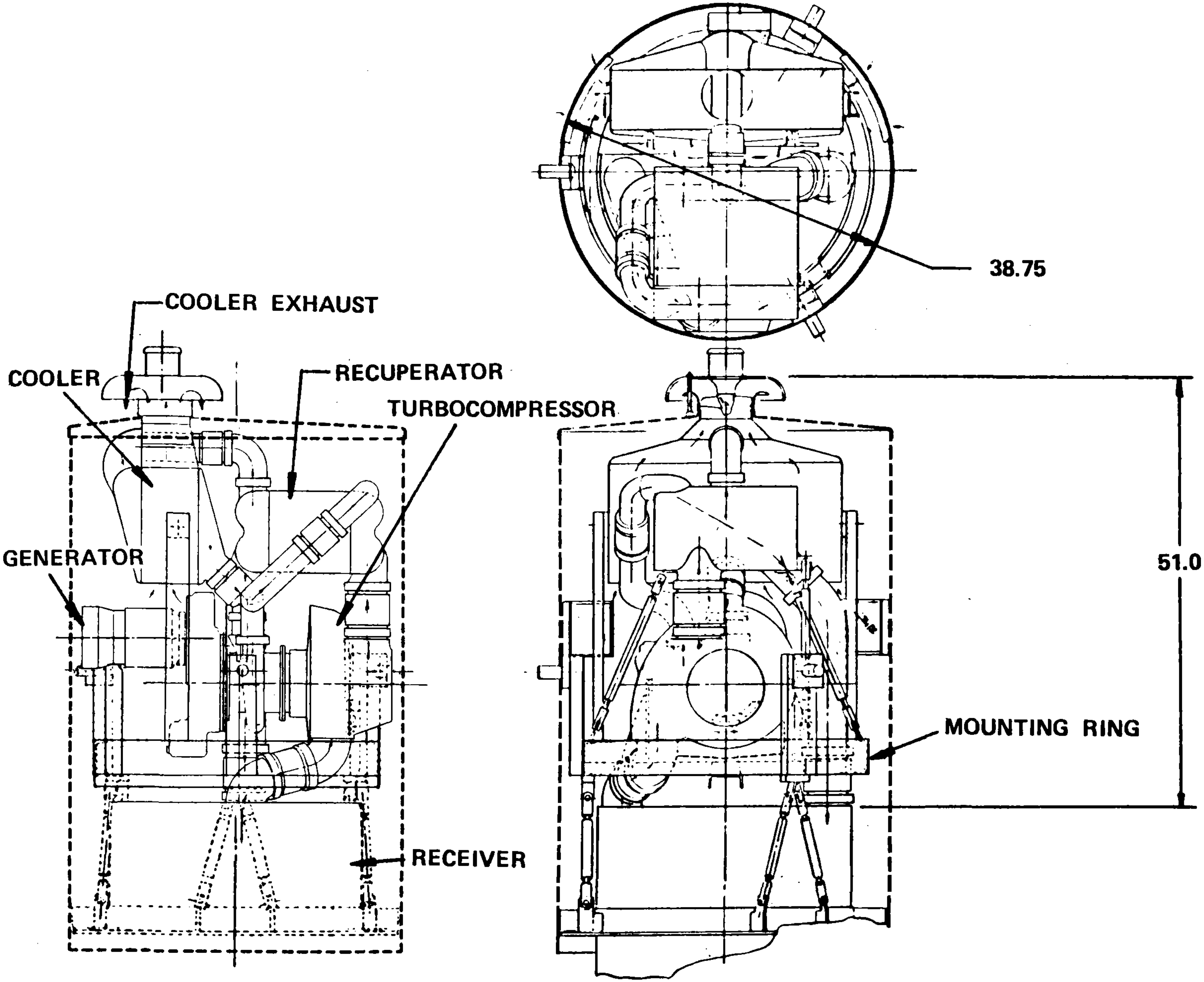

Figure 5-8. PCU Configuration B Conceptual Design.

mainly to the extra weight of the cooler. The Configuration B engine/generator is mounted in a manner similar to that described for Configuration A.

Heat is rejected through a two-pass tubular heat exchanger and atmospheric cooling air is drawn through the unit by a fan that exhausts through the top of the unit to the surrounding environment.

Ducts connecting the components would be 3.0 inch diameter CRES 347. The turbine inlet duct would be fabricated from Hastelloy-X or a non-cobalt containing alloy suitable for the temperature level. Hot ducts would be insulated as required with MIN-K or other suitable high temperature insulation.

The materials recommended for this system are listed in Table 5-V. With the possible exception of the cobalt-containing alloy, Hastelloy-X, all materials are readily obtainable and easily fabricable alloys.

5.3.2 Turbocompressor

The PFE turbocompressor (Arrangement B-3) illustrated in Figure 5-9 consists of a radial outflow compressor and a radial inflow turbine mounted on a combination of gas and oil journal bearings. A gas foil bearing is located between the compressor and turbine, and an oil-lubricated journal bearing is provided between the compressor and gearbox to handle the heavier loads imposed by the spline drive.

5.4 Configuration C

5.4.1 PCU

Configuration C is an open cycle engine/generator PCU containing aerodynamic components customized for 72.7 kW_t design input power level.

A conceptual layout for Engine C is illustrated in Figure 5-10, showing the system profile and center of gravity as assembled on top of the solar receiver. This configuration provides electrical power from a permanent magnet generator directly driven at turbocompressor shaft speed. The system fits entirely within the shadow envelope of the solar receiver, as can be seen on the plan view. The system is considerably more compact than the A or B Engine systems, and the center of gravity is considerably nearer the collector focal point, resulting in lower overhung weight.

Table 5-II lists component weights for Configuration C. The total system weight is 462 lbs, which is considerably less than either the A or B Configurations. The mounting structure for Configuration C is similar to the mounting structure described for Configuration A.

TABLE 5-V. CONFIGURATION B MATERIALS.

Turbocompressor	Turbine Wheel	Inconel 713LC
	Turbine Scroll	Hastelloy-X
	Compressor Impeller	Titanium Alloy
	Compressor Shroud	6061-T6 Aluminum
	Compressor Diffuser	AISI 1010 Steel
	Tie Bolt	Inconel 718
	Bearing Journal	Carburized 1010
	Bearing Carriers	AISI 1010 Steel
	Gearcase	Aluminum Alloy
	Gears (Typical)	AMS 6260 Steel
Recuperator	Plates and Fins	CRES 347
	Manifolds	CRES 347
	Shell	CRES 347
Ducting	Turbine Inlet Duct	Hastelloy-X

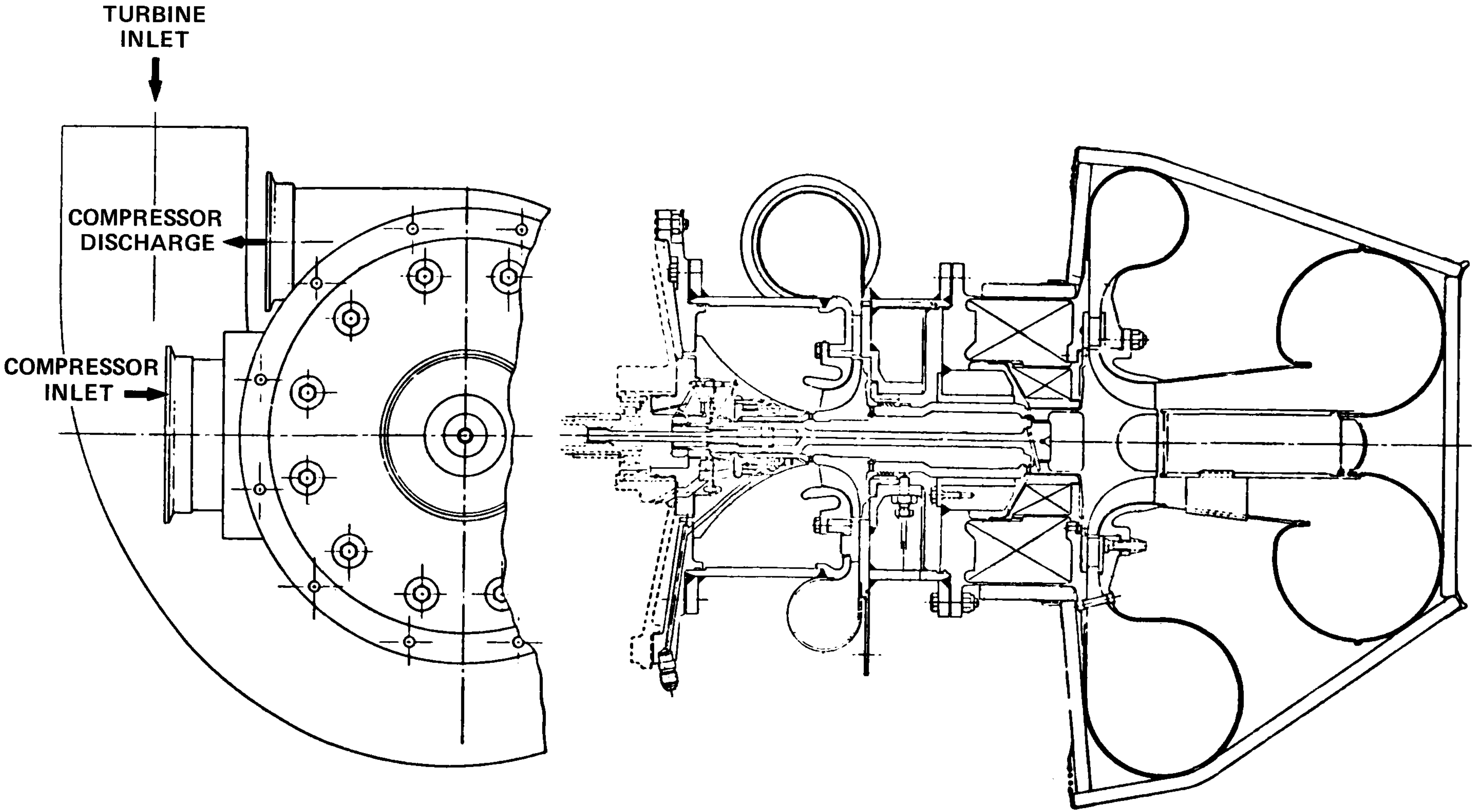

Figure 5-9. Turbocompressor - Arrangement B-3.

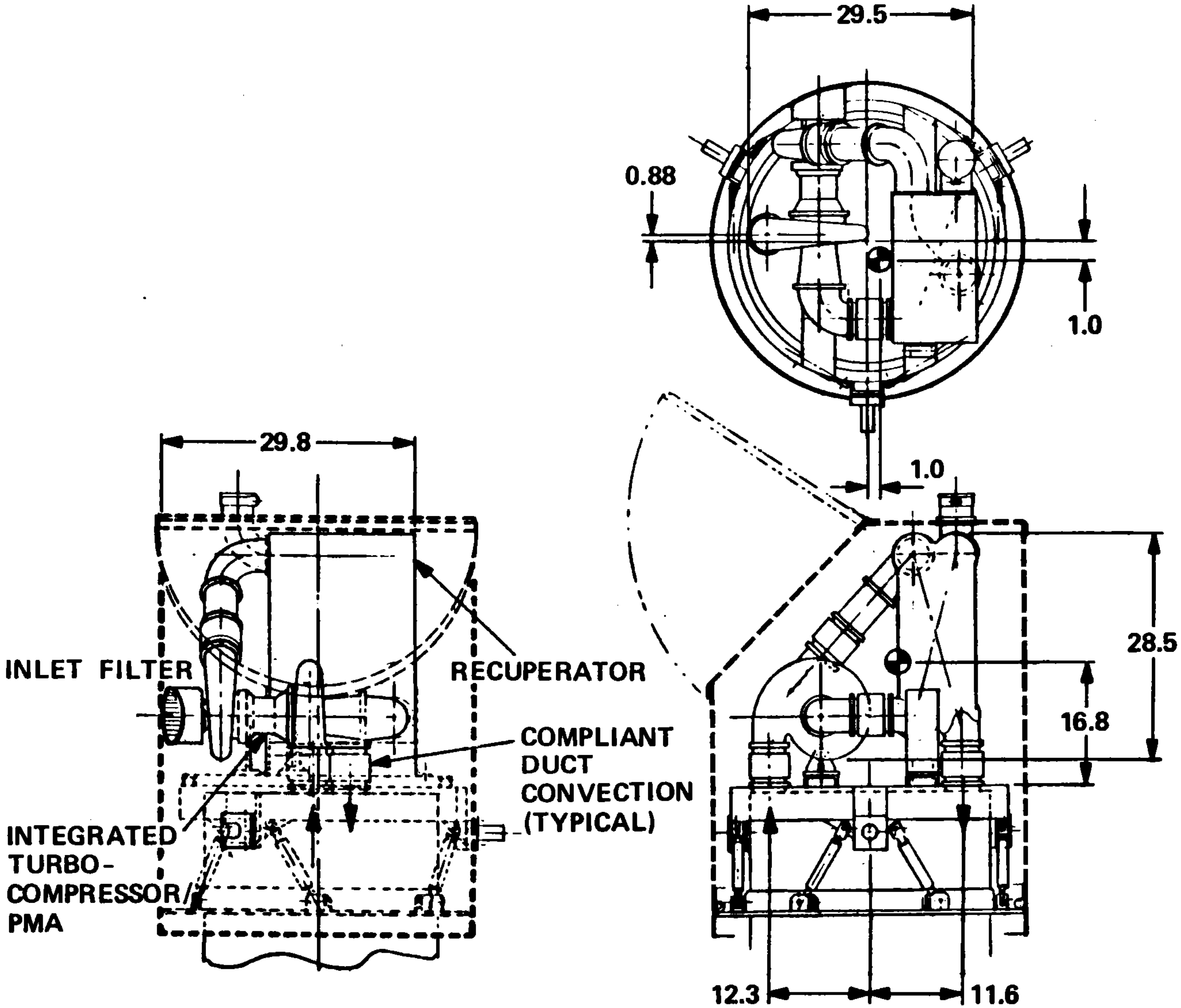

Figure 5-10. PCU Configuration C Conceptual Design.

Also illustrated on Figure 5-10 are the relative locations of the ducts connecting with the solar receiver. Component connecting ducts would be 4.0-inch diameter 347 CRES. The turbine inlet duct would be fabricated from Hastelloy-X or a non-cobalt containing alloy suitable for the temperature level. Hot ducts would be insulated as required with MIN-K or other suitable high temperature insulation. Air is drawn into the unit through a filtered inlet and exhausted to the atmosphere through a diesel engine type exhaust pivot cap or other suitable weatherproof enclosure.

5.4.2 Turbocompressor

The turbocompressor/generator for Engine C is shown in Figure 5-11. This Arrangement C-5 unit consists of a radial outflow compressor and a radial inflow turbine with a permanent magnet generator between the turbine and compressor. The entire rotating group is mounted on gas-lubricated foil journal and thrust bearings. The compact configuration of this unit is characteristic of successful designs employed on the BRU, BRU-F and Mini-BRU units developed by AiResearch for NASA in recent years.

An alternate turbocompressor configuration was designed for early applications where it might be desirable to have a removable generator. This configuration (Arrangement C-2) is illustrated in Figure 5-12. The unit has a back-to-back compressor and turbine overhung on gas lubricated foil bearings, an adaptation of the AGA and GTP36-51 arrangements. The permanent magnet generator (also supported on its own foil bearings) is driven through a coupling.

Still another alternate turbocompressor configuration Arrangement PC-5, appearing very similar to Arrangement C-5 was identified. The PC-5 Arrangement was designed for, and has materials selected as considered appropriate, for a commercialized configuration. This PC-5 Configuration was used for purposes of estimating production costs as reported in Section 8.2.

5.5 Recuperator

All first-generation engine Configurations A, B,and C were based on use of the same recuperator core design. This recuperator would be a plate-fin heat exchanger constructed by the basic bar-and-plate-fin approach as described in Section 5.5.1. High-volume production PCUs, on the other hand, will use plate-fin heat exchangers constructed with formed tube sheets. Consequently, production cost estimates for Configuration PC-5 in Section 8.2 are based on the use of formed tube sheet type of construction.

5.5.1 Recuperator for Configurations A, B, and C

The recuperator for all three Configurations A, B and C is bar and plate-fin type construction. This geometry affords considerable

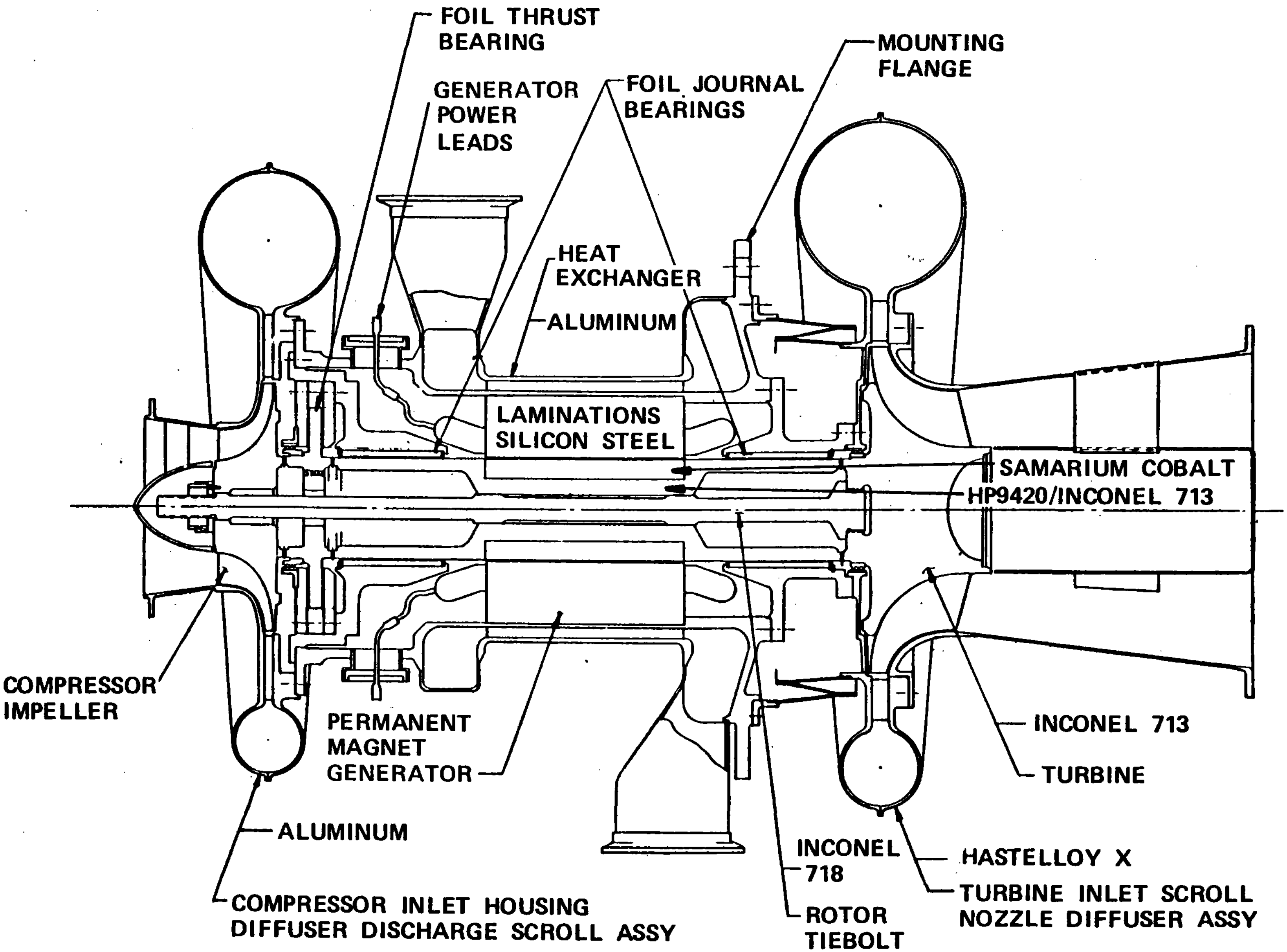

Figure 5-11. Turbocompressor and Generator - Arrangement C-5.

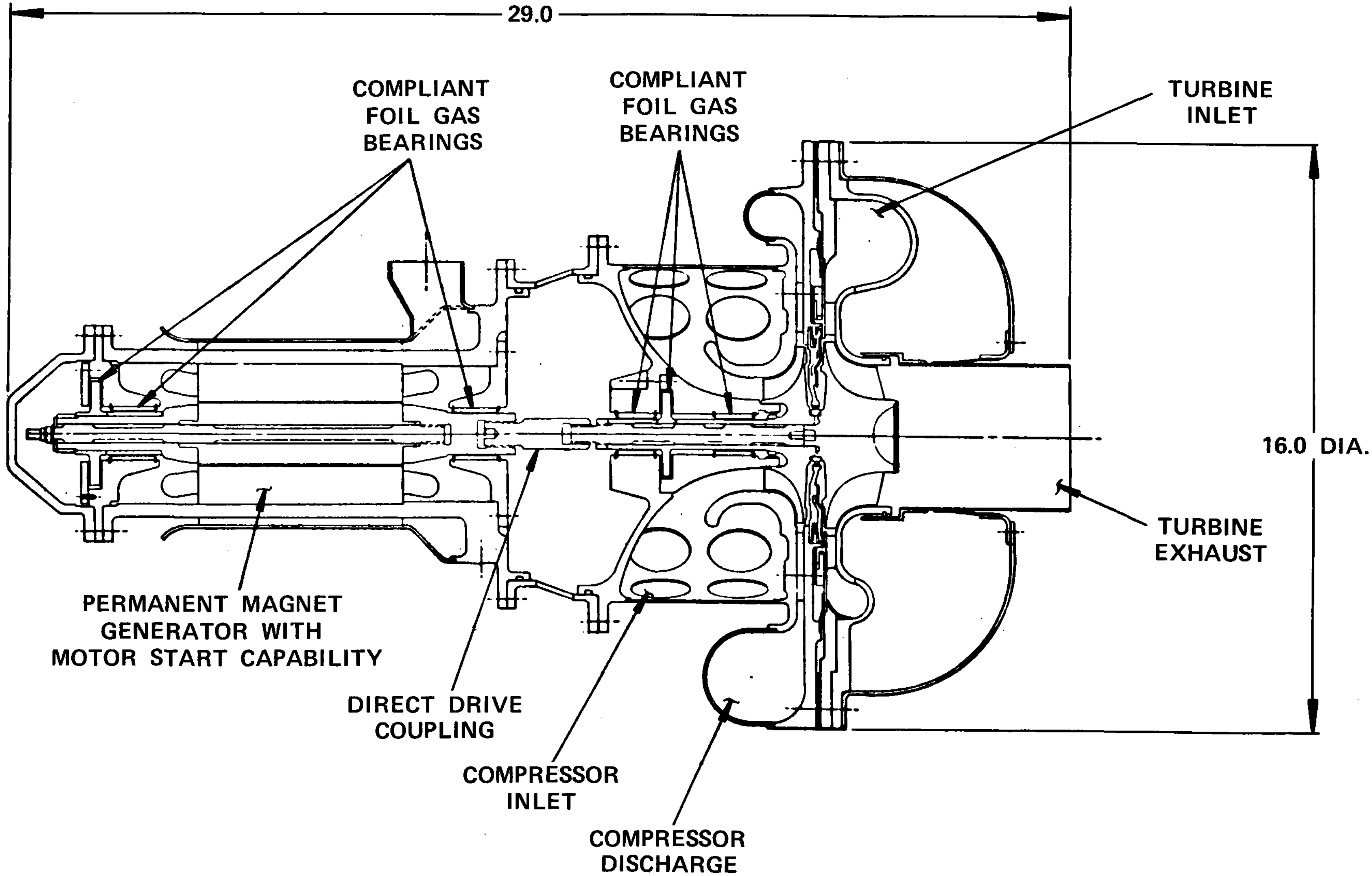

Figure 5-12. Engine C Turbocompressor and Generator - Arrangement C-2.

flexibility useful for developmental applications because the passage heights and fin form can be varied independently to provide customized units for any particular application.

Fabrication of a plate-fin heat exchanger involves stacking the plates and the chosen fin stock to obtain the desired matrix. The side walls of each fluid passage are formed by a solid bar having a height equal to the fin height and a length equal to the passage length. The stack of tube plates, fin stock, and header bars is brazed using suitable alloys to obtain an integral structure referred to as the heat exchanger core. Manifolds and duct connections are welded to the core to obtain the completed heat exchanger.

An artist's sketch of the recuperator concept is shown in Figure 5-13 and a design summary for the recuperator is presented in Table 5-VI. The construction material is 347 stainless steel. Dimensions of the counterflow section of the heat exchanger are 14.7 inches (flow length) by 9.7 inches by 19.1 inches. With the addition of crossflow end sections, the flow length dimension increases to 24.2 inches.

Heat transfer effectiveness of this recuperator when used with Engines A and C is approximately 0.918. Overall pressure loss, i.e., the sum of the low-pressure side and high pressure-side pressure loss, is 2.77 percent.

Heat transfer effectiveness of this recuperator when used with Engine B is approximately 0.912 percent. Overall pressure loss is approximately 1.98 percent.

The core of the Engine B recuperator would utilize the same core as the Engine A and C recuperators. Since Engine B is a closed cycle four header ducts would be employed rather than three as in the Engine A recuperator.

5.5.2 Formed Tube Sheet Recuperator for Production Configuration PC-5

For high-production quantities AiResearch has developed the formed plate heat exchanger. In this concept the use of header bars is avoided by employing plates that are formed to define the complete flow passage. This feature of the formed plate concept avoids the weld-over-braze operations necessary in attaching manifolds to header bar core assemblies.

In the formed plate case, core stacking merely involves stacking the alternate mating formed plates with the desired fin material sandwiched between each pair of plates. Brazing takes place at the formed lip around the plate periphery, resulting in a sheet material-to-sheet material joint. The brazed core requires only the addition of duct connections to the integral manifolds to obtain a complete heat exchanger.

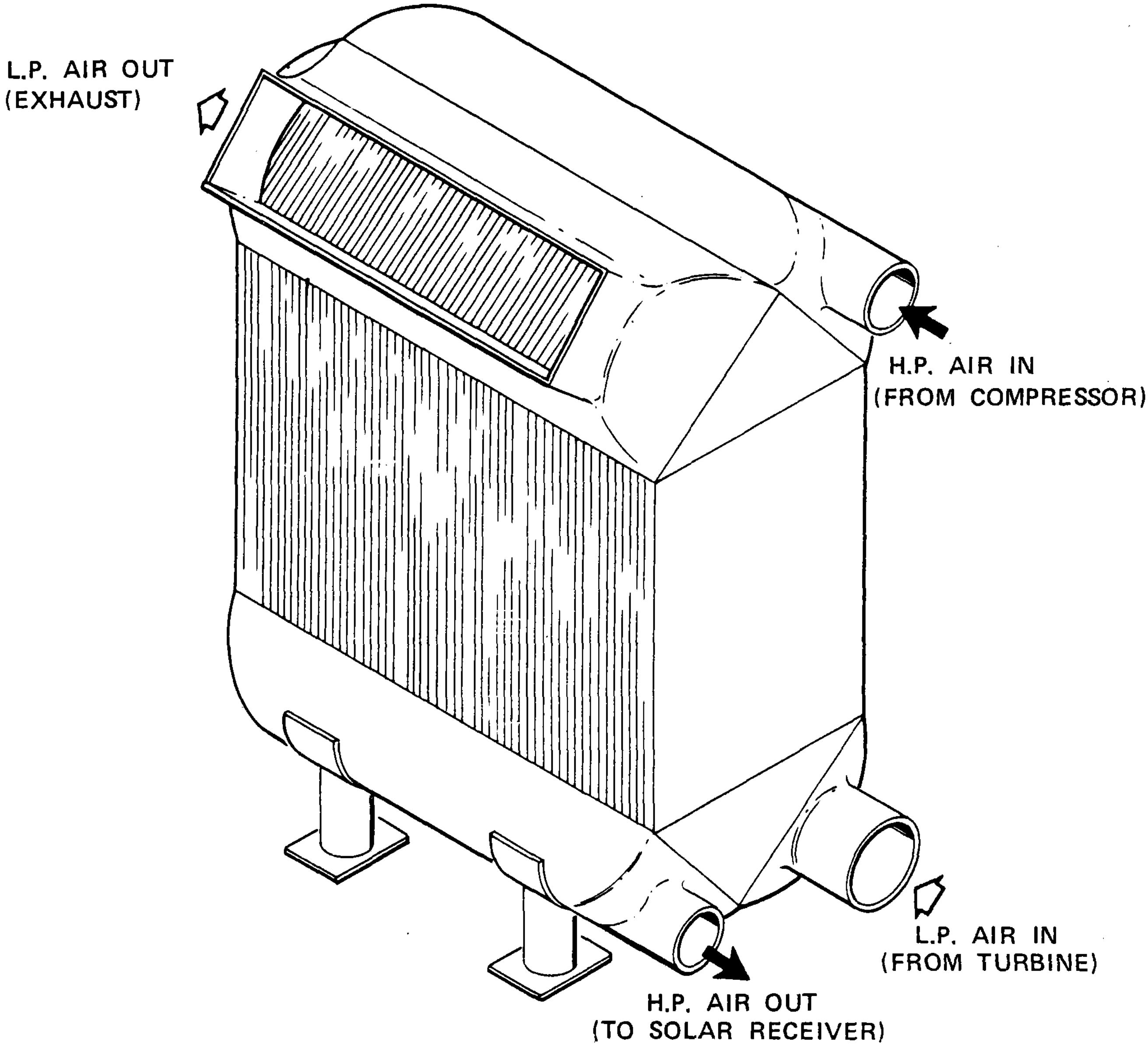

Figure 5-13. Recuperator.

TABLE 5-VI. RECUPERATOR DESIGN SUMMARY.

High-pressure side	
Fin type, counterflow	Offset Rectangular
end section	Plain Rectangular
Fins per inch, counterflow	16
end section	10
Fin thickness (in.), counterflow	0.006
end section	0.010
Plate spacing, in.	0.125
Low-pressure side	
Fin type, counterflow	Offset Rectangular
end section	Plain Rectangular
Fins per inch, counterflow	20
end section	10
Fin thickness (in.), counterflow	0.004
end section	0.010
Plate spacing, in.	0.153
Plate thickness, in.	0.015
Counterflow section length, in.	14.7
End section height (in.),	4.8
End section ratio*	0.59
Overall heat exchanger core length, in.	24.2
Heat exchanger core width, in.	9.7
Heat exchanger stack height, in.	19.1

*Ratio of projected LP passage width to core width.

An artist's sketch of the unit is shown in Figure 5-14. As discussed above, this heat exchanger will utilize the formed tube sheet method of construction rather than the conventional tube sheet/side bar "log cabin" approach.

Since special tooling is required for the tube sheets, this method of construction is most suitable for high volume production. At high production rates, the formed tube sheet design represents a low-cost approach to heat exchanger manufacture. In addition, the elimination of the bulky header bars and side bars from this configuration reduces thermal lags during start-up and shutdown and thus increases the potential cycle life of this design relative to conventional construction. The material for this heat exchanger is 409 stainless steel.

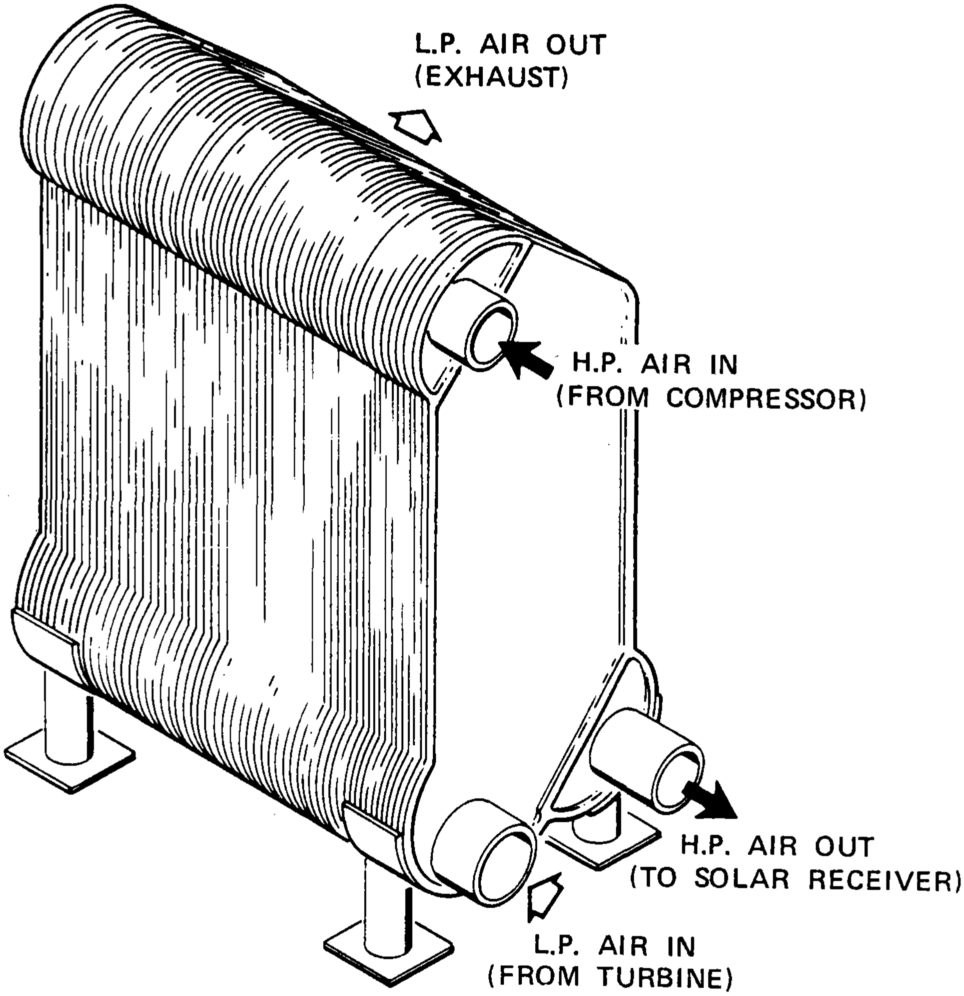

Figure 5-14. Production Recuperator for Configuration PC.

6.0 CONTROL AND STARTING SYSTEMS

The control and starting system concept for a dispersed solar plant using Brayton engines must take into account conditions or requirements such as those listed in Table 6-I. In summary, the control and starting system should be fully automatic, should be "energy source following" (rather than the more conventional "load following") and should allow efficient part power operation.

6.1 Control System Conceptual Design - Open Cycle

6.1.1 Brayton E/G Characteristics and Other Variables Influencing Control System Design

The principal variables involved in the control system design are listed in Table 6-II along with limiting values considered in the study.

Two methods of providing part-power control of the open cycle BE/G for the range of insolation and ambient conditions shown were considered:

(a) Keep N_T constant and reduce T_7

(b) Keep T_7 constant and reduce N_T

To obtain the goal of maximizing BE/G efficiency over a wide range of operating conditions, it was decided to use method (b) and control the engine to operate at design T_7 (1500°F) under all ambient conditions and levels of insolations. Comparing Curve B with Curve A on Figure 6-1 illustrates part-load efficiency advantage of this control concept. With this control concept the engine speed (N_T) will reduce as the insolation or input thermal power (Q_E) falls off, as shown in Figure 6-2. The corresponding reduction in output power (CSP) and change in efficiency (η) are also noted on this figure. Variations of ambient pressure and temperature will cause similar changes in these variables. The effect of ambient temperature on BE/G operation having a constant T_7 control is shown on Figure 6-3 and the effect of ambient pressure (altitude) is shown on Figure 6-4. The combined effect of insolation, ambient pressure and temperature is shown on Figure 6-5.

From Figure 6-5 where the values have been normalized to 1.0 at the design point, it is seen that the engine rotor speed for 72.7 kW_t rated thermal input may vary from a low of 92 percent at sea level, 10°F to a high of 111 percent at 5000 feet, 109°F. With thermal input power reduced to 30 kW_t, the engine rotor speed is 75 percent of design at sea level, 80°F and drops to 68 percent at sea level, 10°F.

TABLE 6-I. CONTROL AND STARTING SYSTEM CONSIDERATIONS - SOLAR BRAYTON ENGINE/GENERATOR.

Item	Character	Consideration
Economics	Capital intensive energy source (concentrator)	Systems should provide for good part power efficiency
Character of insolation	Intermittent, uncontrollable and unpredictable	Systems should automatically start, control and protect E/G and receiver
Load matching	Insolation availability and power demand are not coincidental	Thermal energy storage at Brayton engine temperatures is not attractive Electrical energy storage in large quantities is not attractive Wasting excess energy through load banks increases average cost of energy used Therefore systems should allow delivering all power available to an infinite grid
Flexibility		System should allow stand alone operation

TABLE 6-II. VARIABLES AFFECTING CONTROLS - OPEN CYCLE.

Variables	Constraints
<u>Operating Condition Variables</u>	
Insolation (affecting engine thermal input, Q_E)	30 kW_t to 72.7 kW_t
Ambient temperature (affecting compressor inlet temperature, T_1)	+10°F to +140°F at sea level -20°F to +109°F at 5000 ft
Ambient pressure (affecting compressor inlet pressure, P_1)	Sea level to 5000 ft
Load demand (affecting applied load, CSP)	Assumed to be capable of absorbing all power produced
<u>Independent Control Variables</u>	
Applied load on E/G (CSP)	Controlled by control rectifier
<u>Dependent Variables</u>	
Turbine inlet temperature (T_1)	
Rotor speed (N_T)	
BE/G efficiency (η = CSP/Q_E)	

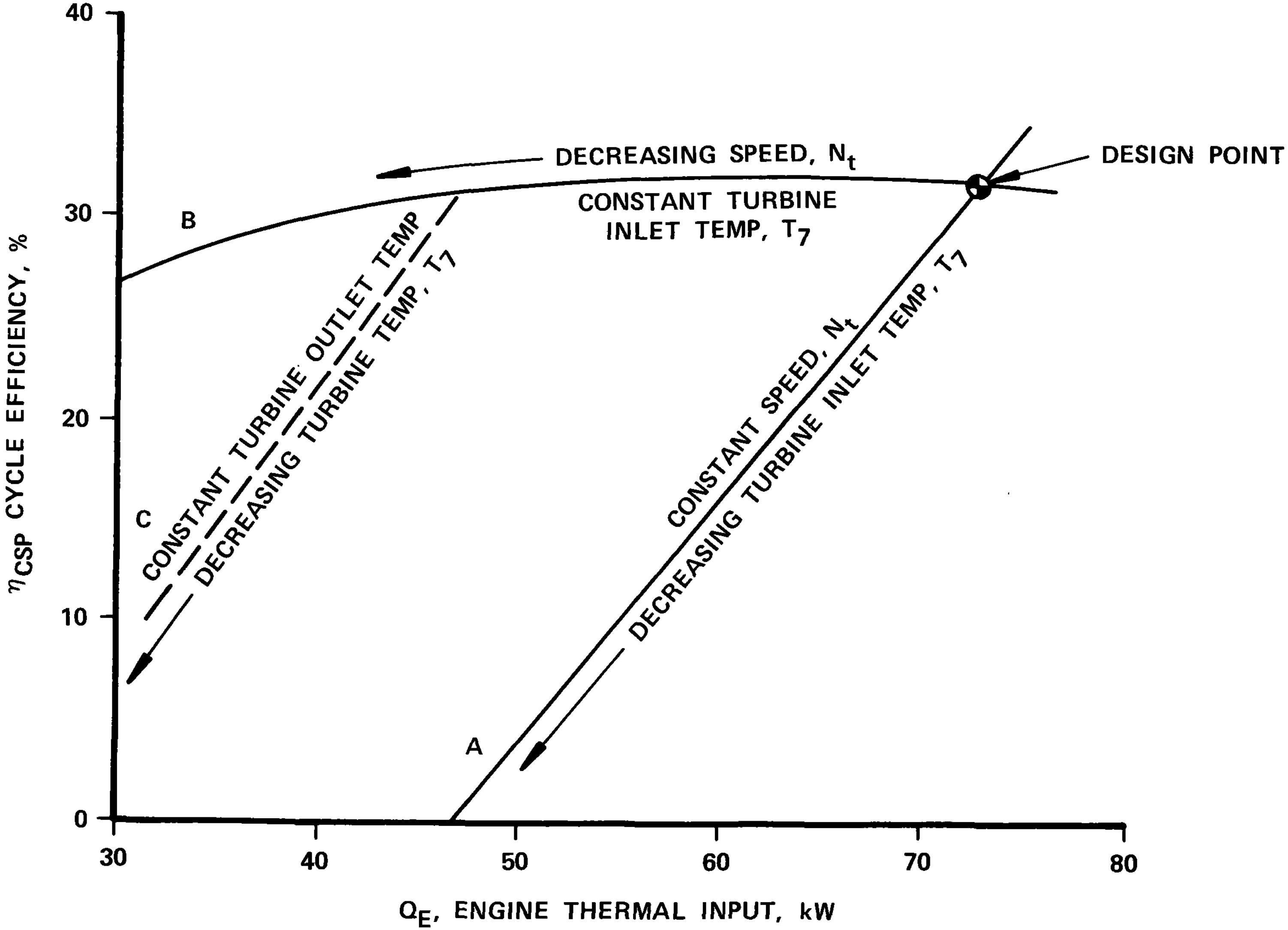

Figure 6-1. Part Power Control Modes.

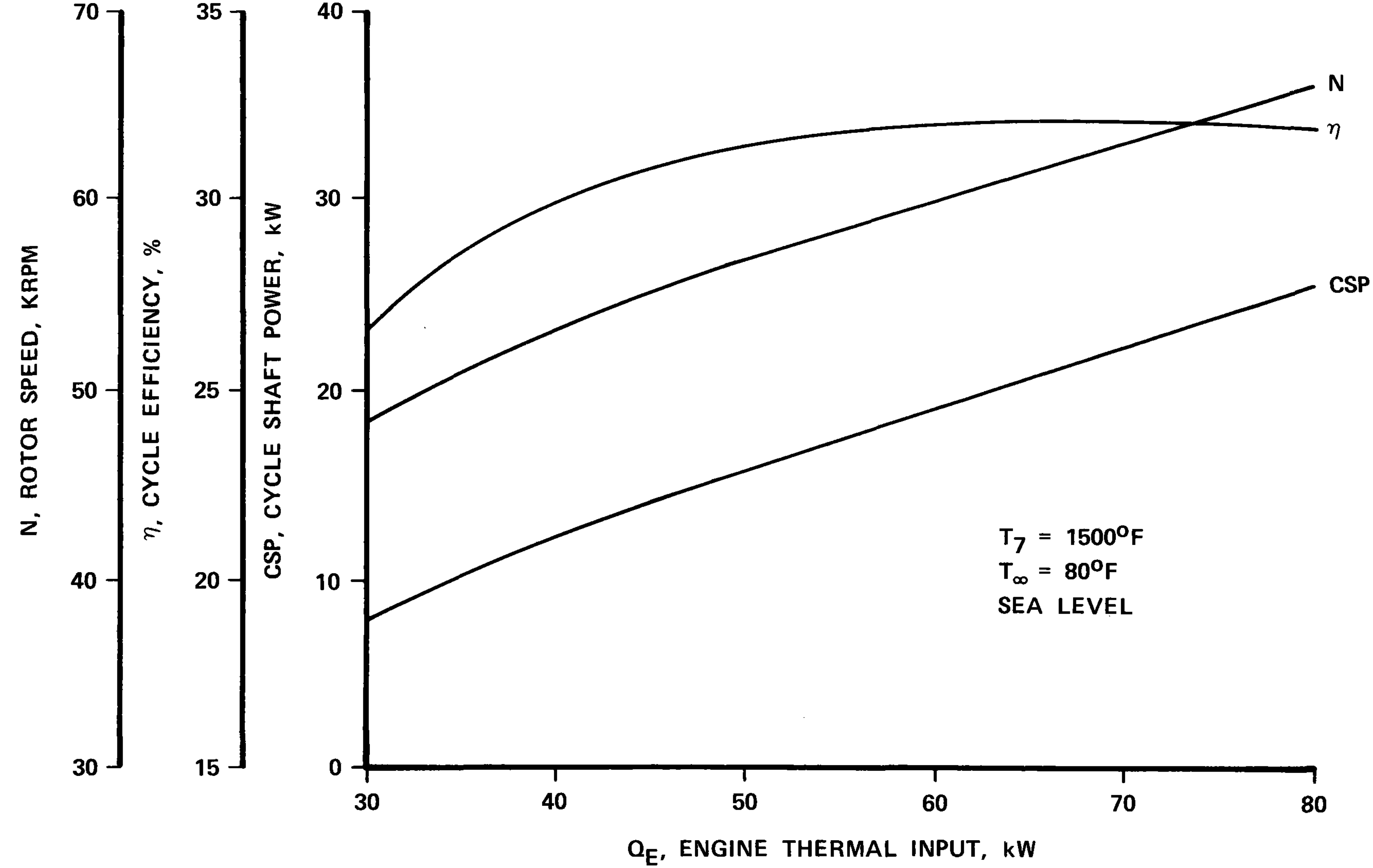

Figure 6-2. Effect of Thermal Input Variation.

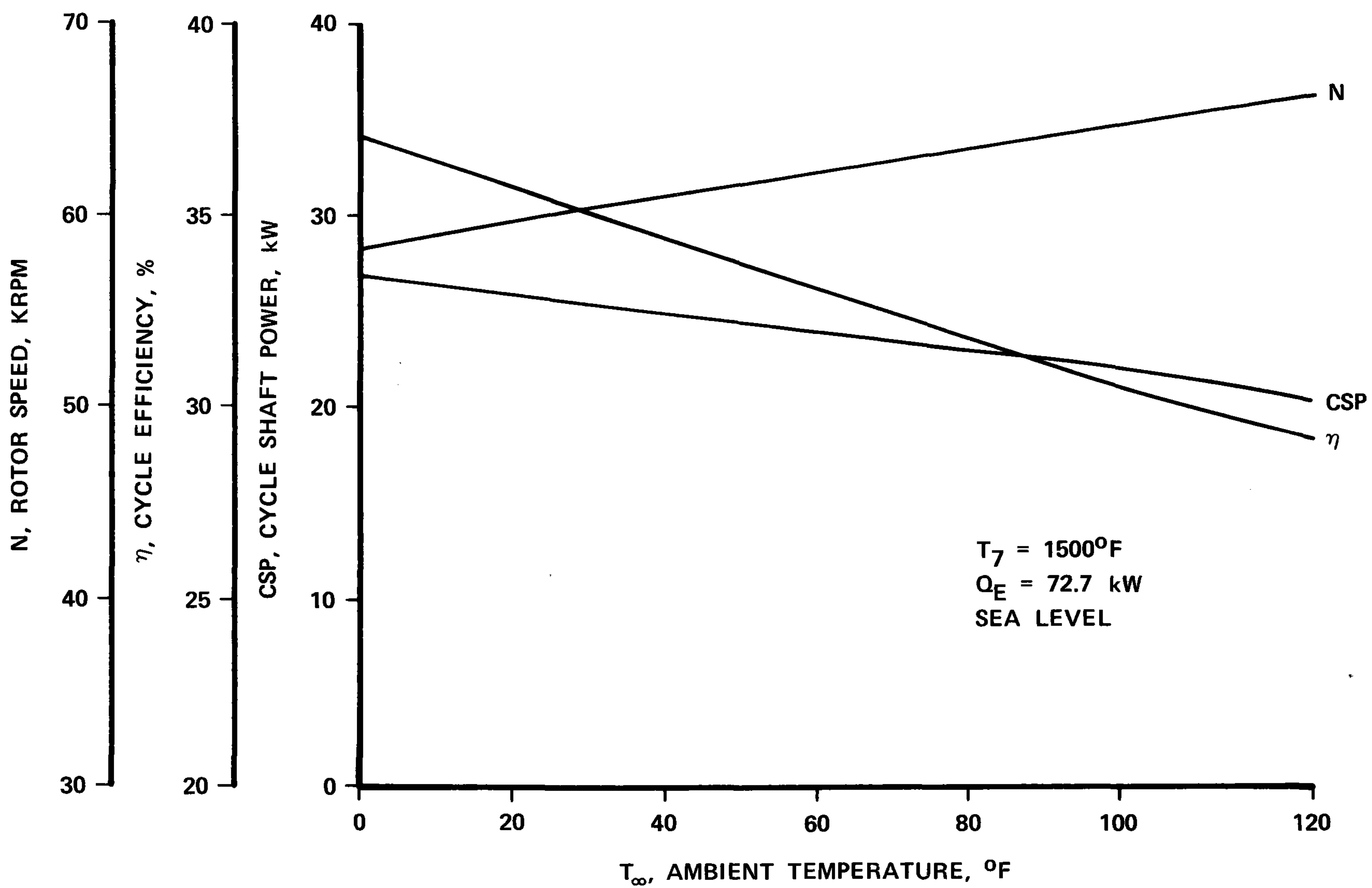

Figure 6-3. Effect of Ambient Temperature Variation.

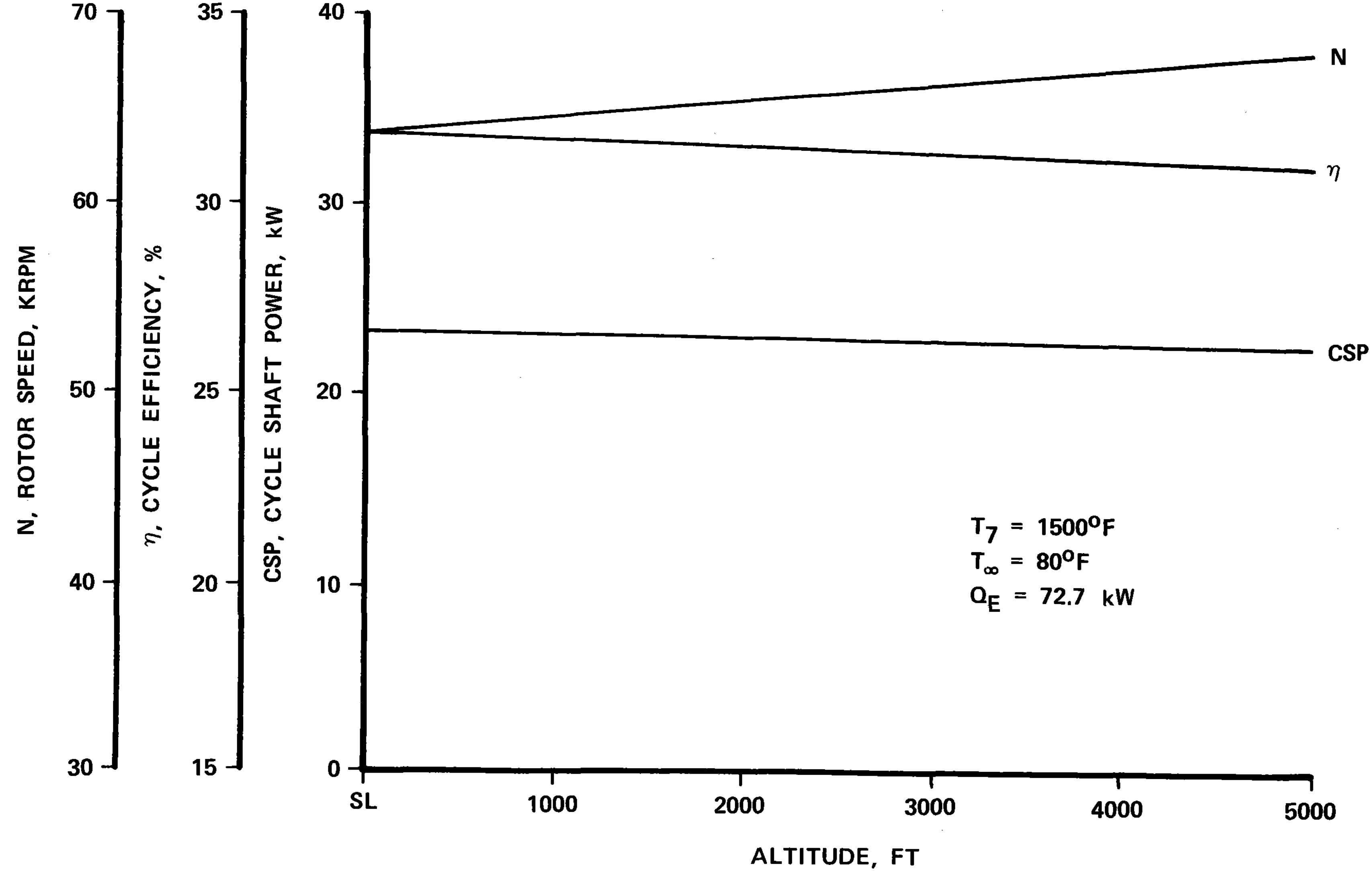

Figure 6-4. Effect of Altitude.

RELATIVE TO DESIGN POINT

5000 FT -20°F	INSOLATION DESIGN	INSOLATION LOW
ENGINE SPEED	0.95	0.70
ENGINE FLOW	0.94	0.56
ENGINE POWER	1.23	0.46

CONDITIONS:

TURBINE INLET TEMPERATURE - 1500°F

POWER LEVEL	INSOLATION INTENSITY	Q_E
DESIGN	1.0 kW/M^2	72.7 kW
LOW	0.4 kW/M^2	30.0 kW

5000 FT 109°F	INSOLATION DESIGN	INSOLATION LOW
ENGINE SPEED	1.11	0.83
ENGINE FLOW	0.95	0.56
ENGINE POWER	0.86	0.35

SEA LEVEL 10°F	INSOLATION DESIGN	INSOLATION LOW
ENGINE SPEED	0.92	0.68
ENGINE FLOW	0.99	0.61
ENGINE POWER	1.17	0.42

SEA LEVEL 80°F	INSOLATION DESIGN	INSOLATION LOW
ENGINE SPEED	1.00	0.75
ENGINE FLOW	1.00	0.61
ENGINE POWER	1.00	0.37

DESIGN POINT

SEA LEVEL 140°F	INSOLATION DESIGN	INSOLATION LOW
ENGINE SPEED	1.07	0.80
ENGINE FLOW	1.01	0.61
ENGINE POWER	0.81	0.31

Figure 6-5. Estimated Off-Design Control Characteristics.

As power level is reduced with a constant T_7 control, the resulting rotor speed decrease causes the turbine exit temperature (T_{10}) and recuperator inlet temperature (T_{11}) to increase as shown by the operating line on Figure 6-6. For some BE/G designs, there may be a T_{10} or T_{11} temperature limit based upon the turbine exducer or recuperator material properties. If so, there will be some low value of power level (hence low rotor speed) below which the constant T_7 control must be biased to avoid exceeding the T_{10} or T_{11} limits. This will cause T_7 to fall below its otherwise constant 1500°F design value. The effects of such a case is illustrated by Curve C on Figure 6-1.

6.1.2 System Control Conceptual Design

The constant turbine inlet temperature variable speed control concept is shown in Figure 6-7. Actual turbine inlet temperature is compared to the temperature setpoint (1500°F) to provide an error signal. This error signal is conditioned to generate a speed setpoint which is compared to actual speed. The resulting error signal generates a current command signal, which is sent to the control rectifier as shown in Figure 6-8. The control rectifier modifies the output current until it equals the current command. Increasing or decreasing the actual current, increases or decreases, respectively, the load on the generator. A change in load, changes the engine speed, thereby closing the speed control loop. Increasing or decreasing the speed, decreases or increases the temperature respectively, thereby closing the loop on temperature.

The control portion of the control rectifier is a transistorized chopper circuit. The chopper circuit is a duty cycle modulator whose output voltage is its input voltage multiplied by the duty cycle.

Rated output current from the control rectifier is 94 amps at 213 v. This load current can be varied electronically by the input current command from the engine controller. A command voltage varying from 0 v to ±10 v scales to a load current ranging from 0 to 100 amps dc. The control logic compares the output dc current to the current command and automatically adjusts the chopper duty cycle to attain the commanded current. The control logic derives operating power from the variable frequency generator power.

The control rectifier is packaged in a natural convection cooled cabinet measuring 20 in. wide x 15 in. deep x 21 in. high. The estimated weight is 75 pounds. The estimated full load efficiency is 96 percent.

6.2 Engine Startup and Shutdown

When the concentrator has been pointed towards the sun and the insolation has increased so that the receiver is hot enough to start engine operation, the engine control will receive a signal and initiate the start sequence. The starter motor will engage and accelerate

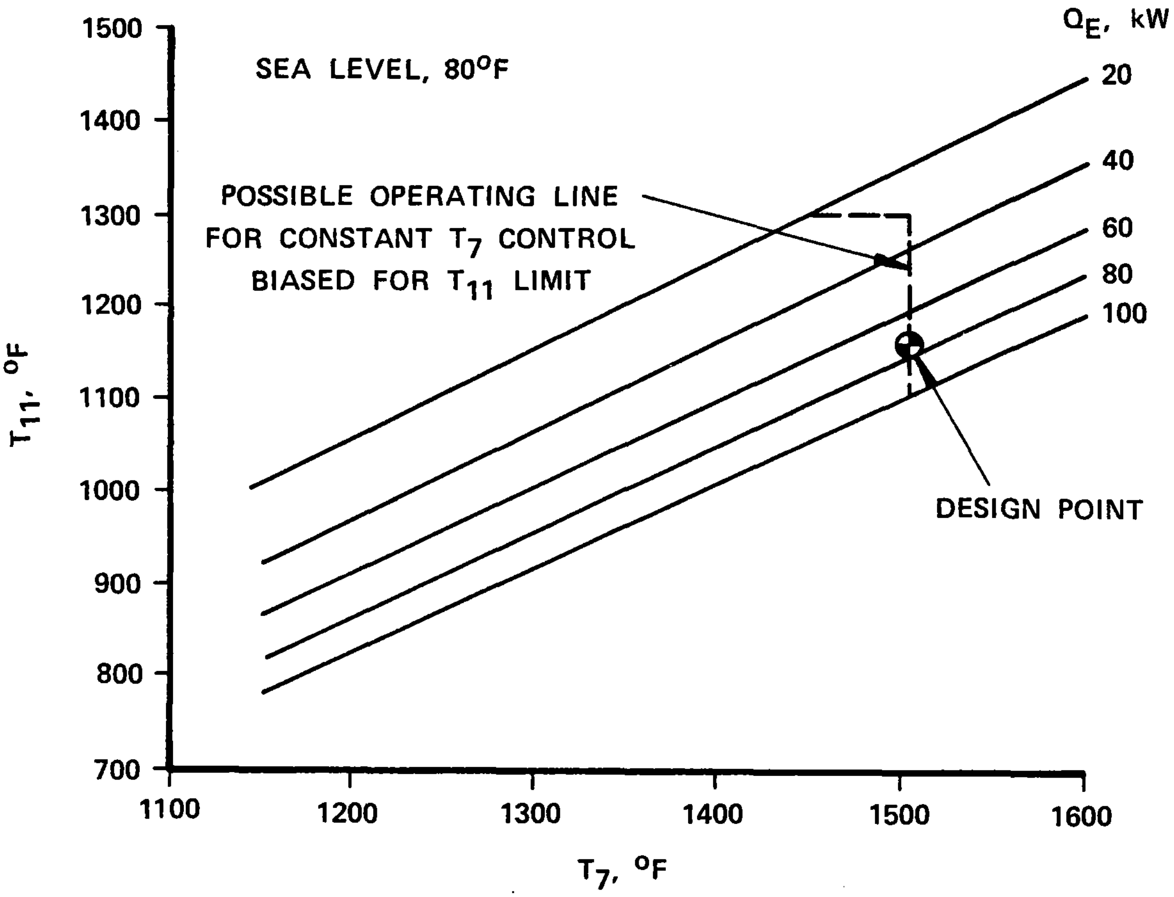

Figure 6-6. Recuperator Inlet Temperature, T_{11}.

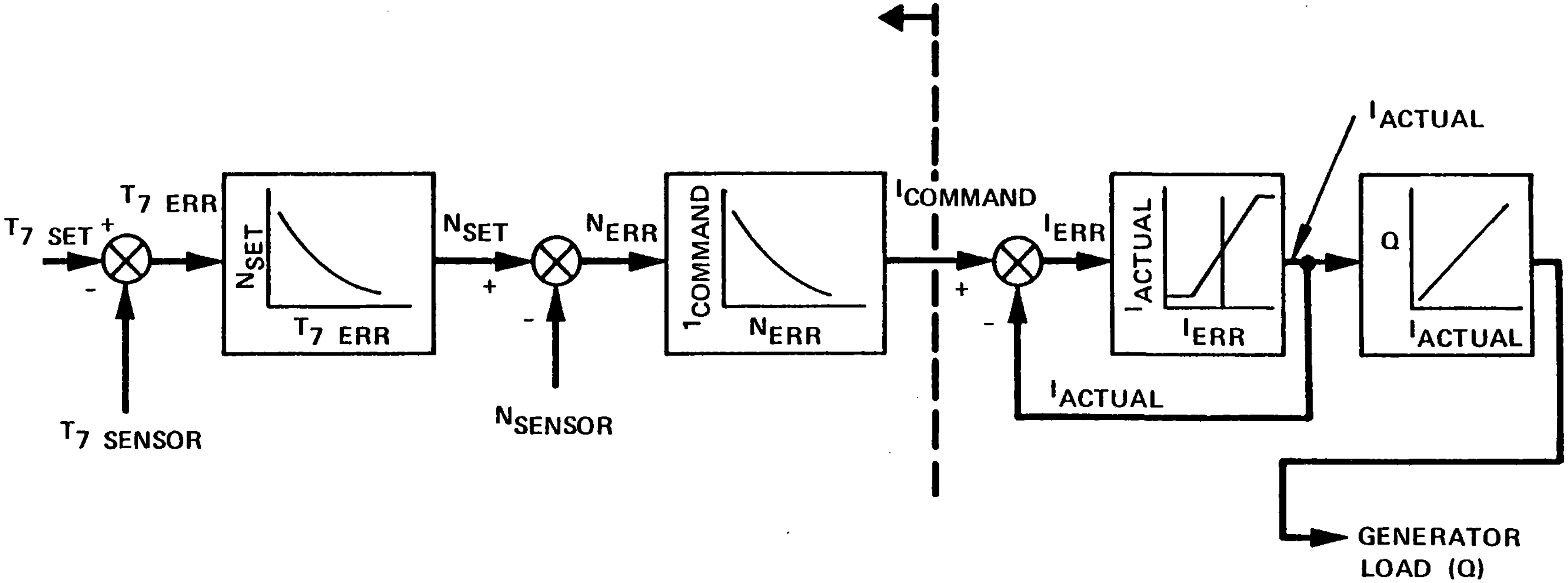

Figure 6-7. Turbine Inlet Temperature/Speed Control Scheme.

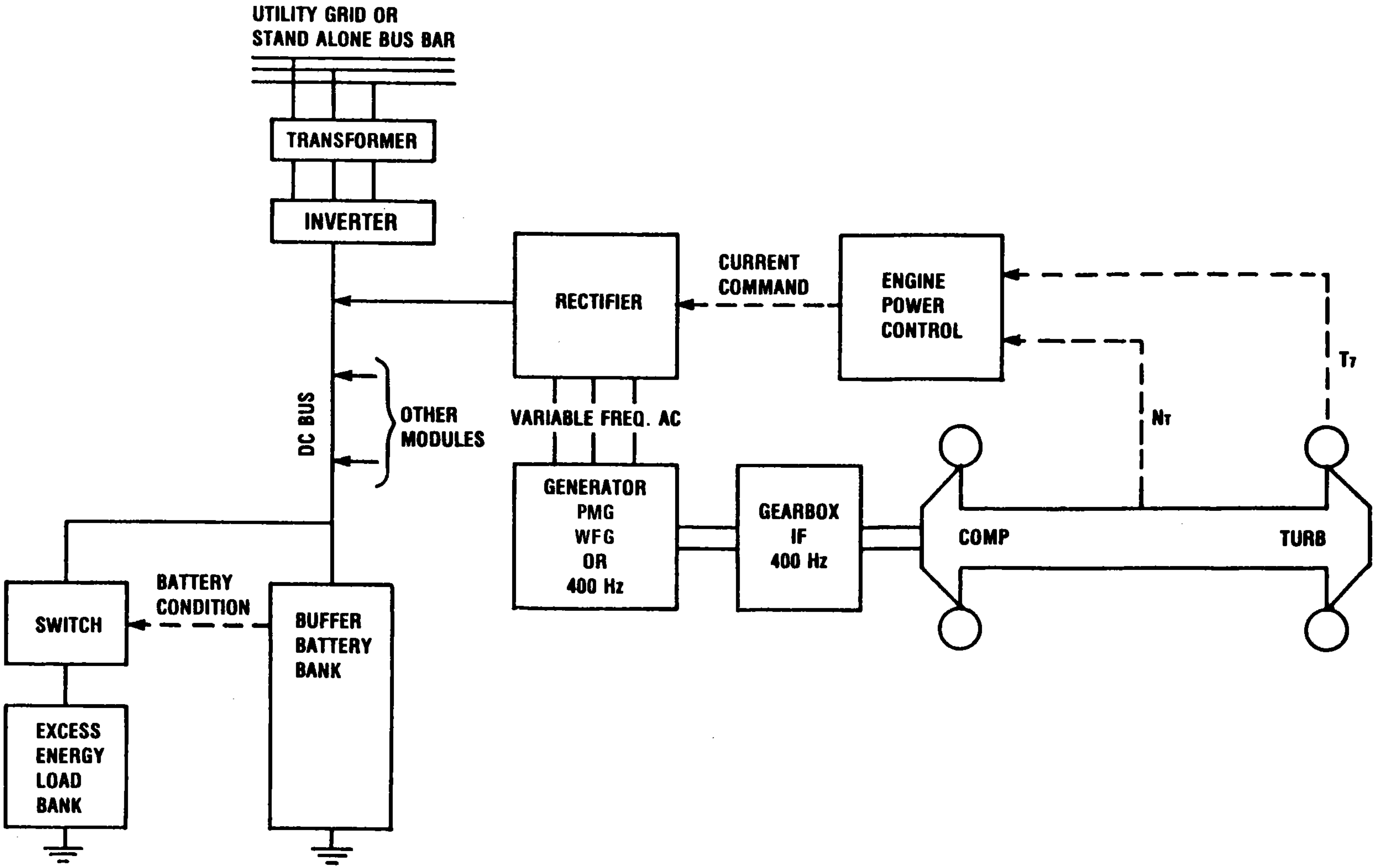

Figure 6-8. Control and Power Conditioning Concept.

the turbocompressor to approximately 65 percent speed. After T_7 increases, the engine should be self-sustaining at this speed and the starter motor will disengage. Since the control logic normally attempts to increase T_7 to 1500°F by reducing N_t, the N_t logic must contain a low N_t limit that is greater than the self-sustaining speed to allow the start cycle to continue. As the insolation increases, turbine inlet temperature will increase to 1500°F and, with further increases, the speed setpoint will be continuously reset upward to maintain a constant 1500°F turbine inlet temperature.

A preset interval timer will start when the starter motor is engaged. The engine control will turn off the starter if the engine does not reach self-sustaining before expiration of the time interval. This is to prevent starter motor damage, which might result, for instance, from a reduction in insolation during startup, allowing the motor to continue running.

In a normal shutdown, the insolation decreases and the N_t setpoint decreases in order to maintain 1500°F turbine inlet temperature. When the N_t setpoint reaches approximately 65-percent speed, the turbine inlet temperature will begin decreasing and, with further decreases in insolation, the engine output power will continue to drop until the engine is no longer self-sustaining. At this point, the engine will decelerate to zero speed.

6.3 Protection Logic

Two conditions are envisioned that will require provisions for avoiding damage to the equipment.

- o Receiver outlet or turbine inlet over-temperature
- o Rotor overspeed.

Should an overtemperature condition or an overspeed condition be sensed, the control will provide a signal to turn the concentrator away from the sun and shut down the BE/G and module. Should subsequent transient analysis of the solar power module show these provisions to be too slow, a fast response valve can be used to bypass flow or thermodynamic energy to provide rapid response to the overspeed and/or overtemperature condition, thus allowing time for the concentrator to be directed away from the sun.

7.0 ENGINE/GENERATOR INTERFACES

7.1 Environment - Attitude With Respect to Gravity

The engine/generators are designed to be mounted at the focus of a concentrator such that the engine will be subjected to a variety of attitudes both while operating and not operating. The required range of attitudes for oil-lubricated Configurations A and B was limited by considering them applicable only to azimuth over elevation type concentrator mounts (as distinct from equatorial mounts). Figure 7-1 shows an azimuth over elevation concentrator in a typical sun tracking position. Daily tracking of the sun is accomplished by a combination of azimuth positioning and elevation positioning. Azimuth positioning rotates the base in a plane normal to the earth's local gravity vector, while elevation positioning tilts the mirror centerline relative to this plane. The daily elevation motion of the Brayton engine/generator assembly relative to the earth's gravity vector will not exceed a maximum of 90° total excursion as shown in Figure 7-2. If the B/EG is designed so the axis about which the turbocompressor rotor turns is oriented perpendicular to the axis of the concentrator and normal to the earth's gravity vector, the oil-lubricated bearings and oil sump will experience a total of only 90° roll motion, and no pitching.

By selecting 45° elevation as the normal design position for Configuration A or B, the BE/G oiling and scavenging systems need to be capable of accommodating only ±45° roll motion. Since the existing hardware selected for the A and B turbocompressors does not now possess this capability, some redesign will be required to accommodate this range of roll motion.

Configuration C should be inherently capable of operation at any roll and pitch attitude, hence offering more freedom of design choice relative to the concentrator mount system and the layout of the turbocompressor within the BE/G assembly. However, extra design attention must be given to any turbocompressor installation that requires an operation over a significant range of pitch attitudes. Thrust bearing loads and stability of the journal bearings must be considered as the axis of rotation departs from the conventional perpendicular relationship to the earth's gravity vector.

Stowing the concentrator and returning the concentrator to the morning position at nightfall will cause the BE/G attitude to change at the rate of 30° per minute through 240° of azimuth and/or 90° of elevation. The engine/generator should not experience unacceptable gyroscopic or other reactions from angular velocities of this magnitude.

If the concentrator stow position is face down (i.e., the concentrator collector axis vertical downward), this would increase the roll motion on the engine to ±90°. This would impose an additional

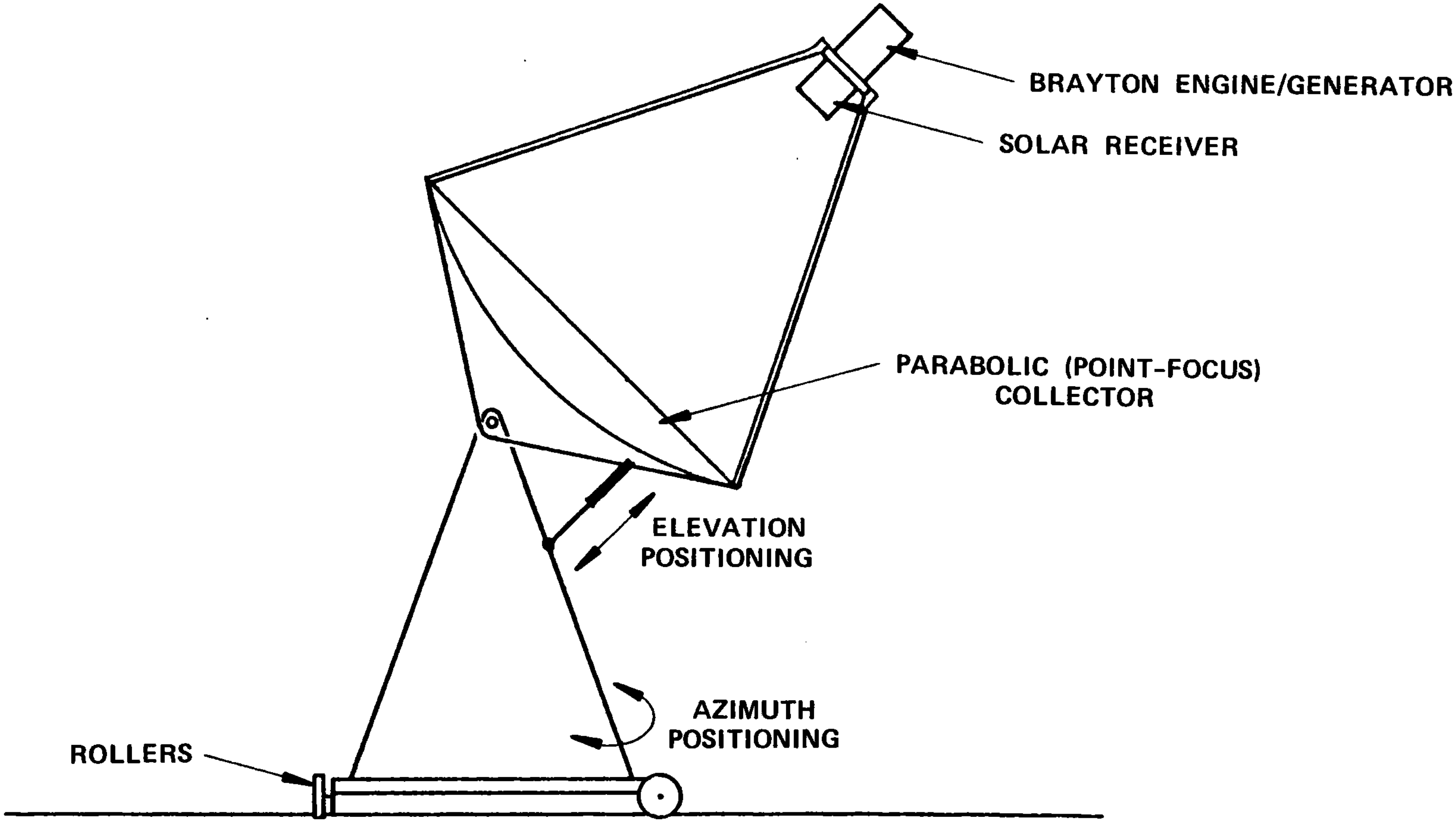

Figure 7-1. Typical Solar Tracking Position.

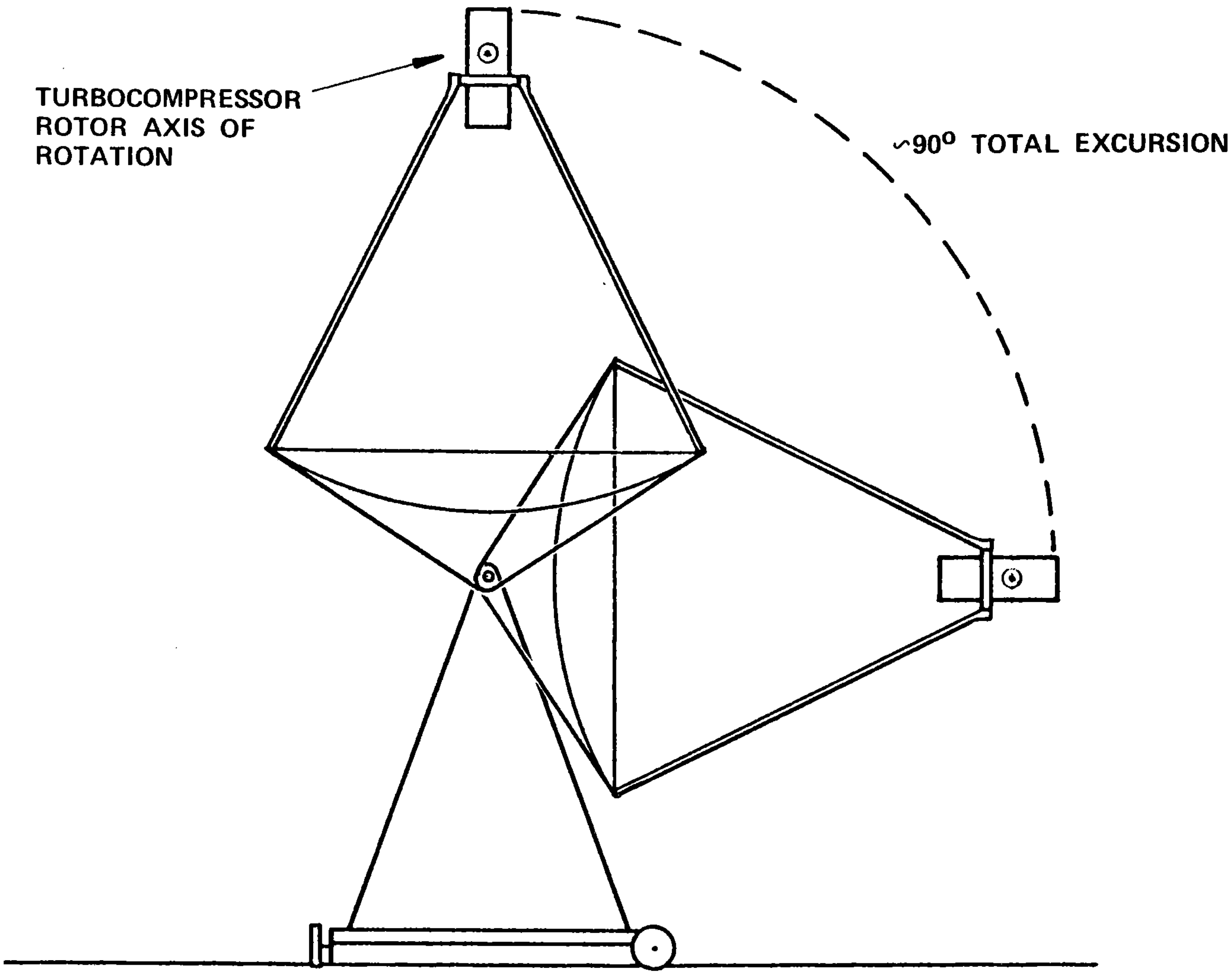

Figure 7-2. Solar Tracking Attitude Extremes.

requirement on the gearbox design. The gearbox design work (and hardware modifications) would be more extensive if the BE/G were required to be operational while in the -90° attitude. (This operational requirement would arise only in the case of a hybrid BE/G).

7.2 Environment - Ambient Pressure, Temperature, Sand, and Dust

Environmental interfaces are considered to include the effect of ambient pressure and temperature, wind, sand and dust. The design altitude range is from sea level to 5000 ft, the design ambient temperature range is -20°F to +109°F at 5000 ft and +10°F to +140°F at sea level, and the design air conditions include blowing sand in wind to 30 mph with gusts to 50 mph. The effects of ambient pressure and temperature on performance are covered in Sections 4.0 and 6.1, in which performance at off-design ambient are estimated for the three Configurations A, B, and C. The ambient pressure and temperature range is expected to fall well within the operating capability limits of the oil lubrication systems for Configurations A and B, and the gas bearing system for Configuration C. Likewise, the effects of wind on E/G performance and control stability should not be significant. Blowing sand will be accommodated by an inlet air filter that will require service at intervals depending on the severity of the entrained contaminants.

7.3 Noise

The major sources of noise in a gas turbine engine are aerodynamic phenomena (compressor and turbine blade passing and broadband noise) and phenomena associated with gear meshing. For an AiResearch generator set utilizing an unrecuperated GTP36-51 gas turbine, typical noise levels around the generator set at a 25-foot radius vary from 74 to 78 dBA at a 20 kW load condition.

The BE/Gs discussed in this report differ from conventional open cycle gas turbines due to the presence of the inlet air filter, insulation, and the recuperator. These three features are expected to substantially attenuate engine noise levels from all sources except the gearbox.

Gearbox noise will remain present in Engines A and B, but is not expected to be at levels that would be of concern. Engine C, which is mounted on gas bearings and is without a gearbox, is expected to be even more quiet.

7.4 Mechanical Interfaces

The engine/generator mechanical interfaces with the rest of the system are listed below. These interfaces appear readily amenable to normal analysis and design with the possible exception of the exhaust duct to atmosphere.

- Hot ducts to and from receiver

  4.0-inch diameter for Configuration A and C
  3.0-inch diameter for Configuration B

- Receiver temperature sensor lines (estimated quantity - 2)
- Structural tie with receiver and concentrator frame
- Control and instrumentation lines
- Electrical power output lines
- Starter motor power lines
- Exhaust duct to atmosphere

The heat exhaust from a solar only engine will be clean air and only pressure drop, temperature and possible atmospheric distortion effects will be of concern in the design phase. For hybrid engines employing fossil fuel combustion, the possibility of contaminating the concentrator surface must be avoided.

8.0 PRODUCTION IMPLEMENTATION

Production implementation task objectives were to assess the technology status, production cost, durability and growth potential for production (or commercialized) versions of open and closed cycle Brayton engines. To facilitate the accomplishment of this task, a production configuration was defined and used as a basis for discussion. This production configuration is an open cycle Brayton engine and was identified as Configuration PC-5. Figure 8-1 depicts this configuration, which differs only slightly from the first generation engine, C-5. The differences are in configuration of detail parts to facilitate mass production and use of appropriate materials. The materials assumed for PC-5 are listed on Table 8-I.

8.1 Technology Status

8.1.1 Production Methods and Component Technology

Production methods were assessed to determine those that might be cost effective for producing the PC-5 configuration at a rate of 10,000 to 100,000 units per year. Table 8-II lists some of the production methods identified for the compressor, recuperator and permanent magnet generator. Table 8-III tabulates key components and an estimate of the development status of the technology for each.

Keeping in mind that the production and component technologies listed in Tables 8-II and 8-III relate to the PC-5, an engine intended for high production rates, it is important to examine to what extent these technologies will be demonstrated in Configurations A, B and C, selected as first-generation engines for test in 1980 and 1981-2. It is impractical to tool up for use of mass production methods for annual production rates in the range from 1 to 100 or even 1000, which are the rates that might be expected for the first generation engines. The key component technologies, however, could all be demonstrated in first-generation engines as discussed and summarized by Figures 5-1 and 5-2, depending on the funds and calendar times available. The impact on test engine availability of incorporating the key technologies is estimated as shown in Table 8-IV. The selected near-term configuration, A-1, relies on oil-lubricated bearings and a gearbox-driven 400 Hz synchronous generator to minimize schedule and cost, and to accommodate use of an existing GTP36-51 engine. Taking approximately 2 to 4 months longer, Configuration A-5 (also based on the GTP36-51), can include both gas bearings and a direct-drive permanent magnet generator. Although the A-7 configuration (a modification of the AGA turbocompressor) already has gas bearings, the turbocompressor is too small for the design thermal input power, 72.7 kw_t. Using this turbocompressor would require (a) operation at a speed higher than current AGA requirements or (b) dumping the thermal energy in excess of the turbocompressor's capability on days with high insolation.

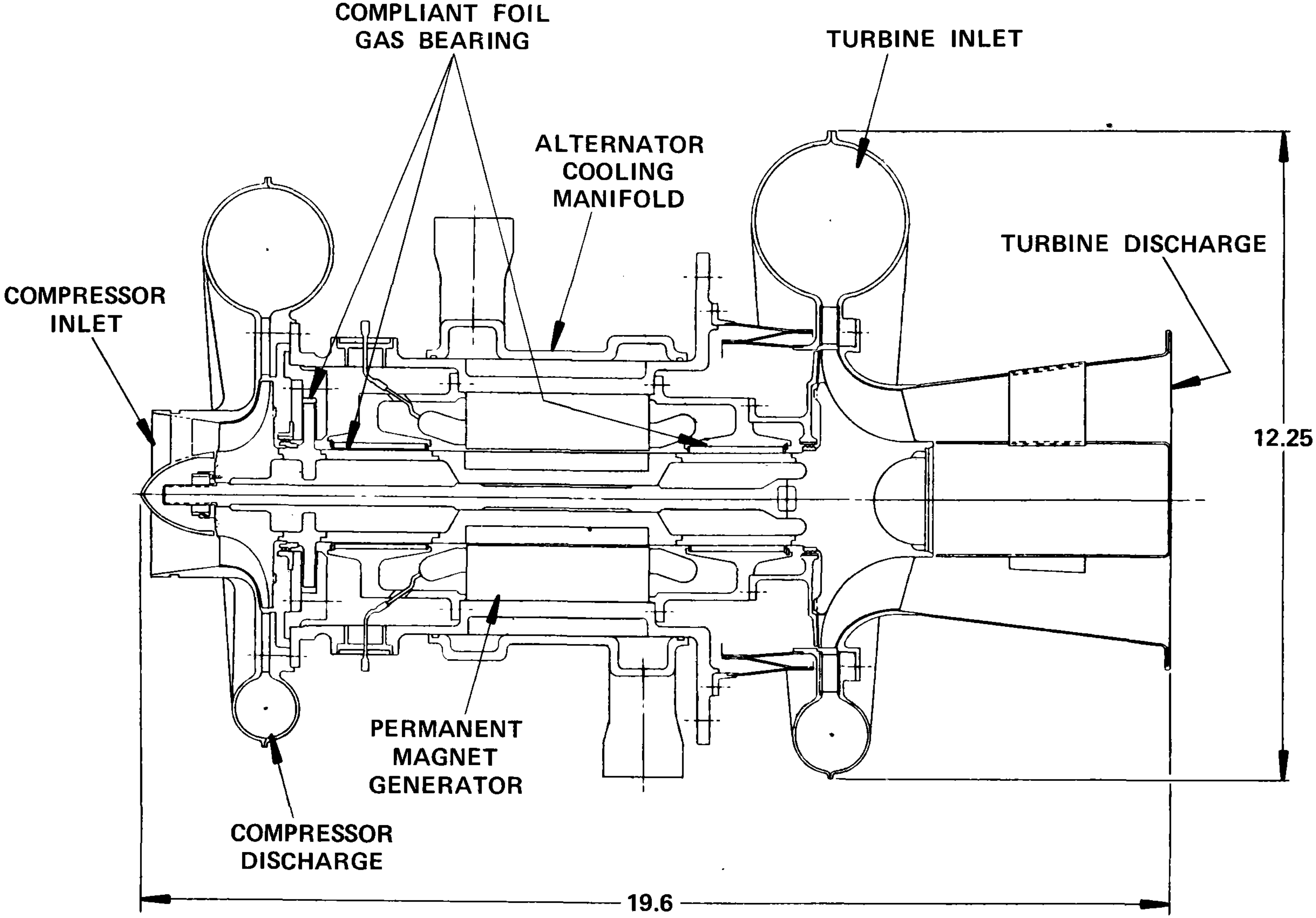

Figure 8-1. Turbocompressor and Generator, Arrangement PC-5.

TABLE 8-I. MATERIALS FOR CONFIGURATION PC-5.

	COMPONENT	MATERIAL
TURBOCOMPRESSOR	TURBINE WHEEL	GMR 225
	TURBINE INLET SCROLL/NOZZLE	HASTELLOY-X
	TURBINE EXHAUST DIFFUSER	ALUMINIZED STEEL
	ALTERNATOR ROTOR	HP9420/INCONEL 713
	PERMANENT MAGNETS	SAMARIUM COBALT
	BEARING JOURNALS	CARBURIZED CARBON STEEL
	THRUST RUNNER	CARBURIZED CARBON STEEL
	TIE	INCONEL 178
	COMPRESSOR NOZZLE/SHROUD	ALUMINUM ALLOY
	MAIN HOUSING AND BEARING SUPPORTS	ALUMINUM ALLOY
	EXTERNAL HEAT EXCHANGER	ALUMINUM ALLOY
	FOIL BEARINGS	TEFLON COATED INCONEL X-750
RECUPERATOR	FINS	CRES 409
	PLATES	CRES 409
	MANIFOLDS	CRES 409
	SHELL	CRES 409
DUCTING	TURBINE INLET DUCT	HASTELLOY-X
	TURBINE DISCHARGE DUCT	ALUMINIZED STEEL

TABLE 8-II. PRODUCTION METHODS FOR 10,000 TO 100,000 UNITS PER YEAR.

Turbocompressors	
Machine Produced Castings	Low Temperature Housing and Aerodynamic Parts
Die Casting	
Low Pressure Permanent Mold	
Permanent Mold	
Automated Investment Castings	Turbine Wheels and Scrolls
Automated Bearing Manufacture	Gas (Foil) Bearings
Hydroforming	Manifolds and Sheet Metal
Inertia Welding	Shaft Parts
Crush Grinding	Aerodynamic Shroud Contours and Shaft Parts
Automated Seam and Spot Welding	Joining Complex Parts
Laser Shaft Balancing	Rotating Group Assembly
Recuperators	
Stamped Tube Sheets	Fin Plates
Forced Hydrogen Circulation Brazing	Plates, Manifolds and Shell
Permanent Magnet Generators	
Automated Windings and Lamination Stamping	Stators
Investment Casting	Rotors

TABLE 8-III. COMPONENT DEVELOPMENT STATUS FOR PC-5.

Key Component	Technology Status
Foil Bearing	Moderate
Permanent Magnet Generator	Moderate
Recuperator	Extensive
Cooler*	Extensive
Engine Control Module & Sensors	Extensive
Compressor Impeller and Diffuser	Extensive
Turbine Stator and Rotor	Extensive

*Closed cycle engines only.

TABLE 8-IV. TECHNOLOGY VERSUS SCHEDULE TIME

Configuration	Key Technologies Included in Demonstrator	Estimated Schedule To First Test Unit
A-1	Open Cycle Solar Engine for 72.7 kW_t High Aerodynamic Performance in Small Size High Degree of Recuperation Variable Speed Control Mode	16 Months
	⇩	
A-5	Light Weight High Performance PMG or WFG Low O & M Cost - All Gas Bearings - No Gearbox - No Starter Motor/Clutch	Plus 2 to 4 Months
	⇩	
C-5	Scaled Aerodynamics, if required to Optimize BE/G for Specific Module Rating	Plus 2 to 4 months

8.1.2 GTCP36-51 Technology Status

The GTP36-51 engine power section was selected as the existing base for the Configuration A requirement on the basis of the following characteristics:

- o An existing proven design
- o A near-optimum performance match with PCU requirements
- o A recent aerodynamic design with high operating efficiency
- o Engine design is a simple, reliable, one-spool rotating group

The GTP36-51 gas turbine (Figure 8-2) was developed for the U.S. Army as prime mover for a ruggedized 30 kW, 50/60/400 Hz field portable generator set. Operating at 80,000 rpm with suitable reduction gearing for each output frequency, the engine has efficient aerodynamic components and displays low noise and vibration characteristics. As a part of a company-sponsored development program, one of these engines was recently coupled to a plate-fin recuperator and demonstrated the expected reduction in fuel consumption and the ability of the combustor to successfully operate with recuperated combustor inlet temperature.

The GTP36-51 gas turbine also is being evaluated in a 600 gpm arctic refueling system. This system has recently completed an 870-hour endurance test and has proven its ability to operate with kerosene and diesel fuels. The system is currently being evaluated in Alaska. As a part of this program, a GTP36-51 gas turbine with unfiltered inlet was recently subjected to a severe environmental test involving extreme temperatures and altitudes, rain, dust, and sand.

The GTP36-51 gas turbine is a modern state-of-the-art engine. Although this engine has not yet been produced in quantity, it is designed for high-volume, low-cost production through the use of simple elements and rugged cast components wherever possible. The power section has a single-spool rotating group consisting of a centrifugal compressor and radial inflow turbine overhung from a rolling element bearing system. It is conservatively estimated that the GTP36-51 could be incorporated into the Configuration A-1 in about 16 months, according to the schedule shown in Figure 8-3.

8.2 Production Cost

Open cycle PC-5 configuration production costs were estimated for a baseline rate of 10,000 units per year. These numbers were then ratioed by empirical factors to obtain costs at other production rates. Table 8-V lists the estimated labor and material costs for the

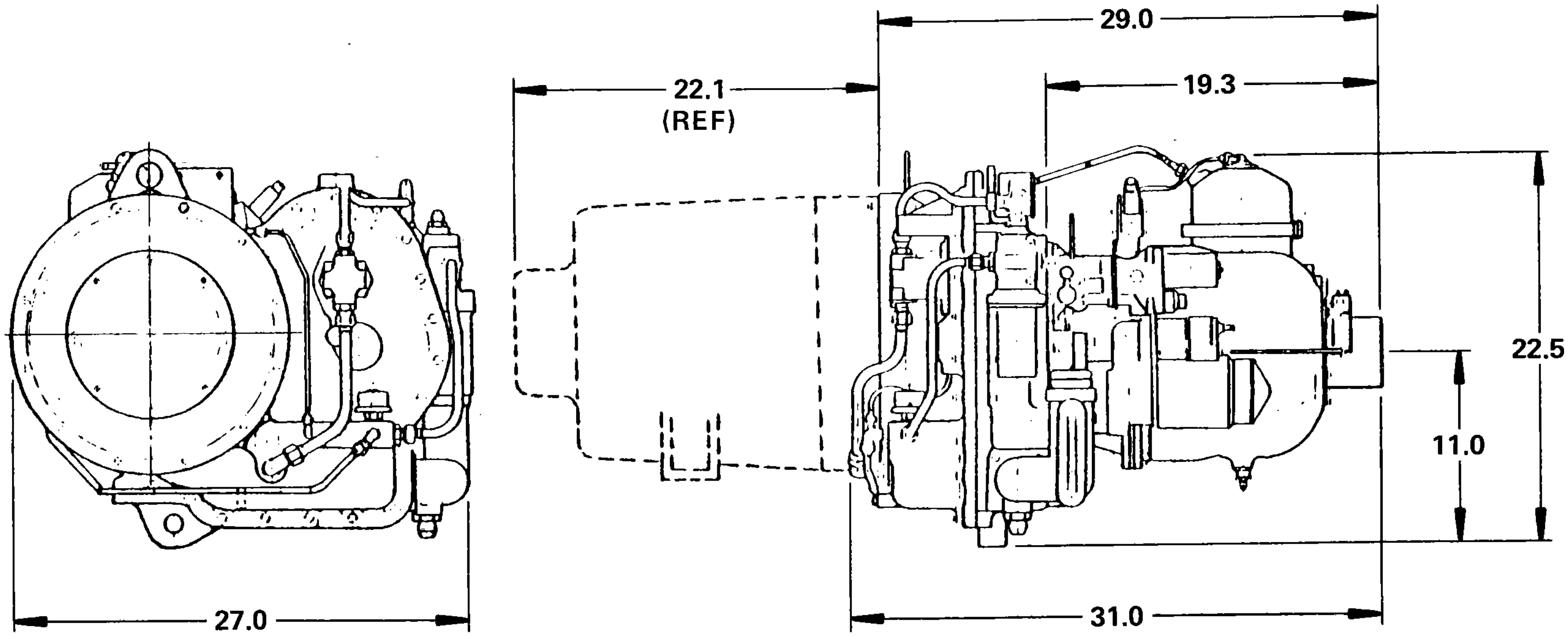

Figure 8-2. Model GTP36-51.

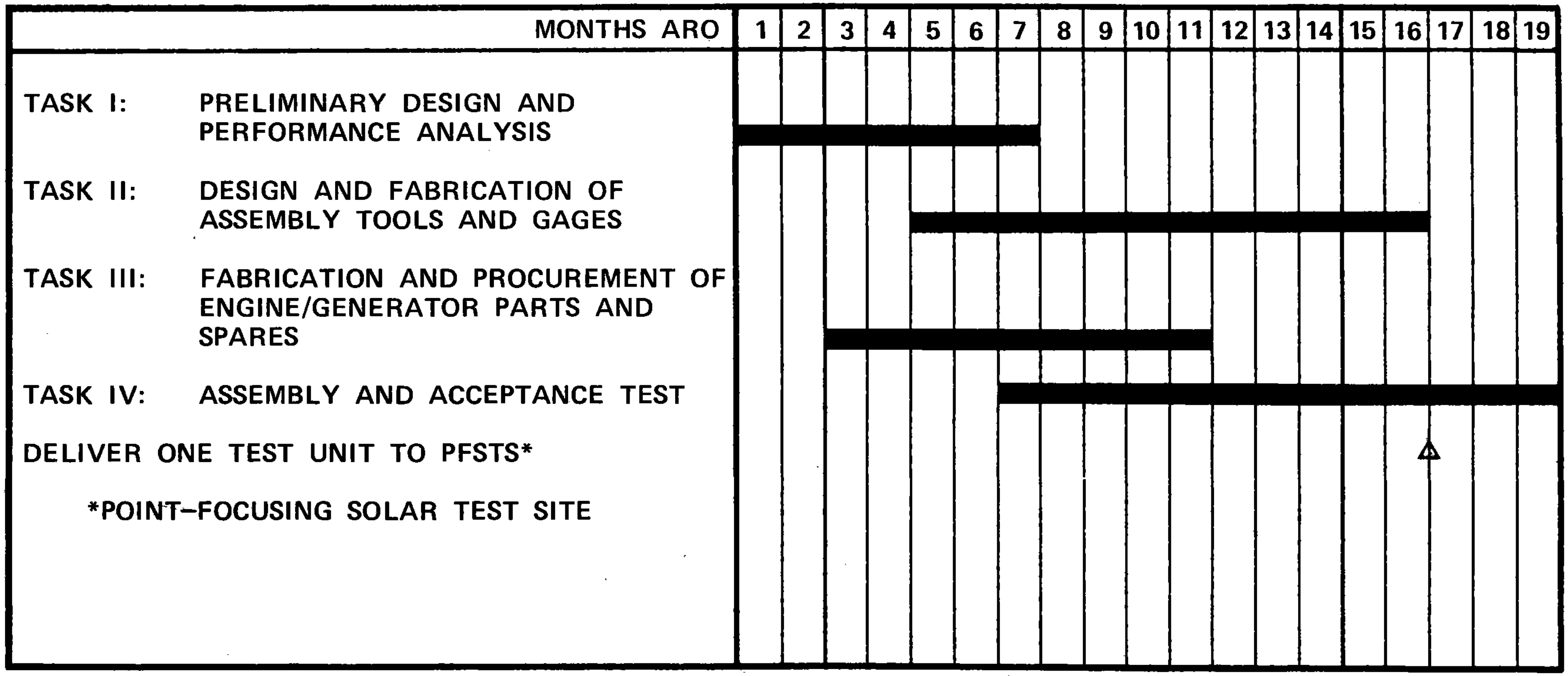

Figure 8-3. Schedule.

TABLE 8-V. PRELIMINARY PRODUCTION COST ESTIMATE - PC-5 CONFIGURATION.

	MATERIAL $(1)	LABOR HRS	MARKUP ON LABOR AND MATERIAL	ESTIMATED PURCHASE PRICE $(1)
TURBOCOMPRESSOR	217	7.5	1.94	890
GENERATOR	302	14.2	1.94	1470
RECUPERATOR	497	12.6	1.94	1750
OTHER PARTS	35	2.7	1.94	236
BELLOWS, DUCTING, FILTER INSULATION, STRUCTURE AND ENCLOSURE				
CONTROLS AND ACCESSORIES				
SENSORS, HARDNESS, ETC.				
CONTROL MODULE				250
FUEL PUMP AND METERING				
RECTIFIER				450
ELECTRONIC START POWER SUPPLY				100
ASSEMBLY AND TEST		2.0	1.94	124
		TOTAL		5270

(1) 1978 DOLLARS
PRODUCTION RATE 10,000/YR
LABOR 32 $/HR

major components. A closed cycle engine configuration would cost about $540 more because of the requirement for a cooler.

Table 8-VI provides estimated factors that may be applied to the baseline 10,000 unit/year production costs to obtain costs for other production rates. For instance, if it were desired to estimate production costs for 1,000,000 units per year, one would multiply the baseline PC-5 cost ($5270) by 0.71 to obtain the cost at the higher production rate.

TABLE 8-VI. ESTIMATED EFFECT OF PRODUCTION RATE

Production (Units/Year)	Normalized Unit Cost
100	3.75
1,000	1.80
10,000	1.00
100,000	0.85
1,000,000	0.71

8.3 Durability

Durability (life) of the Brayton engine/generator is important in estimating the cost of generating power using a solar Brayton plant. A 30-year ultimate objective for commercialized production engines and a 10-year intermediate objective were established as design goals for the purpose of selecting technologies and BE/G component types. Utilizing brushless generators, gas bearings, and avoiding gearboxes and other oil-lubricated components were key elements in designing to meet the ultimate durability goal. In the detail design of commercialized production units, stress levels and materials will first be selected to make the oxidation and rupture or creep compatible with life objectives. When these design and material selections conflict with production cost bogies for labor, machine time or raw material, compromises will be required. In some instances, it may prove more cost effective to add provisions for component maintenance and periodic replacement rather than hold rigidly to an extended design life requirement. The PC-5 configuration, however, is conceptually compatible with the 30-year objective as explained by the durability criteria listed in Table 8-VII.

TABLE 8-VII. DURABILITY CRITERIA.

FAILURE MODES THAT BOUND THE USEFUL LIFE OF THE ENGINE/GENERATOR

Component	Failure Modes
Permanent Magnet Generator	Insulation loss rotor failure
Impeller	Blade fatigue
Turbine	Blade fatigue
Foil Bearings	Loss of foil properties from overtemperature Loss of coating from excessive start/stop
Control Module	Functional failure of temperature sensors
Recuperator	Low cycle fatigue from excessive start/stop cycles Loss of structural capability and pressure integrity from overtemperature

Production engine reliability also was assessed first from the standpoint of possible failure modes and then from the standpoint of expected annual maintenance cost arising from the combination of failure (unscheduled maintenance) modes and scheduled maintenance.

Table 8-VIII lists the estimated MTBFs and estimated unscheduled maintenance costs per unit per year for each major system component. The cost values were derived by assuming 3300 hours/year operation and multiplying by the estimated replacement component cost to arrive at an unscheduled maintenance cost per unit per year. An assumption of maintenance action "on condition" only was made for all operation except inlet air filter replacement. When the unscheduled and scheduled maintenance costs are combined, the estimated total maintenance cost is approximately $116/year.

Table 8-IX lists four alternate concepts for increasing the system life expectancy from 10 to 30 years. Alternative 1 would be to reduce the operating temperatures, accept a performance penalty of 1 or 2 efficiency points, and gain an extension of design life. Alternative 2 would be to replace all life-limiting components at the end of 10 years and again at the end of 20 years so that a 30-year life is achieved. Alternative 3 would be to run the engine to failure, then replace the failed parts and repeating this cycle until 30 year life is achieved. Alternative 4 would be to initially design the E/G for 30 years life.

The effects of these alternatives on BE/G performance, production cost and annual operating cost also are listed in Table 8-IX. A detailed analysis would be required to determine the impact of the alternatives listed on the life cycle cost of the solar power module.

8.4 GROWTH POTENTIAL

Growth potential of the Brayton engine generator was assessed from two points of view, both important contributors toward achieving competitive cost of power produced with Solar Brayton systems.

- o Reduced production and operating costs
- o Increased power conversion efficiency

8.4.1. Reduced Costs

Brayton engine/generator production costs discussed in Section 8.2 were based on the assumed realization of the low cost potential of (a) a high annual production rate (b) a simple, metallic engine design having relatively few parts, and (c) the low maintenance cost of an engine with gas bearings and direct-drive generator. As new low cost materials and manufacturing methods become available, these, too, may be used to further reduce production costs. For

TABLE 8-VIII. MAINTENANCE COST (1978 DOLLARS).

Major Component	Repair/Replace Average Cost ($)	Estimated MTBF (Hours)	Maintenance Cost* Per Unit Per Year	
			Open Cycle ($)	Closed Cycle ($)
Unscheduled				
Turbocompressor	220	70,000	10.3	10.3
Recuperator	510	50,000	33.7	33.7
Permanent Magnet Generator	260	75,000	11.5	11.5
Control Module	60	20,000	9.9	9.9
Sensor Package	60	10,000	19.8	19.8
Ducting and Miscellaneous	70	100,000	2.3	2.3
Cooler	130	50,000		8.6
Scheduled				
Filter Service			10.0	
TOTAL			97.5	96.1

*Based on 3300 hours/year operation.

TABLE 8-IX. ENGINE/GENERATOR LIFE EXTENSION.

Alternative	Changes Relative to 10-Year System		
	Performance	Production Cost	Annualized Operation and Maintenance Cost
(1) TIT and/or rotor speed reduction	Degraded	No Change	Lower
(2) 10-Year replacement of critical parts	No Change	No Change	No Change
(3) Replace parts at failure	No Change	No Change	No Change
(4) Scale engine up geometrically and run at part-load	No Change	Increased	Lower

instance, when ceramic hardware is developed for higher temperature, higher performance automobile gas turbine engines, use of ceramics may also contribute substantially to reduce production costs of solar Brayton engine parts such as the recuperator, turbine rotor and high-temperature housings. Similarly, as the electronics and generator industries achieve economies in manufacturing permanent magnet generators, rectifiers, inverters and microprocesser type controls, these too will be reflected in reduced Brayton engine/generator production costs.

8.4.2 Increased Efficiency

Estimated power conversion efficiencies of the A, B and C configurations selected in this study are listed in Table 8-X. Performance of these engines is a result of an attempt to achieve the best possible efficiency using existing hardware or designs for a 1500°F metallic engine design, and an attempt to rigorously account for all possible losses so that when first-generation demonstrator engines are first evaluated, there will be no surprises. Consequently, when looking down the road at a production configuration, there are several areas listed in Table 8-XI in which potential exists for growth. Some of these are discussed below.

- Turbine Inlet Temperature T_7 - High turbine inlet temperature is one of the most obvious areas for growth. Simply operating the A-1 engine at higher temperatures (with appropriate adjustment in the heat exchanger and ducting design will result in a change in output and efficiency shown on Figure 8-4. Power match with the input thermal power of 72.7 kW_t for operation at turbine inlet temperatures other than 1500°F is achieved by changing the rotor speed as shown in the figure. For the range of T_7 shown, an increase of about two efficiency points at the engine output shaft is achieved per 100°F increase in turbine inlet temperature. The GTP36-51 in its current generator set configuration is designed for 1600°F continuous, and 1750°F standby operation.

  With ceramic components, recuperated Brayton engine operation in the range of 2100 to 2500°F, should be possible, yielding efficiencies at the engine shaft in the 40- to 45-percent range.

- System Pressure Drop - A nominal system pressure drop (including receiver) of about 10 percent was assumed for the A-1 design. Increasing duct diameters and flow passage areas in components such as the recuperator and receiver will result in a system performance gain of about one point efficiency for two points reduction in system pressure loss. Evaluating the cost effectiveness, on a system basis, of

TABLE 8-X. PERFORMANCE SUMMARY, 20 KW_e ENGINE/GENERATOR ASSEMBLIES.

		CONFIGURATION		
		A-1	B-3	C-5
AT THE ENGINE OUTPUT SHAFT				
SHAFT POWER (CSP)	kW_m	22.9	21.6	22.8
EFFICIENCY (CSP $\div$ Q_E)		0.315	0.297	0.314
AT THE SOLAR POWER MODULE TERMINALS				
DC ELECTRIC POWER (MEP)	kW_e	19.1	17.6	20.3
EFFICIENCY (MEP $\div$ Q_E)		0.263	0.242	0.279
AT THE 60 HZ BUS BAR				
60 HZ ELECTRIC POWER (NEP)	kW_e	18.0	16.5	19.1
EFFICIENCY (NEP $\div$ Q_E)		0.248	0.227	0.263

TABLE 8-XI. EFFICIENCY GROWTH POTENTIAL.

- o Higher Turbine Inlet Temperature

  Metallic Concepts
  Ceramic Concepts

- o Larger Recuperator (Increased E_R)

- o Reduced System Pressure Loss Ratio

  (Increased β)

- o Improved Aerodynamic Component Efficiency

  Compressor
  Turbine

- o Increased Generator Efficiency

  - o Increased Rectifier and Inverter Efficiency

- o Reduced Parasitic Losses

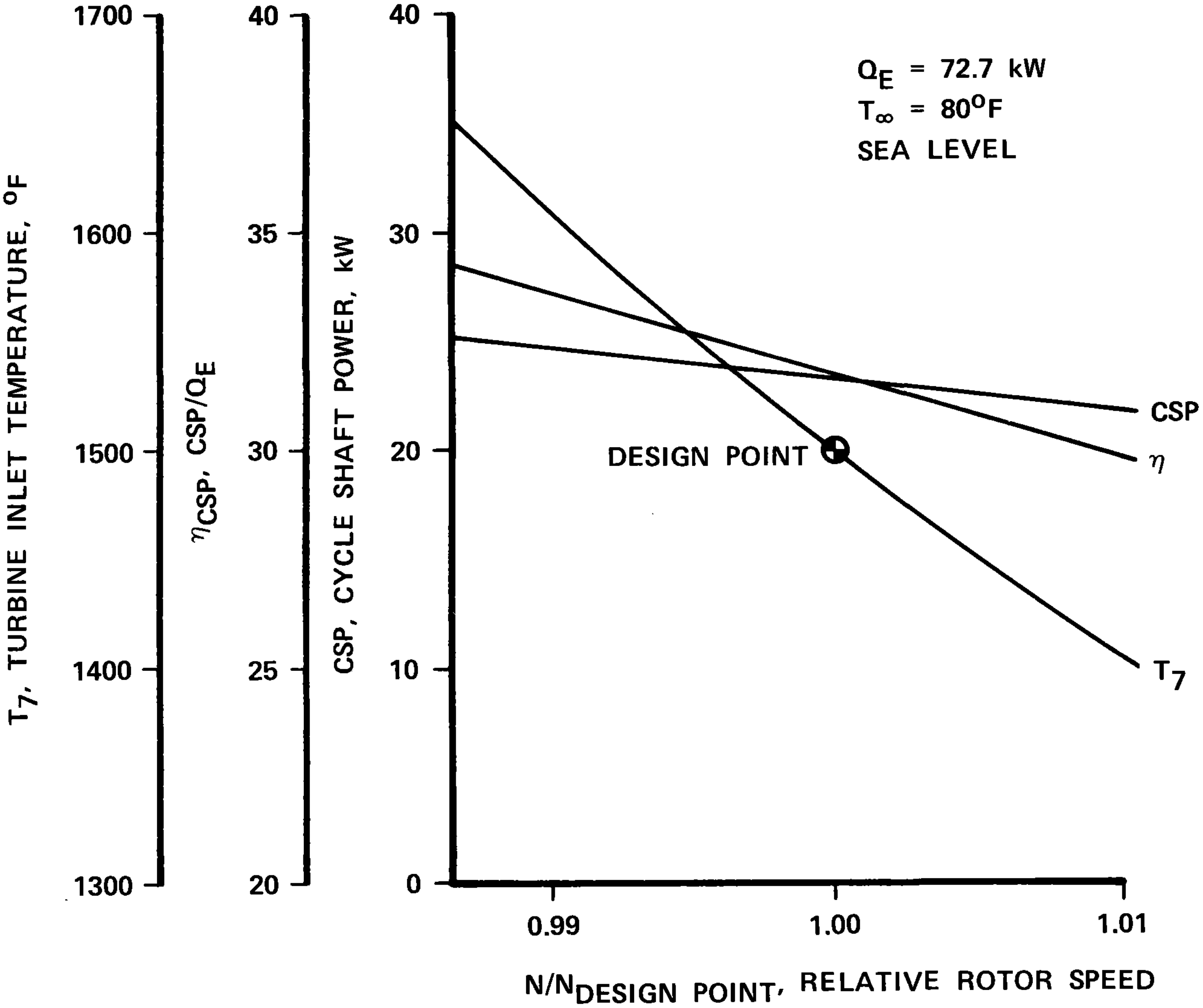

Figure 8-4. Effect of Turbine Inlet Temperature (T_7) on Performance and Speed of Configuration A-1.

changing the system pressure drop would be required prior to making any large change in system pressure drops.

- Recuperator - A highly effective recuperator is part of the Configuration A-1 design. Some additional performance improvement is possible by further increases in the recuperator size. An evaluation indicated a gain of one point efficiency for a 35-percent increase in recuperator size. Since the current A-1 recuperator design was selected on the basis of minimum cost per kilowatt of the complete solar power module, further increases in the recuperator size should be evaluated for overall impact on the overall system cost effectiveness.

- Compressor and Turbine Efficiency - The current aerodynamic performance of AiResearch production gas turbines is an advanced, well developed state of the art. The existing GTP36-51 is an example of this state of the art. Further gains in compressor and turbine performance can however, be expected. For planning purposes, it is noted that approximately two points efficiency at the engine shaft would result from developments that increase the compressor and turbine efficiencies by one point each. Speculation that possible future performance increases are applicable to solar Brayton engines should be tempered until the manufacturing method of the mass-produced components is firmly established, and the impact, if any, that mass production cost considerations will have on compressor and turbine design.

- Electronic Components and Generator Efficiency - Dispersed solar Brayton plant system considerations led to the selection of a variable frequency high speed generator, and rectifer to produce easily paralleled DC power, and an inverter to create 60 Hz power compatible with the 60 Hz power grid. Losses in these components are substantial, and in the A-1 design, reduce the efficiency at the bus bar almost seven points. If it should prove feasible to directly drive a 60 Hz generator, approximately three of these points would be recovered, but an offsetting penalty should then be assessed for the impact that use of induction generators would have on the balance of the 60 Hz grid. In the period prior to full commercialization of solar Brayton plants, some improvement in generator, rectifier, and inverter efficiencies should be expected. Assuming one point improvement in each of these three components would recover approximately 0.6 points BE/G efficiency at the 60 Hz bus bar.

A summary of the potential for growth is provided in Table 8-XII. These values indicate both the current attractiveness of and the potential for growth of Brayton cycle engines for dispersed solar power applications.

TABLE 8-XII. PERFORMANCE GROWTH POTENTIAL.

	Efficiency at Engine Shaft CSP/Q_E (Percent)	Efficiency at 60 Hz Bus NEP/Q_E (Percent)
Baseline (A-1 Configuration)	31.5	24.8
Growth Possibilities		
Increase Turbine Inlet Temperature 150°F	+3.0	+2.4
Reduce System Pressure Drop 2 Points	+1.0	+0.8
Increase Recuperator Size 35 Percent	+1.0	+0.8
Increase Compressor and Turbine Efficiency 1 Point Each	+2.0	+1.6
Use Induction Alternator		+3.0
Increase Efficiency of PMG, Rectifier Inverter 1 Point Each		+0.6
Ceramic Configuration (T_7 = 2100 to 2500°F)	+9.5 to 1.45	+7.2 to 11.2

REFERENCES

1. Allison, H. J., Ramakumar, R. and Hughes, W. L. "A Field Modulated Frequency Down Conversion Power System," IEEE Transactions on Industry Applications, Vol. IA-9, No. 2, March/April 1973.

APPENDIX A

ABBREVIATIONS, ACRONYMS, AND SYMBOLS

APPENDIX A

ABBREVIATIONS, ACRONYMS, AND SYMBOLS

ABC	ATMOSPHERIC BRAYTON CYCLE
AGA	IDENTIFICATION GIVEN TO THE TURBOCOMPRESSOR COMPONENT OF 10-TON REFRIGERATION UNIT BEING DEVELOPED UNDER CONTRACT TO THE AMERICAN GAS ASSOCIATION
BE/G	BRAYTON ENGINE/GENERATOR, ALSO E/G AND PCU
BOP	BALANCE OF PLANT
BRU	BRAYTON ROTATING UNIT. A TURBOCOMPRESSOR PREVIOUSLY DEVELOPED UNDER CONTRACT TO NASA LERC
CBC	CLOSED BRAYTON CYCLE
CSP	CYCLE SHAFT POWER (kW_m)
D_{COMP}	COMPRESSOR WHEEL DIAMETER (INCHES)
D_{TURB}	TURBINE WHEEL DIAMETER (INCHES)
EAL	ELECTRIC ACCESSORY LOAD
E/G	ENGINE/GENERATOR, ALSO PCU
E_r	RECUPERATOR TEMPERATURE EFFECTIVENESS (DIMENSIONLESS)
GEP	GENERATOR ELECTRIC POWER OUTPUT (kW_e)
GTP	GAS TURBINE POWER UNIT
GRI	GAS RESEARCH INSTITUTE
I	INSOLATION (kW/m^2)
m	METER(S)
M	WORKING FLUID MASS FLOW (LBS/SEC). NUMERIC SUBSCRIPTS REFER TO STATIONS IDENTIFIED ON BRAYTON ENGINE/GENERATOR DIAGRAM (FIGURE 3-1)

ABBREVIATIONS, ACRONYMS, AND SYMBOLS (Contd)

M_W, M_F, M_C	MASS FLOW, LBS/SEC, WATER, FUEL, COOLANT
MEP	MODULE ELECTRIC POWER OUTPUT (kW_e)
N_T	ROTATIONAL SPEED OF TURBOCOMPRESSOR (RPM)
N_G	ROTATIONAL SPEED OF GENERATOR (RPM)
N_{GG}	GAS GENERATOR ROTATIONAL SPEED (RPM) FOR MULTI-SPOOL ENGINE
N_{PT}	POWER TURBINE ROTATIONAL SPEED (RPM) FOR MULTI-SPOOL ENGINE
N_{SC}	COMPRESSOR SPECIFIC SPEED - $(W\sqrt{\theta}/\delta)$ RPM-$FT^{3/4}/S^{1/2}$
N_{SC}*	COMPRESSOR INLET SPECIFIC SPEED (DIMENSIONLESS)
NEP	NET ELECTRIC POWER OUTPUT (kW_e)
NSP	NET SHAFT POWER TO GENERATOR (kW_m)
P	PRESSURE (PSIA)-NUMERIC SUBSCRIPTS, WHEN USED, REFER TO STATIONS IDENTIFIED ON ENGINE DIAGRAM (FIGURE 3-1)
PCU	POWER CONVERSION UNIT, ALSO BE/G AND E/G
PEL	PARASITIC ELECTRIC POWER LOSS TO ELECTRIC DRIVEN ACCESSORIES (kW_e)
PFDR	POINT-FOCUSING DISTRIBUTED RECEIVER
PFE	PACIFIC FRUIT EXPRESS
PMG	PERMANENT MAGNET GENERATOR
PPL	PARASITIC PLANT LOSSES
PSL	PARASITIC SHAFT POWER LOSS TO DRIVEN ACCESSORIES (kW)
Q	HEAT FLOW OR THERMAL POWER (kW_t)
Q_C	THERMAL POWER FROM COMBUSTOR (kW_t)
Q_E	THERMAL POWER TO ENGINE = $Q_R + Q_C$ (kW_t)
Q_{EL}	HEAT LOSS FROM ENGINE SURFACES (kW_t)
Q_R	THERMAL POWER FROM RECEIVER (kW_t)

Q_S	HEAT FROM CYCLE TO SINK (kW_t)
REP	RECTIFIED ELECTRIC POWER OUTPUT (kW_e)
r_C	COMPRESSOR PRESSURE RATIO
r_T	TURBINE PRESSURE RATIO
SABC	SUBATMOSPHERIC BRAYTON CYCLE
SAL	SHAFT ACCESSORY LOAD
T	TEMPERATURE, °F, NUMERIC SUBSCRIPTS, WHEN USED, REFER TO STATIONS IDENTIFIED ON BRAYTON ENGINE/GENERATOR DIAGRAM (FIGURE 3-1)
TSL	ROTATING GROUP LOSSES (BEARINGS, SEALS, WINDAGE)
WFG	WOUND FIELD GENERATOR SUCH AS A RICE OR LUNDELL TYPE
β	CYCLE PRESSURE LOSS FRACTION (DIMENSIONLESS, I.E., $\left[\beta = \left(1 - \sum \frac{\Delta P}{P}\right) = (r_T/r_C)\right]$
$\Delta P/P$	PRESSURE LOSS RATIO
η_C	COMPRESSOR EFFICIENCY
η_G	GENERATOR EFFICIENCY
η_{COMB}	COMBUSTOR EFFICIENCY
η_{CSP}	ENGINE CYCLE SHAFT POWER EFFICIENCY = CPS $\div$ Q_E
η_{ETS}	ELECTRICAL TRANSPORT SYSTEM EFFICIENCY
η_{GB}	GEARBOX EFFICIENCY
η_{GEP}	ENGINE ELECTRIC POWER EFFICIENCY AT GENERATOR TERMINALS = GEP $\div$ Q_E
η_{INV}	INVERTER EFFICIENCY
η_{MEP}	MODULE ELECTRIC POWER EFFICIENCY = MEP $\div$ Q_E
η_{NEP}	NET ELECTRIC POWER EFFICIENCY OF PLANT = NEP $\div$ Q_E

ABBREVIATIONS, ACRONYMS, AND SYMBOLS (Contd)

η_R	RECTIFIER EFFICIENCY
η_T	TURBINE EFFICIENCY
TRANS	TRANSFORMER EFFICIENCY

APPENDIX B

PERFORMANCE OF ENGINE/GENERATORS FOR 18.4 TO 63.5 kW_t

TABLE B-I. DESIGN POINTS SELECTED FOR CUSTOMIZED ENGINES.[1]

PERFORMANCE AT DESIGN INSOLATION 0.722 KW/M^2

Cycle Configuration[1][2]	ABC			CBC			SABC		
Concentrator dia, m	7	9	11	7	9	11	7	9	11
Q_E, kW, thermal power to engine	18.4	30.4	45.2	18.4	30.4	45.2	18.4	30.4	45.2
$(\Delta P/P)$, cycle press. loss ratio	0.07	0.07	0.07	0.07	0.05	0.05	0.07	0.09	0.09
T_1-T_∞, °F, ambient-to-comp. ΔT	0	0	0	20	20	20	20	20	20
E_R, Recuperator effectiveness	0.93	0.93	0.93	0.95	0.95	0.95	0.85	0.85	0.85
N_T, krpm, rotor speed	85	75	70	70	70	80	80	70	70
r_C, compressor press. ratio	2.2	2.2	2.4	2.0	2.0	2.2	2.4	2.4	2.4
N_{SC}* compressor specific speed	0.0827	0.093	0.093	0.075	0.075	0.085	0.096	0.107	0.132
N_{SC} compressor specific speed	48.0	55.0	54.8	44.7	46.2	50.4	55.0	62.3	76.8
P_1, comp inlet press, psia	14.69	14.69	14.69	17.1	27.2	30.3	6.25	6.25	6.25
M, RCVR flow, lb/sec	0.184	0.297	0.409	0.213	0.340	0.460	0.145	0.235	0.354
T_5, RCVR inlet temp, °F	1158	1149	1119	1205	1194	1162	1063	1054	1058
P_5, RCVR inlet press, psia	31.6	31.6	34.5	33.3	53.6	65.5	14.65	14.65	14.65
$\Delta P/P_5$ RCVR press loss ratio	0.025	0.025	0.025	0.025	0.025	0.025	0.025	0.025	0.025
η_C, compressor efficiency	0.756	0.782	0.791	0.770	0.781	0.782	0.757	0.777	0.780
η_T, turbine efficiency	0.828	0.851	0.863	0.839	0.850	0.854	0.832	0.856	0.861
Compressor diam									
D_{COMP}, if radial, in.	3.04	3.39	3.83	3.47	3.45	3.24	3.49	3.94	3.93
D_{COMP}, if back-curved, in.	3.35	3.73	4.22	3.82	3.79	3.56	3.84	4.33	4.33
D_{TURB}, in.	3.89	4.46	5.07	4.62	4.56	4.25	4.35	5.04	5.02
η_{MEP}, eng/gen eff, MEP/Q_E	0.279	0.311	0.329	0.282	0.315	0.324	0.218	0.247	0.241
MEP output power, kW_e	5.19	9.45	14.88	5.25	9.57	14.65	4.07	7.50	10.90
Weight of BE/G, lb	163	239	316	300	405	501	237	332	480
Cost of BE/G[2] $	1754	2747	3827	2744	3716	4518	2163	3565	4546

PERFORMANCE AT RATED INSOLATION, 0.900 KW/M^2

	ABC 7	ABC 9	ABC 11	CBC 7	CBC 9	CBC 11	SABC
Q_R, thermal power in kW	23.1	37.8	56.4	23.1	37.8	56.4	
η_{MEP}, eng/gen eff	0.275	0.306	0.323	0.269	0.309	0.312	
MEP, electric power, kW	6.36	11.57	18.24	6.20	11.67	17.58	
BE/G specific cost,[2] $/kW	276	237	210	443	318	257	

[1] Engines have been optimized for a module specific cost of $1000 per design kilowatt at the following conditions: T_∞ = 80°F, P_∞ = 14.69, T_7 = 1500°F, generator/rectifier efficiency = 0.933

[2] Study costs for mass production in 1990 era.

TABLE B-II. DESIGN POINTS[1] SELECTED FOR EXISTING AGA HARDWARE.[2]

PERFORMANCE AT DESIGN INSOLATION, 0.722 kW/m^2

Cycle Configuration	ABC				CBC				SABC			
Concentrator Diameter, m	7	9	11	13	7	9	11	13	7	9	11	13
Q_E, kW, thermal power to engine	18.4	30.4	45.2	63.5	18.4	30.4	45.2	63.5	18.4	30.4	45.2	63.5
Case No.	P1	P7	P9	P17	P3	P10	P14		P5	P12		
$(\Delta P/P)$, cycle press. loss ratio	NS	0.070	0.079	0.082	0.090	0.093	0.093		NS	0.093	NS	NS
$T_1 - T_\infty$, °F, ambient-to-comp ΔT	NS	0	0	0	20	20	20		NS	20	NS	NS
E_r, recuperator effectiveness	NS	0.940	0.940	0.940	0.900	0.900	0.900		NS	0.870	NS	NS
N_t, krpm, rotor speed	NS	62.1	70.7	79.5	74.0	82.0	82.0		NS	81.7	NS	NS
r_c, comp pressure ratio	NS	1.79	2.09	2.45	2.16	2.49	2.49		NS	2.47	NS	NS
P_1, comp inlet press, psia	NS	14.70	14.70	14.70	5.1	6.3	9.5		NS	6.1	NS	NS
N_{SC}, comp specific speed	NS	80	80	80	80	80	80		NS	80	NS	NS
M_5, rcvr flow, lb/sec	NS	0.387	0.493	0.597		0.261			NS	0.246	NS	NS
T_5, rcvr inlet temp, °F	NS	1232	1184	1134		1100			NS	1075	NS	NS
P_5, rcvr inlet press, psia	NS	25.9	30.1	35.4		15.6			NS	14.7	NS	NS
$\Delta P/P_5$, rcvr press loss ratio	NS	0.025	0.025	0.025		0.025			NS	0.025	NS	NS
η_C, compressor eff	NS	0.715	0.770	0.783		0.783			NS	0.784	NS	NS
η_T, turbine eff	NS	0.828	0.833	0.838		0.846			NS	0.846	NS	NS
η_{MEP}, engine/gen eff, $\frac{MEP}{Q_E}$	NS	0.250	0.293	0.310	0.234	0.256	0.259		NS	0.240	NS	NS
MEP, output power, kW_e	NS	7.58	13.30	19.69	4.31	7.78	11.76		NS	7.31	NS	NS
Weight, BE/G, lbs	NS	386	433	495	404	450	493		NS	401	NS	NS
Cost[3], BE/G, $	NS	3633	4046	4576	3370	3586	3712		NS	3163	NS	NS

(1) Engines have been optimized for module specific cost of $1000 per design kilowatt at the following conditions: T_∞ = 80°F, P_∞ = 14.69, T_7 = 1500°F, generator/rectifier efficiency = 0.933

(2) Compressor diameter 3.85 in., Turbine diameter 4.34 in., Design speed 88,760 rpm, N_{SC} = 80

(3) Study costs for mass production in 1990 era.

TABLE B-III. DESIGN POINTS[2] SELECTED FOR EXISTING PFE HARDWARE.[3]

PERFORMANCE AT DESIGN INSOLATION, 0.722 kW/m^2

Cycle Configuration	ABC				CBC				SABC			
Concentrator Diameter, m	7	9	11	13	7	9	11	13	7	9	11	13
Q_E, thermal power to engine	18.4	30.4	45.2	63.5	18.4	30.4	45.2	63.5	18.4	30.4	45.2	63.5
$(\Delta P/P)_{rcvr}$, cycle press loss ratio	0.074	0.075	0.086	NS	0.094	0.094	0.094	0.085	0.091	NS	NS	NS
T_1-T_∞, °F ambient-to-comp. ΔT	0	0	0	NS	20	20	20	20	20	NS	NS	NS
E_R, recuperator effectiveness	0.930	0.930	0.930	NS	0.900	0.930	0.930	0.93	0.930	NS	NS	NS
N_T, krpm rotor speed	46.5	55.7	64.2[1]	NS	65.0	65.0	65.0	65.0	61.1	NS	NS	NS
r_C, compressor press. ratio	1.55	1.84	2.20	NS	2.18	2.18	2.18	2.18	2.01	NS	NS	NS
P_1, comp inlet press, psia		14.70				10.30						
N_{SC}, compressor specific speed	60	60	60	NS	60	60	60	60	60	NS	NS	NS
M_5, rcvr flow, lb/sec		0.349		NS		0.301				NS	NS	NS
T_5, rcvr inlet temp, °F		1202		NS		1154				NS	NS	NS
P_5, rcvr inlet press, psia		26.6		NS		21.5				NS	NS	NS
$\Delta P/P_5$, rcvr press loss ratio		0.025		NS		0.025				NS	NS	NS
η_C, compressor		0.780		NS		0.773				NS	NS	NS
η_T, turbine		0.889		NS		0.893				NS	NS	NS
η_{MEP}, eng/gen eff, $\frac{MEP}{Q_E}$	0.250	0.301	0.321	NS	0.255	0.288	0.297	0.303	0.269	NS	NS	NS
MEP, output power, kW_e	4.61	9.14	14.61	NS	4.67	8.76	13.48	19.15		NS	NS	NS
Weight, BE/G, lbs	275	333	367	NS	353	454	526	637	396	NS	NS	NS
Cost,[4] BE/G, $	2676	3180	3469	NS	2947	3614	3978	4663	3307	NS	NS	NS

(1) Exceeds design speed for the PFE rotor.

(2) Engines have been optimized for module specific cost of $1000 per design kilowatt at the following conditions: T_∞ = 80°F, P_∞ = 14.69, T_7 = 1500°F, generator/rectifier efficiency = 0.933

(3) Compressor diameter = 4.25 in., Turbine Diameter = 4.97 in., Design Speed 60,000 rpm, N_{SC} = 60

(4) Study costs for mass production in 1990 era.

DISTRIBUTION LIST FOR FINAL REPORT

Contract: DEN3-69, (NASACR-159592)

Recipient	Copies
NASA Lewis Research Center Attn: J.A. Heller Mail Stop 500-202 21000 Brookpark Road Cleveland, OH 44135	10
NASA Lewis Research Center Attn: L.W. Schopen Mail Stop 500-305 21000 Brookpark Road Cleveland, OH 44135	1
NASA Lewis Research Center Attn: N.T. Musial, Patent Office Mail Stop 500-318 21000 Brookpark Road Cleveland, OH 44135	1
NASA Lewis Research Center Attn: Library Mail Stop 60-3 21000 Brookpark Road Cleveland, OH 44135	3
NASA Lewis Research Center Attn: Report Control Office Mail Stop 5-5 21000 Brookpark Road Cleveland, OH 44135	1
NASA Headquarters Attn: Ron Scott/RET-14 Washington, DC 20546	2
SERI Attn: J. Fiengold 1536 Cole Boulevard Golden, CO 80401	1
NASA Lewis Research Center	
Attn: A.J. Glassman, 77-2	1
R.J. Stochl, 500-125	1
J.H. Dunn, 500-202	1
R.E. Hyland, 500-202	1
L.I. Shure, 500-202	1
21000 Brookpark Road Cleveland, OH 44135	

DISTRIBUTION LIST (CONTD)

Recipient	Copies
Department of Energy Division of Central Solar Technology 600 E. Street Washington, DC 20545	
Attn: J. Rannels	1
M. Gutstein	1
M. Resner	1
J. Weisiger	5
Jet Propulsion Laboratory 4800 Oak Grove Drive Pasadena, CA 91103	
Attn: V. Truscello (502-201)	1
J. Becker (502-201)	1
A. Marriott (502-201)	1
J. Lucas (502-201)	1
W. Owen (502-201)	1
K. Bahrami	1
N. El Gabalawi	1
W. Carley	1
J. Roschke	1
R. Levin	1
T. Fujita	1
Lawrence Berkeley Laboratory Attn: M. Wahlig Energy & Environment Division University of California Berkeley, CA 94721	1
Pennsylvania State University Attn: Dr. John Kiely Applied Research Laboratory P.O. Box 30 State College, PA 16801	1
Sundstrand Energy Systems	
Attn: T. Bland	1
A. Warren Adam	1
M. Sontucci 4747 Harrison Avenue Rockford, IL 61101	1
Foster-Miller Associates Attn: H. Fuller 135 Second Avenue Waltham, MA 02154	1

DISTRIBUTION LIST (CONTD)

Recipient	Copies
Louis Huang Navy Civil Engineering Lab L-G3 Pt. Hueneme, CA 93043	2
Denis J. Bisantz General Electric, ESPD Bldg. 6, Room 327 Schenectedy, N.Y. 12345	1
T. Nussdorfer Sanders Associates, Inc. 95 Canal St. Nashua, N.H. 03061	1
Curtis-Wright Corp. Power Systems Attn? A.F. Kossar Main & Passaic Sts. Wood-Ridge, NJ 07075	1
Solar Division International Harvester Co. Attn: T.E. Duffy	1
P. Roberts P.O. Box 80966 San Diego, CA 92138	1
Teledyne/CAE Attn: R.J. Macrina 1330 Laskey Rd. Toledo, OH 43601	1
United Technologies Corp. Attn: J.C. Chew 21010 Center Ridge Rd. Cleveland, OH 44116	1
Chrysler Corporation Defense Space Grp./G/Psihas P.O. Box 757 Detroit, MI 48231	1
Rockwell International Corp. Attn: J.W. Wallace, 001-D33 2230 East Imperial Highway El Segundo, CA 90245	1

DISTRIBUTION LIST (CONTD)

Recipient	Copies
Williams Research Corp.	
Attn: Vice President	1
W.J. Bauer	1
2280 W. Maple Rd.	
Walled Lake, MI 48088	
TRW, Inc.	1
Attn: J.N. McCarthy	
23555 Euclid Ave.	
Cleveland, OH 44117	
General Motors Corp.	1
Detroit Diesel/Allison Div.	
Attn: N.E. Eggers/L5	
P.O. Box 894	
Indianapolis, IN 46206	
Westinghouse Electric Corp.	1
Attn: Milton L. Richardson	
1306 Farr Drive	
Dayton, OH 45404	
Mechanical Technology, Inc.	1
Engineering Department	
Attn: Otto Decker	1
968 Albany-Shaker Rd.	
Latham, NY 12110	
Energy Technology, Inc.	1
4914 East 154 Street	
Cleveland, OH 44128	
Arthur D. Little, Inc.	1
Attn: W.P. Feagan	
20 Acorn Park	
Cambridge, MA 02140	
Barber-Nichols Engineering Company	1
6325 West 55 Avenue	
Arvada, CO 80002	
Thermo-Electron Corporation	1
Attn: E. Doyle	
45 First Avenue	
Waltham, MA 02154	

DISTRIBUTION LIST (CONTD)

Recipient	Copies
Fairchild Stratos Division Attn: R. Tadge 1800 Rosecrans Avenue Manhatten Beach, CA 90266	1
Acurex Corporation 485 Clyde Avenue Mountain View, CA 94042 Attn: J.G. Thompson	1
Electric Power Research Institute Attn: J. Bigger P.O. Box 10412 Palo Alto, CA 94303	1
General Electric Company Attn: S.E. Eckard Advanced Energy Programs P.O. Box 15132 Cincinnati, OH 45215	1
General Electric Company Valley Forge Space Center P.O. Box 8661 Philadelphia, PA 19101 Attn: A.J. Poche	1
McDonnel Douglas Astronautics Advanced Solar Energy Systems 5301 Bolsa Avenue Huntington Beach, CA 92647 Attn: R.J. Holl	1
U.S. Army - MERADCOM Attn: W. McGovern DRDME-EM Ft. Belvior, VA 22060	2
Brookhaven National Laboratory Attn: Dr. Paul Auh Opton, NY 11973	1
Argonne National Laboratory Attn: R.E. Holtz Build 330 9700 South Cass Avenue Argonne, IL 60439	1

DISTRIBUTION LIST (CONTD)

Recipient	Copies
Sandia Laboratory Attn: Joe Abbin Division 2324 Albuquerque, NM 87185	1
William Brobeck & Associates 1235 Tenth Street Berkeley, CA 94710	1
Black & Veatch, Inc. Attn: Sheldon Levy 1500 Meadow Lake Parkway Kansas City, MO 64114	1
Boeing Engineering & Construction Co. Attn: D.K. Zimmerman P.O. Box 3707 Seattle, WA 98124	1
Martin-Marietta Corporation Attn: T.R. Heaton P.O. Box 179 Denver, CO 80201	1
Department of Energy Attn: G.H. Thur Code 2221C 20 Massachusetts Ave. Washington, DC 20545	1
Aerojet General Aerojet Liquid Rocket Co. Attn: J.D. Simms P.O. Box 13222 Sacramento, CA 95813	1
Northern Research & Engineering Attn: K. Ginwala 219 Vassar Street Cambridge, MA 02139	1
Institute of Gas Technology Attn: E.B. Ahlers Proposal Preparation 3424 S. State Street Chicago, IL 60616	1

DISTRIBUTION LIST (CONTD)

Recipient	Copies
Burns & Roe, Inc. Attn: J.J. Willson International Sq., Suite 220 1876 K. Street, NW Washington, DC 20006	1
Battelle Columbus Labs. Attn: Sue A. Tiller 505 King Avenue Columbus, OH 43201	1
Stone & Webster Engineering Corp. Attn: Robert G. Paine 245 Summer Street Boston, MA 02107	1
Franklin Inst. Research Lab. Attn: Ed Rosenberg Proposals Manager 20th & The Parkway Philadelphia, PA 19103	1
Desert Research Inst. Attn: Jerry O. Bradley 1500 Buchanan Boulevard Boulder City, NV	1
Solaramics, Inc. Attn: Harold Felix 1301 East El Segundo Blvd. El Segundo, CA 90245	1
Honeywell Attn: James K. Fisher 2600 Ridgway Parkway Minneapolis, MN 55413	1
Research Analysis & Develop., Inc. Attn: F. Macon 4615 Northpark Dr. Suite 204 Colorado Springs, CO 80907	1
Sigma Research, Inc. Attn: E. Saaski 2952 George Washington Way Richland, WA 99362	1